An Assessment and Predictive Modelling of Land use and Mangrove Cover Change Dynamics in the Sundarbans Biosphere Reserve from the Perspective of Climate Change

Thesis submitted for the degree of

Doctor of Philosophy (Ph.D.) in Science

of

Jadavpur University

Submitted by

SOURAV SAMANTA

School of Oceanographic Studies

Faculty of Interdisciplinary Studies, Law & Management

Jadavpur University Kolkata, West Bengal, India

2025

DETAILS OF THESIS

1. Index no. and Date of Registration	Index No. D-7/ISLM/43/18 dated 21 February 2018
2. Title of the thesis	An assessment and predictive modelling of land use and mangrove cover change dynamics in the Sundarbans Biosphere Reserve from the perspective of climate change
3. Name and designation of the supervisor	Prof. Sugata Hazra Professor School of Oceanographic Studies Jadavpur University
4. Email ID of the supervisor	sugata.hazra@jadavpuruniversity.in

5. List of publications

a. Journal articles

i. **Samanta, S.,** Hazra, S., Mondal, P.P., Chanda, A., Giri, S., French, J.R. and Nicholls, R.J., 2021. Assessment and attribution of mangrove Forest changes in the Indian Sundarbans from 2000 to 2020. *Remote Sensing*, *13*(24), p.4957.

ii. **Samanta, S.,** Hazra, S., French, J.R., Nicholls, R.J. and Mondal, P.P., 2023. Exploratory modelling of the impacts of sea-level rise on the Sundarbans mangrove forest, West Bengal, India. *Science of The Total Environment*, *903*, p.166624.

b. Conference

i. **Samanta, S.,** Giri, S., Chanda, A., Hazra, S. 2021, March. Assessment of mangrove degradation due to repeated cyclones in the Sundarbans using satellite-derived canopy density model and vegetation Indices. In Geospatial Science For Digital Earth Observation (GSDEO).

6. List of patents: Nil

STATEMENT OF ORIGINALITY

I, **Sourav Samanta** (Reg. no. **D-7/ISLM/43/18**) registered on **February 21, 2018** do hereby declare that this thesis entitled "**An assessment and predictive modelling of land use and mangrove cover change dynamics in the Sundarbans Biosphere Reserve from the perspective of climate change**" contains literature survey and original research work done by the undersigned candidates as part of Doctoral studies.

All information in this thesis has been obtained and presented in accordance with existing academic rules and ethical conduct. I declare that, as required by thesis rules and conduct, I have fully cited and referred all materials and results that are not original to this work.

I also declare that I have checked this thesis as per the "Policy on Anti Plagiarism, Jadavpur University, 2019", and the level of similarity as checked by iThenticate software is 9%.

Sourav Samanta.

Signature of the candidate with date: 20.02.2025

20.02.2025

Signature of the Supervisor with date and seal:

Dr. SUGATA HAZRA
Professor (Retired)
School of Oceanographic Studies
Jadavpur University, Kolkata-32

CERTIFICATE FROM SUPERVISOR

This is to certify that the thesis entitled "**An assessment and predictive modelling of land use and mangrove cover change dynamics in the Sundarbans Biosphere Reserve from the perspective of climate change**" submitted by Sourav Samanta, who got registered (registration no **D-7/ISLM/43/18**, dated **February 21, 2018**) his/her name under the Faculty of Interdisciplinary Studies, Law & Management for the award PhD (Arts/Science/Engineering/Pharmacy) degree of Jadavpur University is absolutely based upon his/her own work under the supervision of **Prof. (Dr.) Sugata Hazra** and that neither his/her thesis nor any part of the thesis has been submitted for any degree/diploma or any other academic award anywhere before.

20.02.2025

Signature of the Supervisor/s

Dr. SUGATA HAZRA
Professor (Retired)
School of Oceanographic Studies
Jadavpur University, Kolkata-32

Acknowledgment

This research, which forms the foundation of my PhD thesis, would not have been possible without the unwavering support and guidance of numerous individuals and organizations. I am deeply grateful to everyone who has contributed in various ways to the successful completion of this work.

First and foremost, my heartfelt gratitude, after the Almighty, goes to my mentor and supervisor, Prof. Sugata Hazra. His endless encouragement, motivation, and invaluable guidance have been instrumental in shaping this research. Throughout this journey, he has been more than just a supervisor—he has been a mentor, a teacher, a friend, and a colleague. His unwavering faith, patience, and constant support have been a source of immense inspiration, and for that, I am profoundly grateful.

I extend my sincere appreciation to Prof. Tuhin Ghosh, Director, School of Oceanographic Studies, for his support and assistance in facilitating my research and ensuring the smooth completion of all official formalities.

I am also deeply grateful to Dr. Abhra Chanda, Secretary, Faculty of Interdisciplinary Studies, Law, and Management, for his valuable insights, assistance, and encouragement throughout my research journey. My special thanks go to Dr. Rahi Soren for her kind support and to Mr. Subhas Acharya (Ex. Officer, Sundarban Development Board, Government of West Bengal) for his generous help.

I would like to express my sincere gratitude to Prof. Robert J. Nicholls (University of East Anglia & University of Southampton) and Prof. Jon R. French (University College London) for their valuable suggestions and insightful corrections to my writing.

I gratefully acknowledge the financial support from the "Towards a Sustainable Earth: Environment-Human Systems and the UN Global Goals" (TaSE) program under the project "Opportunities and Trade-offs between the SDGs for Food, Welfare, and the Environment in Deltas." This work was made possible through funding from NERC Grant NE/S012478/1, Formas Grant 2019-00045, and the UKIERI-DBT (Grant BT/IN/TaSE/70/SH/2018-19) under the UK-India Education Research Initiative.

I also extend my gratitude to the School of Oceanographic Studies, Jadavpur University, for providing the necessary infrastructural facilities and to the Research and PhD Sections of Jadavpur University for their support and cooperation.

I express my sincere appreciation to Mr. Partho Protim Mondal for his encouragement, guidance, and support during my research. My thanks also go to Dr. Sandip Giri, Dr. Kaberi Samanta, and Dr. Anirban Mukhopadhyay for their valuable guidance and assistance. Additionally, I am grateful to my colleagues from the TaSE team—Mr. Partho Protim Mondal, Dr. Sandip Giri, Miss Ondrila Basu and Mrs. Sudipa Pal—for their encouragement and collaboration.

A special acknowledgment is due to my fellow research scholars at the School of Oceanographic Studies, Jadavpur University, whose camaraderie and insights have enriched this journey.

I would also like to extend my thanks to my colleagues at Bongs Prayukti International for their encouragement and assistance.

Finally, the most profound source of strength, inspiration, and encouragement throughout this journey has been my family. My deepest gratitude goes to my parents, Mr. Gour Gopal Samanta and Mrs. Jharna Samanta; my brother, Mr. Subhendu Bikas Samanta; my sister-in-law, Mrs. Sarmistha Samanta; my nephew, Sharbendu Samanta; and my wife, Mrs. Bithika Biswas. Their unwavering support, love, and belief in me have been the cornerstone of my academic journey.

I sincerely apologize if I have inadvertently missed mentioning anyone. Please know that I am deeply appreciative of each and every contribution made toward the completion of this research.

Abstract

The Indian Sundarbans, together with Bangladesh, comprise the world's largest mangrove forest. Despite the official cessation of reclamation, the mangroves in this region continue to face significant threats from both anthropogenic and environmental pressures. These include conversion into aquaculture farms, hydrological changes caused by upstream water diversions, sediment starvation due to the loss of riverine flow, repeated cyclone landfalls, wave action from the Bay of Bengal, and the ongoing effects of relative sea-level rise.

This study builds on previous research to assess mangrove extent, genus composition, and health indicators from 2000 to 2020, using vegetation indices derived from Landsat and MODIS satellite imagery with maximum likelihood supervised classification. The findings indicate that approximately 110 km² of mangroves disappeared within the Reserve Forest due to erosion, while 81 km² of mangroves were gained through plantation and regeneration within the inhabited part of the Sundarbans Biosphere Reserve (SBR). However, these gains occurred outside the contiguous mangrove belt and only partially compensated for carbon loss from degraded primary forests. Genus composition analysis, incorporating field surveys and published literature, indicates a shift toward more salt-tolerant mangrove species, with a decline in freshwater-dependent genera such as Heritiera, Nypa, and Sonneratia. Vegetation health indicators such as the Enhanced Vegetation Index (EVI) and the Normalized Difference Vegetation Index (NDVI) exhibit a monotonic degradation trend, particularly in sea-facing areas of the mangrove forests, driven by increasing salinity, rising temperatures, and declining pre-monsoon and post-monsoon rainfall.

This study also integrates predictive modelling to examine future land use and mangrove cover dynamics up to 2050, utilizing a Cellular Automata-Markov (CA-Markov) model for land use change projections and the Sea Level Affecting Marshes Model (SLAMM) to assess mangrove vulnerability under climate-induced sea-level rise (SLR) scenarios. Between 2000 and 2020, mangrove cover declined by 4%, wetlands by 50%, and single-cropped agricultural land shrank by 38.4%, while urban settlements increased by 64.7% and aquaculture expanded at the cost of agricultural land. By 2050, urban settlements are projected to expand by 155.9%, mangrove cover may shrink by an additional 9.7%, and aquaculture could rise by 25.4%, exacerbating biodiversity loss and ecosystem degradation. Furthermore, exploratory simulations of the

Indian Sundarbans' evolution up to 2100 under various SLR scenarios indicate that 42% to 80% of mangrove cover could be lost if current management practices continue. Managed realignment could mitigate some losses but would require significant trade-offs, including the relocation of human settlements and repurposing of productive land.

These findings highlight the pressing need for integrated coastal zone management (ICZM), sustainable urban development, climate-resilient agricultural practices, mangrove restoration, and ecosystem-based adaptation strategies to protect the ecological health and socio-economic stability of the Sundarbans. Without proactive conservation efforts and cross-border collaboration between India and Bangladesh, the long-term survival of the Sundarbans is at risk. This research offers scientific evidence to guide policymakers in creating sustainable strategies that strike a balance between development and conservation, ensuring that the Sundarbans continues to function as both an ecological buffer and a vital socio-economic resource for future generations amidst the climate crisis.

Table of Contents

Acknowledgment ..... **iv**

Abstract ..... **vi**

Table of Contents ..... **viii**

List of Table ..... **xii**

***List of* Figure** ..... **xii**

ACRONYMS ..... **xiv**

1. Introduction **2**

1.1 Background of the study area *2*

1.1.1 Shelf zone: 2

1.1.2 Mid-basinal zone: 3

1.1.3 Coastal domain: 4

1.2 The history of land reclamation *5*

1.3 Objectives: *6*

1.3.1 LULC change analysis and future projections: 6

1.3.2 LULC modelling under socio-economic and climatic conditions: 6

1.3.3 Mangrove health assessment and forest decline analysis: 7

1.3.4 Habitat transition modelling in the Sundarbans: 7

1.4 Statement of the problem: *8*

1.5 The gap in the previous researches: *9*

2. Literature Review **11**

2.1 Land use/landcover prediction and scenario-based dynamics modeling in Sundarbans Biosphere Reserve 11

2.2 Mangrove Change and Health change *13*

2.2.1 Significance of Global Mangrove Forests 13

2.2.2 Mangrove Health Assessment 14

2.3 Mangrove Future *15*

3. Study area, present status and problems in Sundarbans **19**

3.1 Number of islands *20*

3.2 Tide: *21*

3.3 Sea level rise *21*

3.4 Land subsidence *21*

3.5 Land surface temperature *22*

3.6 River water temperature *22*

3.7 Land elevation *22*

3.8 River bathymetry *23*
3.9 Geology *23*
3.10 Geomorphology *24*
3.11 Drainage *24*
3.12 Groundwater *25*
3.13 Climate *25*
3.14 Land use and Land cover *25*
3.15 Soil *26*
3.16 Vegetation *27*
3.17 Transport and communication *27*
3.18 Agriculture *28*
3.19 Aquaculture and fishing *28*
3.20 Industry *29*
3.21 Demography *29*
3.22 Culture: *31*
3.23 Literacy *32*
3.24 Cast *33*
3.25 Working population *33*
3.26 Pollutions *34*
3.26.1 Soil Pollution: 34
3.26.2 Air Pollution: 34
3.26.3 Water Pollution 35
3.27 Hazards *35*

4. Methodology 40

4.1 Land use Methodology *40*
4.1.1 Satellite data 40
4.1.2 Land use/land cover classification and accuracy assessment 40
4.1.3 Crop classification 41
4.1.4 Accuracy assessment 42
4.1.5 Generation of Scenario-wise transition probability matrix: 43
4.2 Land Use Change Allocation using Cellular Automata-Markov (CA-Markov) model *44*
4.3 Mangrove change Methodology *45*
4.3.1 Mangrove extent 45
4.3.2 Mangrove Species Classification 46
4.3.3 Mangrove Health Indicators 46
4.3.4 Temperature and Rainfall Estimation 47
4.3.5 Correlating Climatic variability with vegetation health 47
4.3.6 Estimating Cyclone Impact on Mangroves 48
4.3.6.1 Canopy density 48

4.3.6.2 Enhanced Vegetation Index (EVI) 48

4.4 Mangrove Future 48

4.4.1 SLAMM overview 48

4.4.2 Raster input layers 49

4.4.2.1 DEM and slope 49

4.4.2.2 Wetland habitat layer 50

4.4.2.3 Subsidence layer 51

4.4.2.4 Flood defence (dike) layer 52

4.4.3 Model parameters 52

4.4.4 Data-driven modelling of coastal land loss due to erosion 53

4.4.5 SLR scenarios 54

4.4.6 Management scenarios 54

5. Results 57

5.1 Analysis of LULC transformation within the last two decades 57

5.1.1 Land use Change between 2000-2010: 57

5.1.2 Land use Change between 2010-2020: 58

5.2 Accuracy results: 64

5.3 Driver of Land use changes: 65

5.4 Land use/ land cover future projection 67

5.4.1 Land use change between 2020-2030: 67

5.4.2 Land use change between 2030-2050: 71

5.5 Mangrove status of last two decade 74

5.5.1 Change in mangrove forest area 74

5.5.2 Change in Mangrove Species Composition 76

5.5.3 Change in mangrove health indicators 78

5.6 Drivers of change 79

5.6.1 Salinity rise 80

5.6.2 Relative sea-level rise 82

5.6.3 Temperature Rise 84

5.6.4 Changes in Rainfall 84

5.6.5 Short term degradation due to cyclones 86

5.7 Mangrove Future 90

5.7.1 Impact of Sea-Level Rise on Sundarbans Mangrove Extent 90

6. Discussions 98

6.1 Land use dynamics 98

6.2 Land Use/Land Cover Changes and Future Projections discussion 99

6.3 Mangrove Change discussion 101

6.4 Mangrove Future discussion 103

7. Conclusions 106

7.1 Land use change in the transition zone and the future projection 106

7.2 Changes in the mangrove forest 108

7.3 Future of the Mangrove Forest: *109*

References: **111**

List of Table

Table 1 Demographic status of SBR Blocks 30
Table 2 Decadal growth of Population in the SBR Blocks 31
Table 3 Data Used for crop classification 41
Table 4 Climate-induced eustatic SLR scenarios used in this study (derived from Nicholls et al., 2021). 54
Table 5 Summary of the model runs and the scenario assumptions. 54
Table 6 Land use change Matrix 2000-2010 (area in sq. km) 61
Table 7 Land use change Matrix 2010-2020 (area in sq.km) 63
Table 8 Accuracy assessment results 65
Table 9 Drivers of land use/ land cover change 65
Table 10 Land use change matrix 2020-2030 (area sq. km) 70
Table 11 Land use change matrix 2030-2050 (area sq. km) 73
Table 12. The Indian Sundarbans mangrove forest area over time. Numbers in parenthesis show average annual change over the proceeding five years, with negative indicating loss and positive indicating gain. 75
Table 13 Area (and percentage area) of principal mangrove genera in 2000 and 2020. 78
Table 14 Drivers of change for mangroves in the Indian Sundarbans. Driver types: L—legacy; C—contemporary; S—shock. (Samanta et al. 2021) 80
Table 15 Summary of changes in mangrove area for the combined SLAMM and empirical shoreline erosion model simulations for the various SLR, accretion and management scenarios. 90

List of Figure

Figure 1 Location of the Study area (Source: Dubey et al. 2016) 20
Figure 2 Methodology for land use / land cover change and LULC projection 45
Figure 3 Comparison of ground-surveyed elevations with CoastalDEM, SRTM, and TanDEM datasets at Mousuni Island: a) A map indicating the survey transect location.b) An elevation comparison between surveyed data and DEM products along transect A-A'. 50
Figure 4 Key input layers for SLAMM simulations: a) Elevation derived from the CoastalDEM dataset.b) Topographic slope. c) Presence of dikes.d) Land use and land cover. 51
Figure 5 Methodology for SLAMM model 52
Figure 6 Land use / land cover change between 2000-2010 in Sundarbans Biosphere Reserve 58
Figure 7 Land use and land cover change between 2010-2020 in Sundarbans Biosphere Reserve 59
Figure 8 Land use/ Land Cover change (2020-2030) 69
Figure 9 Land use / Land cover prediction 2030-2050 72
Figure 10 Mangrove area loss/gain in the sea-facing islands (numbers 1 to 9). 75
Figure 11 Distribution of dominant mangrove communities of the Indian Sundarbans in 2000 and 2020. 77
Figure 12 Trends in vegetation indices in terms of improving health and declining health from 2000 to 2020 using the Mann–Kendall test on EVI and NDVI, derived from Landsat and Modis data ((a)—Landsat NDVI MK test; (b)—Landsat EVI MK test; (c)—MODIS NDVI MK test; (d)—MODIS EVI MK test). 79
Figure 13 Comparison between salinity zones and mangrove health (MODIS EVI MK test). (A) the inset map showing the different salinity zones in SBR and (B) the spatial variability of EVI MK. 81
Figure 14 Mean sea-level rise at Diamond Harbor. MTL stands for mean tide level (source: Permanent Service for Mean Sea Level (https://www.psmsl.org/data/obtaining/stations/417.phpaccessed on 21 January 2021) and Kolkata Port Trust). 82
Figure 15 Relationship between sea-level rise and loss of mangrove island area due to erosion. MTL stands for mean tide level. 83

Figure 16 Annual rainfall, maximum temperature and minimum temperature variability in (a) summer, (b) monsoon, (c) post-monsoon, and (d) winter season during 2000–2020 in the SBR. 85
Figure 17 Adjusted R square (a–d), partial R EVI-rainfall (e–h), and EVI-maximum temperature (i–l). 86
Figure 18 Change in the forest canopy density (FCD) of the mangroves after cyclones Bulbul (2019) and Amphan (2020). 88
Figure 19 Change in the enhanced vegetation index (EVI) of the mangroves after two consecutive cyclones in 2019 and 2020. 89
Figure 20 Simulated mangrove area changes due to the net effect of accretion and erosion for RCP2.6 (Run 1), RCP4.5 (Run 2) and RCP8.5 (Run 3) SLR scenarios using a baseline vertical mangrove accretion rate of 3 mm yr-^{1} and assuming the Continued Protection scenario 91
Figure 21 Simulated mangrove loss gains for RCP2.6 (Run 4), RCP4.5 (Run 5) and RCP8.5 (Run 6) scenarios, for a vertical mangrove accretion rate of 6 mm yr^{-1} to represent a plausible threshold for mangrove response to SLR, and assuming the Continued Protection scenario. 92
Figure 22 Simulated mangrove loss/gain for RCP2.6 (Run 7), RCP4.5 (Run 8) and RCP8.5 (Run 9) SLR scenarios using a baseline vertical mangrove accretion rate of 3 mm yr^{-1} and assuming the Managed Realignment scenario (inland migration of mangroves allowed). 94
Figure 23 Simulated mangrove loss/gain for RCP2.6 (Run 10), RCP4.5 (Run 11) and RCP8.5 (Run 12) SLR scenarios using a baseline vertical accretion rate of 6 mm yr^{-1} and assuming the Managed Realignment scenario (inland migration of mangroves allowed). 95

ACRONYMS

ANN- Artificial Neural Network

AVI - Advanced Vegetation Index

BAU- Business as Usual

BI - Bare Soil Index

CA-MCA - Cellular Automata–Markov Chain Analysis

Coastal DEM - Coastal Digital Elevation Model

DEM - Digital Elevation Model

DJF – December-January-February

DN- Digital Number

DTH- Direct-to-Home

ENSO - El Niño-Southern Oscillation

ENVI - Environment for Visualizing Images

ETM+ - Enhanced Thematic Mapper plus

EVI - Enhanced Vegetation Index

FCD - Forest Canopy Density

FLAASH- Fast Line-of-sight Atmospheric Analysis of Hypercubes

GBM - Ganges–Brahmaputra–Meghna

GDTR- Great Diurnal Tide Range

GNDVI - Green Normalized Difference Vegetation Index

GPS - Global Positioning System

IMD- India Meteorological Department

IPCC - Intergovernmental Panel on Climate Change

JJA-Jun-July-August

K- Kappa Coefficient

LAI - Leaf Area Index

LiDAR - Light Detection and Ranging

LP - Linear Programming

LST - Land Surface Temperature

LULC- Land Use and Land Cover

MAB - Man and Biosphere

MAM- March-April-May

MCE- Multi-criteria Evaluation

MLP–MCA - Multilayer Perceptron–Markov Chain Analysis

MK- Mann-Kendall

MODTRAN4 - MODerate resolution TRANsmission 4

MOLA- Multi-objective Land Allocation

MSL - Mean Sea Level

NDVI - Normalized Difference Vegetation Index

NDWI- Normalized Difference Water Index

NH – National Highway

NPP- Net Primary Productivity

NWI - National Wetlands Inventory

OA - Overall Accuracy

OLI - Operational Land Imager

PA - Producer's Accuracy

PTC - Percentage Tree Cover

RCP- Representative concentration pathways

SBR- Sundarbans Biosphere Reserve

SH- State Highway

SI - Shadow Index

SLAMM - Sea Level Affecting Marshes Model

SLR – Sea Level Rise

SON- September-October-November

SRTM- Shuttle Radar Topography Mission

STR- Sundarbans Tiger Reserve

TanDEM - TerraSAR-X add-on for Digital Elevation Measurement

TI - Thermal Index

TM - Thematic Mapper

UA - User's Accuracy

UNESCO- United Nations Educational, Scientific and Cultural Organization

USGS - United States Geological Survey

UTM- Universal Transverse Mercator

VI - Vegetation Index

VNIR - Visible and Near-infrared

WWF- World Wide Fund

YBP - Years Before Present

Chapter 1

1. Introduction

The Sundarbans Biosphere Reserve (SBR), designated as a World Heritage Site in 1987 and a Ramsar site in 2019, is home to around 4 lakhs 44 thousand people (as per the 2011 census) and nearly 100 Royal Bengal Tigers, thriving within its distinctive and rich mangrove ecosystem. Over the past two decades, the SBR has experienced significant transformations driven by both natural and human-induced factors. Reports indicate rapid conversion of agricultural lands and marginal forests into human settlements and aquaculture areas (Chopra et al., 2009; DasGupta et al., 2019). Additionally, the decline in mangrove habitats areas (Giri et al., 2007) and the deterioration of their health (Ishtiaque et al., 2016) have raised serious concerns about the sustainability of this global heritage site.

This research aims to develop probabilistic models' framework to forecasting various land use and land cover (LULC) change pathways influenced by different socioeconomic drivers. Furthermore, it seeks to model changes in mangrove forest cover under various climatic scenarios in the SBR up to the year 2050.

1.1 Background of the study area

The development of the modern jagged coastline of the Bengal Basin has been significantly influenced by Quaternary processes associated with the formation of the Bhagirathi-Hooghly delta. Within this context, three distinct sections have been delineated, with the Shelf zone being one of them (Roy and Chatterjee, 2015).

1.1.1 Shelf zone:

Extending from the western margin of the cratonic mass to the Bhagirathi-Hooghly River in the east and from Farakka in the north to the Digha-Haldia line in the south, the Shelf zone has been meticulously studied by numerous researchers. Notably, Ghosh and Majumdar place the Neogene-Quaternary boundary within this zone, specifically between the Mio-Pliocene Bhatrab Banki Formation and the Pleistocene Lalgarh Formation. The Lower Lalgarh Formation, found at higher topographic levels, signifies primary laterite development over Pleistocene boulder conglomerates, while the Upper Lalgarh Formation, occurring at lower elevations, contains vertebrate fossils dating back to the Middle to Upper Pleistocene, along with Palaeolithic tools. This stratigraphic sequence is identified by various names across different districts, such as the Baltora Formation, Illambazar Formation, Kharagpur Formation, and Worgram Formation, reflecting its regional development. The Lalgarh Formation, characterized by a flat-topped but dissected tableland, is not only prevalent along the entire

western margin of the Bengal Basin but also extends to the western fringe of the Mahanadi delta in Orissa. Deep dissection of this tableland has led to the formation of gullies and ravines, often exposing the underlying Mio-Pliocene rocks. Younger than the Pleistocene Lalgarh Formation, A substantial accumulation of alluvial terrace deposits (T3) sediments, known as the Sijua Formation, has been identified. These sediments, characterized by ferruginous, brown, compact, sandy loam with multiple caliche horizons, represent the Older Alluvium and are associated with Late Pleistocene to Early Holocene ages. Another sequence of alluvial terrace (T2) sediments, without any palaeosol horizon, borders the Shelf zone at lower elevations. Referred to as the Daintikri Formation, these sediments comprise greyish-black to black fine sand, silt, and clay and are recognized as the Younger Alluvium. The age of the Daintikri Formation has been determined to be Middle Holocene based on a decomposed wood sample dating 4810±120 years before present (YBP). This formation forms a lower level alluvial plain, featuring typical paradeltaic fluvial fans and other geomorphic elements like aggraded relict channels and oxbow lakes. In the Shelf zone itself, sediments ranging from Late Holocene to present-day form the floodplains (T0) and occasionally develop into narrow, low-relief incipient terraces (T1) within major river channels.

1.1.2 Mid-basinal zone:

Extending from the eastern shore of the Bhagirathi-Hooghly River to the India-Bangladesh border, the Mid-basinal zone features low-lying alluvial plains composed of deltaic and estuarine sediments dating back to the Holocene period. This region encompasses three distinct deltaic plains, each shaped by the influence of fluvial, estuarine, and tidal processes.

The Oum Oum Formation consists of greyish-black, clayey, and muddy mature sediments deposited by migrating meandering channels and Mid-Holocene tidal mudflats. It is positioned at a relatively elevated topographic level, ranging from 10 to 20 meters above mean sea level. This formation spans across Murshidabad, Nadia, and North 24-Parganas districts, with mangrove wood from Oum Oum providing a radiocarbon date of 6175±125 years before present. Consequently, the deltaic Oum Oum Formation, dated to the Middle Holocene, is considered equivalent to the para-deltaic Daintikri/Panskura Formation of the Shelf zone.

The Calcutta Formation consists of greyish-black, muddy sediments of estuarine deltaic origin, found in and around Calcutta at elevations ranging from 4 to 9 meters above mean sea level. This geological formation spans multiple districts, including Nadia, North and South 24-Parganas, Burdwan, Hooghly, Howrah, and Midnapore. Geomorphic features such as tightly

compressed two-phase meander channels, partly alluviated paleo-meander scars, tidal mudflats, infilled tidal channels and creeks, salt marshes and swamps, and dry salt pans characterize the surface of the Calcutta Formation. Radiocarbon dating of peat samples collected from Metro rail excavations assigns a Late Holocene age to this formation, with dates ranging from 3470±110 to 2640±150 years before present.

The Sunderban Formation consists of immature deltaic sediments, primarily composed of greyish-black, sticky fine sand, silt, clay, and mud, forming a tidal-estuary delta. Radiocarbon dating suggests its age ranges between 2900±4022 to 1710±110 years before present, placing it within the Late Holocene to Present era. Situated at elevations below 4 meters above mean sea level, this formation dominates the southern part of the South 24-Parganas district, experiencing regular tidal inundation. The region features extensive mudflats, mangrove swamps, marshes, creeks, and estuaries, characteristic of an active delta plain. Additionally, numerous muddy islands along the east coast support dense mangrove forests.

1.1.3 Coastal domain:

The coastal domain represents a narrow tract of coastline characterized by beach ridges and intervening tidal flats situated between Digha and Haldia in the Hooghly estuary. Morpho stratigraphically, this coastal complex can be categorized into two units: the older Contai Formation and the younger Digha Formation.

In the Contai-Paniparul belt of the Midnapore district, four dissected and partially penetrated beach ridges run parallel to the present coastline, indicating ancient shorelines. These beach ridges, occurring at a height of 6 meters above MSL, are composed of red and brown sediments. Radiocarbon dating has assigned a phase of 5760±140 years before present to the Contai Formation. This aligns it with the Daintikri/Panskura Formation of the fluvial domain (Shelf Zone) and the Oum Oum Formation of the deltaic domain (Mid-Basinal Zone).

South and southeast of the Contai Formation, the terrain is flat, featuring sandy beaches and intertidal mudflats extending to the beach-dune complex of the present-day coast. The Digha Formation, a more recent geological unit, is located at an elevation of 2 to 3 meters above mean sea level. Radiocarbon dating results, indicating an age of approximately 2920±120 years before present, place this formation within the Late Holocene to Present era. Consequently, the Digha Formation is contemporaneous with the Sunderban Formation.

1.2 The history of land reclamation

The history of land reclamation in the Sundarbans Biosphere Reserve, spanning India and Bangladesh, is deeply rooted in both ancient and colonial times, with significant transformations over centuries. Early reclamation efforts trace back to pre-historic settlements, where marshy tracts were gradually cleared for subsistence agriculture using rudimentary tools and shifting cultivation techniques (Chatterjee, 2016). The process intensified during the Mauryan (4th century BCE - 2nd century BCE) and Gupta (4th century CE - 6th century CE) empires, with the introduction of more structured water management systems, including embankments and canals, to facilitate irrigation and protect settlements from tidal inundation (Roy & Dhar, 2021). By the medieval period (7th-12th century CE), reclamation efforts expanded under various local rulers who focused on clearing forests and controlling riverine landscapes for food security and settlement expansion (Bandyopadhyay, 2019). The Islamic period (13th-16th century CE) witnessed large-scale land conversion, particularly under the Delhi Sultanate and Mughal Empire, which encouraged agrarian expansion through state-sponsored irrigation projects and embankment construction to reclaim coastal lands (Eaton, 1993). The Baro Bhuniya system (1576-1612 CE) under the Mughal rule played a crucial role in integrating zamindars (landlords) into reclamation efforts, leading to significant deforestation and the transformation of wetlands into arable land (Habib, 1999).

During the colonial era (1757-1947 CE), British administrators systematically expanded land reclamation, motivated by revenue collection and agricultural productivity. The Henckell's Scheme (1783-84 CE) was one of the earliest large-scale reclamation projects, which involved extensive embankment construction along tidal channels to prevent saline water intrusion and enable rice cultivation (Chatterjee, 1990). The Sundarbans was classified into three revenue districts by the British, and a structured approach was developed to lease out land to settlers who would clear and cultivate the mangrove forests (Pargiter & Ascoli, 2002). However, many of these reclamation projects led to unintended environmental consequences, including soil salinization and increased vulnerability to flooding due to disrupted tidal hydrology (Ghosh et al., 2015). The post-independence period saw both India and Bangladesh continuing reclamation initiatives using modern engineering techniques. Efforts included large-scale irrigation projects, embankment reinforcement, and polder construction aimed at increasing agricultural output and supporting rural livelihoods (Das & Das, 2023). However, these interventions often failed to account for the dynamic fluvio-geomorphological nature of the

region, leading to issues such as waterlogging, sedimentation, and land subsidence (Gour, 2021).

In recent decades, the focus has shifted towards sustainable land management, reforestation, and ecosystem-based adaptation to counteract the ecological degradation caused by historical reclamation efforts. Climate change-induced sea-level rise, frequent cyclones, and increasing salinity have necessitated alternative approaches like mangrove restoration, controlled embankment breaching, and community-led water resource management (Dutta, 2023). Several contemporary studies highlight the need for integrating traditional knowledge with modern scientific techniques to ensure long-term environmental stability while addressing the socio-economic needs of the region's inhabitants (Richards & Flint, 1990). Thus, while land reclamation in the Sundarbans Biosphere Reserve has played a pivotal role in shaping its history, ongoing efforts must balance development with conservation to sustain both human livelihoods and ecological integrity.

1.3 Objectives:

The primary objective of this research is to analyze and project land use and land cover (LULC) changes and assess mangrove health. Additionally, it aims to model future habitat transitions in the Sundarbans Biosphere Reserve (SBR) under varying socio-economic and climatic conditions. The specific objectives are:

1.3.1 LULC change analysis and future projections:

- Study LULC changes over two decades (2000-2020) using remote sensing techniques.
- Project future land use scenarios for 2030 and 2050 under a Business-As-Usual (BAU) scenario.

1.3.2 LULC modelling under socio-economic and climatic conditions:

- Model future LULC changes in the SBR under different socio-economic and climatic conditions using a hybrid CA-Markov Chain model.
- Generate projections based on past trends and discuss them with stakeholders for future planning and sustainable management.

1.3.3 Mangrove health assessment and forest decline analysis:

- Analyze changes in mangrove health and forest area decline from 2000 to 2020, emphasizing climatic drivers.
- Utilize remotely sensed data, ground validation, and vegetation indices to assess spatial, temporal, and seasonal variations in mangrove extent, species composition, and health.
- Investigate the influence of historical and ongoing drivers, including land reclamation, temperature rise, declining rainfall, sea-level rise, and disturbances such as cyclones and storm surges.

1.3.4 Habitat transition modelling in the Sundarbans:

- Model habitat transitions in the Sundarbans, including mangrove loss and migration, under various climate change and sea-level rise (SLR) scenarios throughout the 21st century.
- Employ a hybrid approach combining the Sea Level Affecting Marshes Model (SLAMM) to simulate habitat changes caused by land subsidence and flooding, considering the presence and absence of protective embankments.
- Integrate an empirical model to capture shoreline erosion due to SLR.
- Conduct exploratory simulations under different regional climatic pathways (RCP 2.6, RCP 4.5, and RCP 8.5), which represent varying levels of greenhouse gas emissions and global temperature rise. These simulations factor in geological subsidence and the mangroves' capacity for vertical accretion.

To achieve the first two objectives, LULC changes for the years 2000, 2011, and 2020 have been analyzed using Landsat TM, ETM+, and OLI satellite data with a supervised classification technique. A hybrid CA-Markov Chain model has been used for projecting future LULC scenarios under the Business-As-Usual scenario for the year 2030, which has been discussed with various stakeholders for future planning.

To address the third objective concerning mangrove health assessment, this research analyzes the variations in both the extent and health parameters of the mangroves within the Indian Sundarbans Forest from 2000 to 2020 using remotely sensed data and ground truthing. Changes in mangrove forest area, species composition, and health indicators across the Indian

Sundarbans have been assessed using Landsat and MODIS satellite imagery. The assessment is conducted at spatial, temporal, and seasonal levels by directly measuring forest area changes and developing health-related indicators, such as various vegetation indices. To evaluate the potential factors influencing observed changes in mangrove ecosystems, this study examines historical drivers such as land reclamation, progressive factors like temperature rise and declining rainfall, sea-level rise, and sudden disturbances, including frequent cyclones and storm surges.

To address the fourth objective concerning the response of the Sundarbans mangrove forest to progressive climate change and sea-level rise scenarios, a hybrid model is employed. This model integrates the Sea Level Affecting Marshes Model (SLAMM) to simulate habitat changes driven by subsidence and inundation, constrained by the presence or absence of protective embankments, with an empirical model capturing shoreline erosion induced by sea-level rise. The study conducts a series of exploratory simulations considering regional climatic pathways (RCP 2.6, RCP 4.5, and RCP 8.5) with future climate trends for global SLR. Additionally, geological subsidence in the delta region is accounted for, along with constraints on the mangroves' ability to vertically accrete.

1.4 Statement of the problem:

The Sundarbans region is facing an array of environmental challenges, including increasing erosion, sea-level rise, cyclone frequency and intensity, population growth, changes in salinity, water unavailability, unplanned land conversion, embankment breaching, and various forms of pollution (soil, water, air). These factors, coupled with deforestation and subsidence, contribute to the loss of mangroves, deterioration of their health, and overall changes in LULC in the SBR region (Bera and Maity, 2019; Ghosh et al., 2015; Hazra et al., 2002; Mandal and Hosaka, 2020; Hazra and Samanta, 2016; DasGupta et al., 2019; Sardar and Samadder, 2021).

The Sundarbans is highly susceptible to the adverse effects of climate change. Rising sea levels, coupled with the growing frequency and intensity of cyclones, are accelerating the degradation of mangroves, both in terms of their overall health and spatial coverage. This ongoing trend is projected to persist, leading to further submersion of mangrove forests throughout the century, posing significant ecological and socio-economic challenges for the region. (Das et al., 2020; Ishtiaque et al., 2016; Awty-Carroll et al., 2019; Payo et al., 2016).

1.5 The gap in the previous researches:

Dutta and Deb (2012) produced a LULC change map of the SBR using Landsat satellite images concentrating on mangrove change. The findings showed a decline in open mangroves over time, which is just the opposite of the dense mangrove area. Sahana and Sajjad 2019 revealed that the LULC of the SBR has been diversely changed during 1975-2015. Research findings indicate a significant rise in settlement expansion, swamp formation, and water-logged areas, accompanied by a noticeable decline in vegetation and plantation cover within the region. DasGupta et al. (2019) conducted a study to analyze decadal land-use changes in the Indian Sundarbans delta, with a particular focus on mangrove cover loss and the trade-off between declining agricultural land and the expansion of aquaculture. Similarly, Sardar and Samadder (2021) examined historical trends in land-cover changes from 1998 to 2018, while also projecting future shifts in land distribution. Their study further explored the broader landscape dynamics of the Sundarbans using landscape ecological parameters. However, none of this research concentrated on the classification of cropland into cropping areas of three intensities, distinction between fringe mangroves and reserve forest or classification based on species composition and health of the mangrove forest, and their changes.

In this proposed research work, LULC will be classified into fifteen (15) classes. This will be a first attempt of this kind where LULC is classified considering three crop systems (mono-crop, double-crop, and triple crop). In the study, the prediction of LULC will be done up to 2050.

Xu et al. (2020) carried out land-use change and driver's analysis using biophysical and socioeconomic parameters in Bangladesh. This study will analyze drivers of land change in the SBR using more parameters than the study carried out by Xu et al. (2020). Mangrove change due to sea-level rise is already studied by Payo et al. (2016) using the SLAMM model in Bangladesh with certain limitations (GDTR=0). This research will produce the mangrove change in SBR in a more sophisticated way using the SLAMM model and RCP scenarios. Future projection of shorelines with sea-level rise will be done for calculating future mangrove loss in the SBR. Ishtiaque et al. 2016 have generated MODIS-based ecosystem health on Sundarbans. Awty-Carroll et al. (2019) have made Landsat based health conditions from 1988 to 2018 using classification and NDVI. High resolution and accurate mangrove species mapping and species-specific health deterioration assessment will be carried out in this research for future planning and policymaking.

Chapter -2

2. Literature Review

2.1 Land use/landcover prediction and scenario-based dynamics modeling in Sundarbans Biosphere Reserve

The 20th century has borne witness to an unparalleled environmental upheaval fueled by the escalating forces of population growth and development. The changes in land use and land cover are acknowledged as outcomes of population-induced pressures on the environment, exerting significant influence on global environmental change and sustainability (Meyer and Turner 1992; Roberts et al. 1998; Pocewicz et al., 2008; Mishra and Rai, 2016). Crucially, material on the dynamics of LULC is deemed essential for the effective and sustainable planning and utilization of land and its associated natural resources (Sheeja et al., 2011; Mishra and Rai, 2016).

Riverine deltas, as exemplified by the Sundarbans, display inherent dynamism due to their intricate geomorphological features, the exploitation of natural resources, and socio-economic factors. The presence of diverse landforms within this complex delta, coupled with elements such as resource exploitation, population growth, aquaculture and agriculture expansion, deforestation, rapid urbanization, and climate change, frequently propels the landscape toward a non-linear transformation (Felsenstein and Lichter 2014; Montanari et al. 2014; Morgado et al. 2014, DasGupta et al., 2019).

Understanding the future patterns of land use and the trajectory of transformation is therefore crucial for the Sundarbans. This comprehension holds significance from the perspective of policy governance aimed at conserving natural resources, mitigating disaster risks, formulating appropriate adaptation strategies, and assessing trade-offs and synergies for sustainability (Bryan et al. 2016; DasGupta et al., 2019).

The analysis of future land-use patterns through scenario-based approaches has evolved into an effective decision-making tool, recognizing the socio-ecological complexities and non-linearities of land-use dynamics (Kates et al., 2001; Schoemaker, 2004; Swart et al., 2004; Bryan et al. 2016). Scenarios offer credible projections of future events by incorporating a structured set of assumptions about various influencing factors. These narratives help in understanding potential developments over time by analyzing the interactions between social, economic, environmental, and technological drivers. (Nakicenovic et al., 2000; Alcamo and Henrichs, 2008; Bryan et al., 2016; DasGupta et al., 2019). They are particularly effective for

long-term sustainability assessments, considering diverse possibilities, incorporating various spatio-temporal processes, human regulatory violations, and stakeholders' perceptions (Swart et al., 2004).

In contrast to model-based linear projections of land use, scenario analysis offers the advantage of projecting future scenarios in alignment with different policy implementations. While the precision of scenario predictions cannot be guaranteed, the outcomes can assist policymakers in optimizing their objectives through suitable policy implementation (Feng and Liu, 2016; DasGupta et al., 2019). Scenarios may take a qualitative, quantitative, or hybrid form, with qualitative scenarios presented as narrative texts or storylines and quantitative scenarios illustrated numerically through graphs, tables, or numbers. The combination of both types is often necessary to leverage the advantages of each (Alcamo and Henrich, 2008). Recent scenario exercises are primarily structured based on the 'Story-and-Simulation' approach by Alcamo (2001), where storylines are developed to feed into dynamic models (Kok, 2009).

The extensive utilization of land-use simulation models has been validated through advancements in remote sensing and numerical computation (DasGupta et al., 2019). Over the past twenty years, numerous studies have explored scenario-based land-use projections to delineate trajectories for the sustainable utilization of diverse landforms (He et al. 2006; Mozumder and Tripathi, 2014; Boron et al., 2016; Bryan et al., 2016; Mishra and Rai, 2016; Kolb and Galicia, 2018; DasGupta et al., 2019).

Diverse integrated simulation frameworks, such as Cellular Automata–Markov Chain Analysis (CA-MCA) and Multilayer Perceptron–Markov Chain Analysis (MLP–MCA), facilitate the simulation and visualization of the non-linear transformation of land use. Among these, MLP–MCA stands out as the most widely adopted, employing a 'feed-forward Artificial Neural Network' (ANN) and a 'Markovian stochastic process (i.e., MCA)' (Mishra and Rai, 2016; DasGupta et al., 2019). The MLP comprises three layers – input, output, and multiple hidden layers – offering the advantage of automatically generating numerous parameter values, minimizing the need for a training dataset, and saving model standardization time (Civco 1993; Atkinson and Tatnall 1997; Chan et al. 2001; Mishra and Rai, 2016). Another notable benefit of MLP is its capability to model many or all transitions simultaneously (Eastman, 2009). MCA, on the other hand, is the most frequently employed model for simulating changes and trends in urban land use (Sang et al. 2011; Arsanjani et al. 2013). The Markovian stochastic

process in MCA involves various transition probability metrics of Land Use and Land Cover (LULC) changes, which are then used to predict plausible future LULC scenarios.

Capitalizing on the robustness of the MLP–MCA model, the same has been applied in the current study to formulate four future LULC scenarios for the Sundarbans Biosphere Reserve (SBR) based on narrative storylines. These scenarios entail land allocation under different land-use classes, incorporating diverse policy assumptions and developing short-term projections for 2030. The objective of these scenario analyses is to offer plausible directives to policymakers for crafting acceptable and implementable policies to foster the development of a sustainable Sundarbans delta.

2.2 Mangrove Change and Health change

2.2.1 Significance of Global Mangrove Forests

Mangrove forests, spanning approximately 136,000 km² across tropical and subtropical coastal regions, are among the most productive ecosystems on the planet (Giri et al., 2011; Alongi, 2009). These unique coastal forests provide essential ecosystem services (Field et al., 1998; Dodd & Ong, 2008), acting as crucial habitats for both marine and terrestrial species (Nagelkerken et al., 2008). They also play a fundamental role in sediment and nutrient exchange within coastal and estuarine environments (Wolanski, 1995; Dittmar et al., 2006).

Beyond their ecological significance, mangroves contribute to natural disaster mitigation by reducing the destructive impact of extreme waves and storm surges (Zhang et al., 2012; Arkema et al., 2013; Menéndez et al., 2020). Recent studies have further recognized their function as a significant global carbon sink, making them vital in climate change mitigation efforts (Donato et al., 2011; Alongi, 2014). Given their ecological and climatic importance, conservation and restoration initiatives for mangrove forests have gained global attention (Duarte et al., 2013).

Despite their critical role, mangrove forests have suffered substantial losses over the past century due to extensive land reclamation for aquaculture, urban expansion, and coastal development (Valiela et al., 2001; Thomas et al., 2017). Over the last five decades, up to 35% of the world's mangroves have disappeared (Giri et al., 2010), with an estimated annual global loss ranging between 0.3% and 0.7% (Hamilton & Casey, 2016). Between 2000 and 2016, over 60% of mangrove loss was attributed to land-use changes. However, in recent years, direct human-induced degradation has shown a decreasing trend due to growing conservation efforts.

Apart from anthropogenic factors, mangroves are also highly vulnerable to climate variability and environmental changes. Shoreline erosion and extreme weather events have significantly contributed to global mangrove loss, with 27% attributed to erosion and 11% to extreme weather conditions since 2000 (Goldberg et al., 2020). Additionally, climate warming and rising sea levels have led to mangrove expansion into salt marsh areas (Thomas et al., 2017). While this shift may help counteract erosion and increase terrestrial carbon storage—due to the high belowground carbon sequestration capacity of mangrove ecosystems (Doughty et al., 2016)—any acceleration in mangrove degradation could offset these potential benefits.

2.2.2 Mangrove Health Assessment

Efforts to understand mangrove health involve not only mapping changes in mangrove forest areas but also deriving higher-level metrics for a comprehensive view of overall ecosystem health (Hamilton and Casey, 2016, Goldberg et al. 2020). Mangrove ecosystems exhibit remarkable ecological stability and resilience; however, they are highly sensitive to variations in tidal inundation, salinity levels, and soil chemistry (Alongi, 2008; Kuenzer et al., 2011). Evaluating the health of mangrove forests typically involves assessing factors such as tree height, aboveground biomass and carbon storage, as well as the extent of forest fragmentation. These indicators provide crucial insights into the overall condition and sustainability of mangrove habitats. (Simard et al. 2019; Lee et al., 2020; Atwood et al. 2017; Tang et al. 2018; Bryan-Brown et al. 2020).

Remote sensing, in conjunction with ground observations, provides a comprehensive understanding of mangrove health. Optical remote sensing studies utilize vegetation canopy characteristics to derive surrogate indices such as the Normalized Difference Vegetation Index (NDVI), Enhanced Vegetation Index (EVI), Green Normalized Difference Vegetation Index (gNDVI), and Normalized Difference Water Index (NDWI) (Giri et al. 2007; Chellamani et al. 2014; Pastor-Guzman et al. 2018; Huete et al. 2002; Maryantika and Lin, 2017; Abd-El Monsef and Smith, 2017). Supporting measures and derived data products, including Percentage Tree Cover (PTC), Leaf Area Index (LAI), and Net Primary Productivity (NPP), play a crucial role in assessing mangrove health at a regional scale. These metrics provide valuable insights into vegetation density, canopy structure, and overall ecosystem productivity, enabling more comprehensive monitoring and management of mangrove forests. (Ishtiaque et al. 2016).

Despite these advancements, the identification of stressors and health assessment, particularly in the Sundarbans area, remains limited and recent. Remote sensing data from multiple sources

and times are recommended for a more accurate evaluation of mangrove health. Quantitative analysis of mangrove changes, as demonstrated by Paul et al. 2017 and Rahman et al. 2010, enhances conservation and management effectiveness. Previous remote sensing applications in the Sundarbans have primarily concentrated on analysing land cover changes, characterizing key features, and conducting forest mapping. These studies have leveraged satellite imagery and geospatial techniques to monitor habitat dynamics, assess vegetation health, and track environmental changes over time, contributing to improved conservation and management efforts in the region. (Islam et al. 1997; Kundu et al. 2021; Chatterjee et al. 2015; Bera and Maity, 2019; Rahman et al. 2011; Sánchez-Arias et al. 2011; Sahana et al. 2015; Rahman, 2020).

2.3 Mangrove Future

Mangroves emerge as exceptionally productive ecosystems on Earth, playing a vital role in providing crucial ecosystem services like raw material and food supply, defence against coastal erosion and storm surge, water purification, support for fisheries, carbon sequestration, and contributions to tourism and recreation (Sriyanie, 2008; Carugati et al., 2018; Barbier et al., 2011). However, the vulnerability of coastal ecosystems to ongoing sea-level rise (SLR) presents a substantial threat. Rising sea levels can lead to increased salinity intrusion, shoreline erosion, habitat loss, and ecosystem instability, ultimately endangering biodiversity and the sustainability of these fragile environments. (Nicholls and Cazenave, 2010), exacerbated by additional factors related to climate change and human-induced pressures.

The impact of SLR on mangroves may lead to their loss through submergence, as insufficient vertical sedimentation fails to maintain surface elevations (Woodroffe et al., 2016; Saintilian et al., 2020). Additionally, increased rates of shoreline erosion and retreat contribute to mangrove loss (Wu et al., 2015). A high SLR scenario, projected by Spencer et al. (2016), anticipates potential losses of up to 78% of the world's coastal wetlands by 2100. Nevertheless, Schuerch et al. (2018) suggest that losses may be mitigated or avoided where accommodation space allows for landward migration.

Climate-driven SLR is expected to result in the loss of 10 to 15% of mangrove forests by 2100, as projected by Alongi (2008). Regionally, Gilman et al. (2006) predict a 13% decline in mangrove forests in the Pacific islands by the end of the century. The degradation of mangrove ecosystems, coupled with the loss of associated services, brings about multiple adverse impacts, with the reduction of natural protection against storm surges standing out as a critical consequence (Menéndez et al., 2020).

The vulnerabilities discussed are particularly evident in the Sundarbans, an extensive mangrove forest covering approximately 10,000 km2, recognized as the world's largest continuous mangrove expanse (Sarker et al., 2016). Situated between India and Bangladesh, the Sundarbans boast rich biodiversity and serve as the primary habitat for the critically endangered Royal Bengal Tiger. Despite its significance, varying outcomes have been projected in assessments of the effect of SLR on the Bangladesh Sundarbans.

Huq et al. (1995) anticipated complete inundation and loss of the Bangladesh Sundarbans under a 1.0 m SLR, while Loucks et al. (2010) predicted substantial inundation, particularly considering 2000 as a base year and a SLR of 0.28 m. In contrast, Mukul et al. (2019) foresaw the entire Bangladesh Sundarbans being submerged by 2070 in response to climate change and SLR. Lovelock et al. (2015) offered a more optimistic outlook, suggesting that the Sundarbans mangroves could withstand a larger SLR scenario of 1.48 m by 2100. Similarly, Payo et al. (2016) estimated that under a 1.48 m sea-level rise (SLR) scenario, the Bangladesh Sundarbans would experience only a 10% reduction in mangrove coverage by the year 2100. Given the Sundarbans' local, regional, and global importance, these divergent findings underscore the need for further analyses to enhance our understanding of future changes and their management implications.

Over the past few years, various models have been developed to assess the impacts of SLR on coastal habitats, facilitating improved management strategies. For instance, specialized modelling efforts in the Mississippi delta have been undertaken, although their applicability to other locations is limited due to high data requirements (Costanza et al., 1990; Reyes et al., 2000; White et al., 2019). More generalized models, such as the Sea Level Affecting Marshes Model (SLAMM), have been employed globally for exploratory analysis in wetland environments (Akumu et al., 2011; Li et al., 2015; Payo et al., 2016; Tabak et al., 2016; Cole Eckberg et al., 2017; Prado et al., 2019). SLAMM simulates key processes influencing coastal wetland habitat types at broad spatial and temporal scales, considering habitat transitions in response to SLR (Craft et al., 2009; McLeod et al., 2010; Clough et al., 2016). While SLAMM has been utilized in the Sundarbans of Bangladesh (Payo et al., 2016), incorporating static inundation assumptions and a constant shoreline erosion rate, it lacks consideration of increased vertical sediment accretion with rising sea levels. Furthermore, the model neglects the non-linear land loss under time-varying SLR, an important process in the region (Samanta et al., 2021).

The findings from these simulations are utilized to elucidate the potential consequences of a significant managed realignment, facilitating inland northerly migration of mangroves. The study also explores the impacts of such realignment on human activities within the region.

Chapter-3

3. Study area, present status and problems in Sundarbans

The Indian Sundarbans Biosphere Reserve is situated at the northernmost point of the Bay of Bengal, and the southern end of the state of West Bengal with a geographical extension of 21° 32′ N–22° 40′ N and 88° 05′ N–89° 51′ E. It is an archipelago of around 102 low-lying islands connected with intricate river networks. he Indian section of the Sundarbans Biosphere Reserve (SBR) is bounded by the Ichamati-Kalindi-Raimongal river to the east, the Hugli river to the west, the Dampier-Hodges line to the north, and the Bay of Bengal to the south (Giri et al., 2022). Spanning an area of 9,630 square kilometers, the Indian SBR encompasses core, buffer, and transition zones (Sahana et al., 2022) (Figure 1). The core area is highly protected and prohibits all sorts of human activities. The Sundarbans Biosphere Reserve (SBR) consists of a core and buffer zone, collectively forming the Reserve Forest, which spans 4,263 square kilometers. Within this protected region lies the Sundarbans Tiger Reserve (STR), covering 2,585 square kilometers. Surrounding the uninhabited core zone and its continuous mangrove forest is the transition zone, extending over 5,367 square kilometers. This area is home to approximately 4.44 million people, (based on the 2011 census) (Samanta, 2018). Currently, the populated region of the Sundarbans Biosphere Reserve (SBR) falls within 19 administrative blocks, with 13 situated in the South 24 Parganas district and the remaining six in the North 24 Parganas district. (Giri et al., 2021, Giri et al., 2022, Chand et al., 2012). The Indian Sundarbans mangrove, located within the Sundarbans Biosphere Reserve (SBR), gained recognition from UNESCO in 1989 under the Man and Biosphere (MAB) Program. The river Hugli, the westernmost estuary of the Sundarbans, represents the initial deltaic branch of the Ganga River. The eastern boundary of the Sundarbans Biosphere Reserve (SBR) is formed by the river Raimangal. The Dampier–Hodges line, established from a survey conducted in 1829–1832, serves as the northern limit of the Sundarbans. At present, the inhabited regions of the Sundarbans Biosphere Reserve (SBR) are spread across 19 administrative blocks, commonly known as the 'Sundarban blocks.' These include 13 out of the 36 blocks in South 24 Parganas and 6 out of the 22 blocks in North 24 Parganas.

The Biosphere Reserve experiences a gradient of salinity resulting from freshwater flows from mainstream rivers and tidal ingress from the sea, exhibiting spatial and temporal variations. Generally, salinity is higher closer to the coast, while the water tends to be nearly fresh on the inland side limit of the Sundarbans.

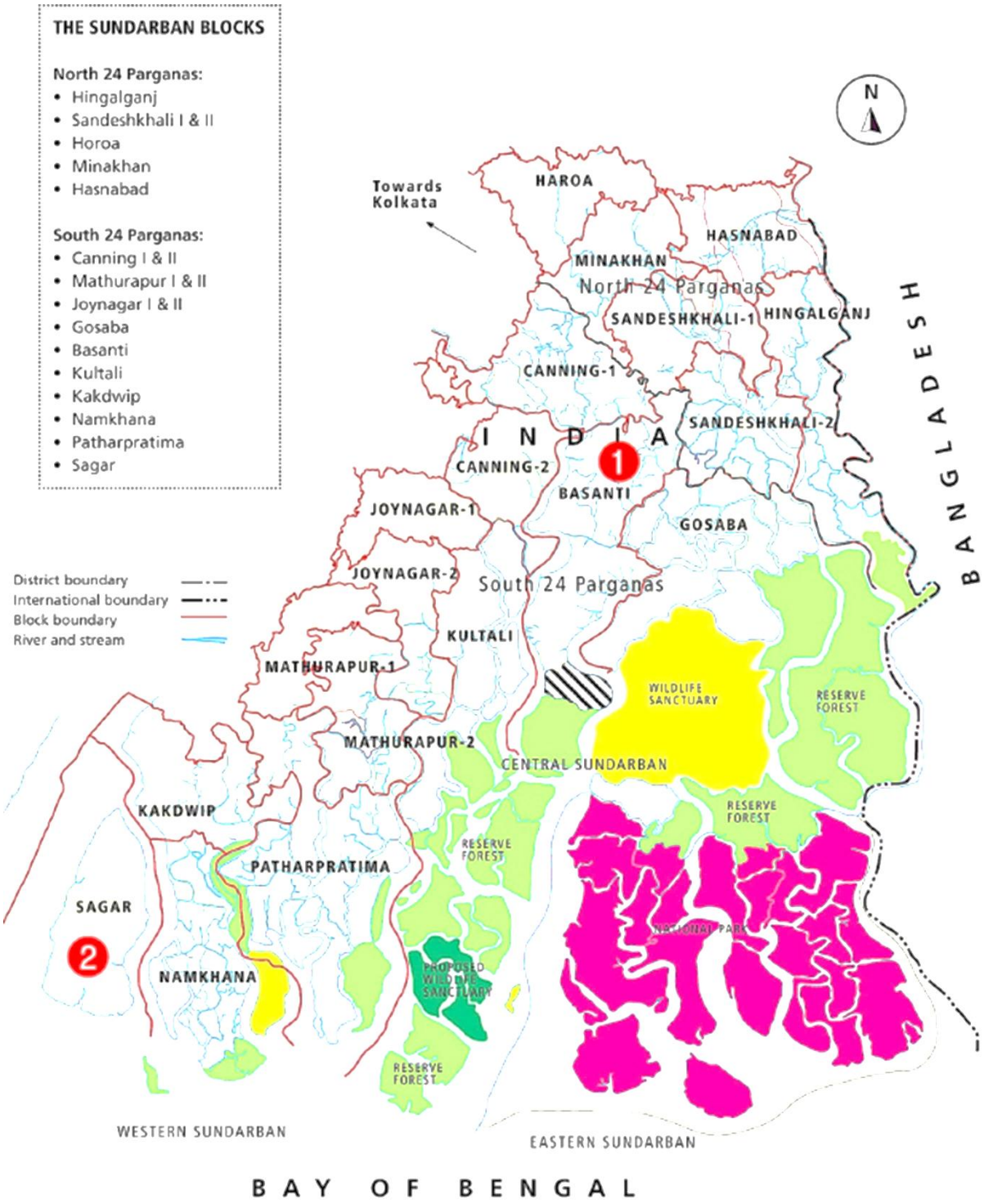

Figure 1 Location of the Study area (Source: Dubey et al. 2016)

3.1 Number of islands

The dynamic nature of the delta, with ongoing processes such as sedimentation, erosion, and accretion, can lead to changes in the number and size of islands. The number and size of islands

can fluctuate over time due to factors like tidal influences, river dynamics, and anthropogenic activities.

The delta comprises of 102 Low-altitude islands, of which 54 islands are occupied by mangrove inhabiting (Chaudhuri, A.B., 2007).

3.2 Tide:

In the Sundarbans, the tidal cycle follows a semi-diurnal pattern with minimal diurnal inequality. The influx of high water along the estuaries is intricate, influenced by resonance and other factors that disrupt any simple pattern in the amplitude of tidal rise and fall. The tidal amplitude in the Sundarbans Estuarine System (SES) in India ranges from 3.5 to 4 meters. Depending on the season, the tidal range can fluctuate between 1 to 6 meters (Chatterjee et al. 2013).

3.3 Sea level rise

Tide gauge records from the northern Bay of Bengal exhibit significant interannual variability in mean sea level, primarily influenced by the El Niño-Southern Oscillation (ENSO), the Indian Ocean Dipole (IOD), and fluctuations in river discharge (Becker et al., 2020). The most comprehensive Indian tide gauge records, maintained at Diamond Harbor on the Hugli estuary, indicate a linear sea-level rise trend of 3.75 mm per year from 1948 to 2020. Given the tidal range of approximately 5 meters, these records also capture sea-level variations influenced by the 18.6-year nodal cycle (Samanta et al., 2021).

Furthermore, the observed sea-level rise trend at Diamond Harbor closely corresponds with the absolute sea-level increase of 3.11 ± 0.44 mm per year in the northern Bay of Bengal between 1993 and 2010, as determined through satellite altimetry data (Ghosh et al., 2018).

3.4 Land subsidence

We analyzed net subsidence rates based on the comprehensive review by Brown and Nicholls (2015), which compiled 205 measurements across different methodologies and timescales for the Ganges–Brahmaputra–Meghna (GBM) delta. Among various land uses in the delta, the Sundarbans exhibited the lowest net subsidence rate, with a mean of −2.8 mm/year and a median of −2.0 mm/year. This relatively lower subsidence rate in the Sundarbans is likely due to sediment deposition from upstream flow and minimal soil compaction.

Brown and Nicholls (2015) emphasized that the median subsidence rate is more representative than the mean, as large individual subsidence measurements can disproportionately affect the

average. Following this approach, we adopted a net subsidence rate of −2.4 mm/year for the Sundarbans, consistent with the findings of Ghosh et al. (2019).

3.5 Land surface temperature

The Sundarbans, a vast mangrove forest spanning Bangladesh and India, exhibits diverse ecological characteristics, and its land surface temperature plays a crucial role in understanding the region's environmental dynamics. Land surface temperature (LST) refers to the temperature of the Earth's surface as measured from a satellite or other remote sensing platforms. The Sundarbans experience distinct variations in land surface temperature due to its geographical features, including the intricate network of water channels, mudflats, crop land, aquaculture, mixed settlement and densely vegetated islands. Remote sensing technologies, such as satellite-based thermal infrared sensors, are commonly employed to capture Sundarbans' land surface temperature. These observations contribute to research on climate change, habitat health, and the overall resilience of the Sundarbans.

The typical surface temperature of SBR has risen at a rate of 0.041 °C per decade (Thakur et al. 2021). However, Sahana et al. (2016) identified the mean surface temperature in the study area has experienced a rise of 0.54 °C per decade. The LST varies between 15–30-degree C. But the LST varies in different land use.

3.6 River water temperature

Between 1980 and 2007, the aquatic temperature in the Sundarbans experienced a significant rise, increasing by 0.5°C per decade. In comparison, the global sea surface temperature exhibited a slower warming trend, rising by approximately 0.06°C per decade. (Mahadevia and Vikas, 2012). This rapid temperature rise in the sea holds significant consequences for aquatic life, particularly impacting the Sundarbans area due to its nature as an estuarine delta. Moreover, this shift detrimentally affects the overall health of the mangrove ecosystem.

3.7 Land elevation

The Sundarbans Biosphere Reserve (SBR) is a low-lying coastal ecosystem, with most areas lying between 0 to 5 meters above mean sea level (MSL) (Mukhopadhyay et al., 2018). The Indian Sundarbans have an elevation range of 0.2 to 2.1 meters, while the Bangladesh Sundarbans range from 1.5 to 3.0 meters (Ghosh et al., 2015; Rahman et al., 2011). This makes the region highly vulnerable to sea-level rise (SLR), land subsidence, and tidal inundation.

Studies indicate that land subsidence rates range from 2 to 4 mm per year, combined with SLR of 3–8 mm per year, posing a serious threat to coastal stability (Brown & Nicholls, 2015; Pethick & Orford, 2013). Satellite-based elevation models (SRTM, LiDAR) reveal continuous erosion, sediment deposition, and shifting tidal channels, further influencing the landscape (Rogers et al., 2017).

The low elevation of the Sundarbans has severe implications, especially during cyclones such as Aila (2009) and Amphan (2020), which caused massive flooding in areas below 1.5 meters (Mukherjee et al., 2021). Efforts such as mangrove restoration, coastal embankments, and sediment management are essential to mitigate the risks of land degradation and rising sea levels (DasGupta & Shaw, 2019). Future research should focus on high-resolution elevation mapping and sustainable adaptation strategies to ensure the long-term resilience of the Sundarbans.

3.8 River bathymetry

The bathymetry of Sundarbans rivers is categorized by a network of channels, tidal creeks, and estuarine zones, creating a diverse and ever-changing aquatic landscape. As one of the world's largest mangrove ecosystems, the Sundarbans depends on a delicate interplay between freshwater and tidal flows. Therefore, bathymetric data is essential for comprehending the hydrodynamic behavior of its rivers. It also contributes to studies on sedimentation patterns, erosion, and the overall health of the rivers, facilitating sustainable development and conservation efforts in this ecologically significant region.

According to a recent study conducted by Bhui et al. (2022), the depth of the rivers ranges from 0 to 75 meters.

3.9 Geology

The Ganga-Brahmaputra (G-B) delta's evolution is marked by high sedimentation rates, forming a distinctive alluvial deposit on both sub-aerial and subaqueous delta regions. The multi-branching channel network underscores its unique development. Notably, the G-B system maintains a delta at different sea level phases. About 18,000 years ago, a lower sea level created a deep channel, including the Swatch of No Ground. Subsequent transgressions led to sediment accumulation. Robust monsoons in Tibet around 15,000 years ago intensified sediment flux. Over the last 7,000 years, sediment deposition increased, forming the Sundarbans, the world's largest mangrove swamp, with distinct saline and freshwater sub-areal

facies. (Goodbred and Kuehl, 2000; Goodbred and Kuehl, 1999; Mikhailov et al., 2006; Sarkar et al., 2009; Allison, 1998).

The majority of the Indian Sundarbans is situated in the lower delta plain, shaped by ongoing estuarine deposition of sand and silt. In contrast, a minor portion in the north and northeast is characterized by a composition of sand, silt, and clay derived from ancient estuarine deposits.

3.10 Geomorphology

The Sundarbans Biosphere Reserve (SBR) is a coastal plain estuary shaped by the Ganges-Brahmaputra-Meghna (GBM) delta, comprising low-lying islands with elevations not exceeding 3 meters above Mean Sea Level (MSL) (Chatterjee et al., 2013). These islands are crisscrossed by tidal creeks and estuarine channels, forming a dynamic landscape influenced by sediment deposition, tidal action, and fluvial processes. The primary tidal channels remain active throughout the tidal cycle, redistributing water and sediments, while interconnected secondary channels facilitate nutrient exchange and salinity balance. High tides inundate intertidal areas, depositing sediments that eventually form tidal flats, which, over time, rise in elevation and support mangrove colonization until they surpass tidal limits (Mukhopadhyay et al., 2018). The geomorphic features of the Sundarbans are classified into six major types, including beaches, delta marshes, young and older delta plains, mudflats, paleo-ridges, creeks, spits, and tidal swamps (Hazra et al., 2002). The region's highly dynamic geomorphology is shaped by coastal erosion, sea-level rise, subsidence, and sediment transport, necessitating remote sensing-based monitoring and sustainable conservation strategies to mitigate erosion, saline intrusion, and habitat degradation in this ecologically fragile delta.

3.11 Drainage

The Sundarbans, once renowned for its multitude of islands separated by an intricate network of interconnected channels, has witnessed significant transformation. Land reclamation has played a substantial role in altering this distinctive system, particularly in the interior regions. A considerable number of channels have undergone conversion into agricultural land, residential areas, or aquaculture ponds. The drainage system of the Indian Sundarbans comprises nine major estuaries—Muriganga, Hugli, Thakuran, Saptamukhi, Bidya, Matla, Raimangal, Harinbhanga, and Gosaba—extending from south to north. Additionally, the region is interlaced with numerous intersecting creeks.

With the exception of Hooghly and Muriganga, none of the estuaries possesses freshwater sources due to their disconnection from their parent river following the eastward diversion of

the Ganga in the 12th century (Morgan and McIntire, 1959) and subsequent anthropogenic modifications.

3.12 Groundwater

Groundwater in the Sundarbans is crucial for sustaining various ecological processes, such as facilitating mangrove growth, preserving wetlands, and regulating soil salinity. Moreover, it serves as a key freshwater source for local communities living in and around the biosphere reserve.

However, the Sundarbans face challenges related to groundwater salinity intrusion, especially in areas closer to the coast. Human activities, such as over-extraction of groundwater for agricultural and domestic purposes, also impact the groundwater balance in the region (Bhadra et al. 2020).

3.13 Climate

The Sundarbans Biosphere Reserve (SBR) has a tropical monsoon climate, with high humidity, seasonal rainfall, and rising temperatures due to climate change. The mean annual temperature ranges between 20°C and 35°C, with summer peaks exceeding 40°C and winter minimums as low as 2–4°C in some areas (Sahana et al., 2021). Seasonal temperature trends show a significant rising pattern, particularly in Canning and Sagar stations, with projections suggesting an increase of up to 6.4°C by the end of the century (Sahana et al., 2021).

Rainfall is monsoon-driven, with 75–80% of the total precipitation occurring between June and October. The annual rainfall ranges between 1,500 mm and 2,500 mm, with the highest levels recorded in July and August (Sahana et al., 2019). Recent studies indicate erratic rainfall trends, with an increase in heavy precipitation events leading to flooding, erosion, and increased salinity. However, there is also evidence of declining winter rainfall, affecting agriculture and freshwater availability (Samanta et al., 2021). The combined impact of temperature rise and altered rainfall patterns has intensified climate-induced vulnerabilities, including sea-level rise, extreme weather events, and mangrove degradation. Adaptation measures such as mangrove conservation and improved hydrological monitoring are essential to mitigate these environmental challenges (Sahana et al., 2022).

3.14 Land use and Land cover

The Sundarbans Biosphere has undergone significant land use changes over the decades, driven by both natural and anthropogenic factors. Major conversions include mangrove to agricultural land due to population pressure (Datta & Deb, 2012), mangrove to urban expansion caused by infrastructure development (Hossain et al., 2024), and mangrove to aquaculture driven by the shrimp farming industry (Chowdhury & Hafsa, 2022). Other notable transitions include agricultural land to urban expansion (Roy et al., 2024), water bodies to agricultural land due to

land reclamation (Khan et al., 2021), and mangrove to bare land caused by deforestation and illegal logging (Kundu et al., 2019). Climate change-induced effects such as natural vegetation to eroded land and eroded land to water bodies have been linked to sea level rise and coastal erosion (DasGupta et al., 2019). Economic factors have driven agricultural land to aquaculture (Thakur et al., 2021), while urban to abandoned land is increasingly common due to climate migration and loss of livelihoods (Sardar & Samadder, 2021). Studies utilizing remote sensing, GIS, and machine learning have mapped these transformations over decades, revealing the urgent need for sustainable management (Quader et al., 2017).

3.15 Soil

The deltaic alluvium in the region has developed over time through the deposition of silt transported by rivers, resulting in a diverse range of soil types. The moribund delta primarily consists of sandy loam, with certain areas containing stiff clay. The Sundarbans mangrove forests, along with a reclaimed northern strip, are dominated by clayey soils, while the coastal regions feature fresh sandy deposits with high salinity levels. In the mature delta and along the Madhumati River, the soil consists of clayey loams, which gradually transition into sandier compositions as they approach the Meghna estuary. Moving further east along the Padma River, the soil primarily consists of pure silt loams. Additionally, peat deposits are found in the central swampy areas, whereas the northernmost regions contain fine silty clay (Naskar and Guha Bakshi, 1987)

The proportion of silt and clay is notably higher in the middle and inner sections of the delta compared to the outer coastal areas. The silt varies in color, appearing pale brown, grey, or greyish-black. The loamy soil, often referred to as black soil or sodium clay, contains ferrous sulfide. The surface layer exhibits a grey to greyish-black hue, while the subsoil appears grey with a blend of clay and sand. At greater depths, the sand grain size changes, and the coloration ranges from grey to blackish-grey.

The soils of the Sundarbans mangrove ecosystem are relatively young and characterized by low oxygen levels. The pH of these soils typically ranges between 7 and 8, with a generally high humus content. Chemical analysis indicates the presence of 0.02–0.9% nitrogen, 0.06–0.1% phosphate, 0.1–0.5% potash, 0.0–6% calcium oxide, and 0.5–1.0% carbon (Naskar and Guha Bakshi, 1987, Chaudhuri and Choudhury, 1994).

3.16 Vegetation

The Sundarbans, the world's largest mangrove forest, predominantly spans non-reclaimed areas. India claims 3% (4740 km2) of the global mangrove expanse, with the Sundarbans accounting for nearly half of that share. According to the Indian State of Forest Report in 2015, the Indian Sundarbans cover 2103 km^2 of mangrove area, with 990 km2 being highly dense, 700 km2 classified as dense, and 416 km^2 designated as open forest. Among the 50 major mangrove species globally, 26 are identified in the Indian Sundarbans (Mandal and Nandi, 1989). The name "Sundarbans" is derived from the renowned Heritiera fomes, locally known as Sundari. Other common species include Bani (Avicennia), Garan (Ceriops sp.), Keora (Sonneratia apetala), Golpata (Nypa fruticans), Baen (Avicennia officinalis), Dhundul (Carapa obovata), and more. Bani, with variants like Black Bani (Avicennia marina), White Bani (Avicennia alba), and Peara Bani (Avicennia officinalis), is the most widely distributed species. Notably, the Sundarbans is the sole mangrove area where the Royal Bengal Tiger and crocodile coexist. Recognizing its significant ecological value and distinctiveness, the Sundarbans attained UNESCO World Heritage Site status in 1987

3.17 Transport and communication

The majority of the Indian Sundarbans now boasts well-established connections to both rail and road networks. The road density stands at 4.25 km/km^2, a substantial improvement compared to the national average of 0.66 km/km^2 (Mistri and Das, 2020). However, the condition of roads is often compromised due to inadequate maintenance. Key highways such as NH-12 (Dalkhola to Bakkhali), SH-1 (Bangaon to Kulpi), and SH-3 (Krishnangar to Gosaba) play a pivotal role in linking these remote islands with other districts. Additionally, the Sundarbans is directly accessible through three vital local railway routes: Sealdah to Namkhana (109 km), Sealdah to Canning (46 km), and Sealdah to Hasnabad (77 km). The railway network connecting Sealdah and Diamond Harbour (60 km) also contributes significantly to the region's transportation services (Fig.). Ferry services are prevalent among the islands, utilizing hand boats or machine boats (Bhatbhati) as primary modes of inter-island connectivity. In fringe villages with limited bus services, auto-rickshaws, electric autos, machine vans, and trackers are extensively employed. Notably, Sundarbans has experienced recent advancements with the widespread availability of electricity, cable, DTH, and internet services.

3.18 Agriculture

Agriculture stands as the predominant economic activity in the Indian Sundarbans, a tradition that has been upheld since the initial cultivation of the land and continues to thrive. Approximately 60% of the people is actively involved in the farming sector (Sanchez-Triama et al., 2014). The primary crop in this region is paddy, with Amman (Kharif paddy) being the dominant variety cultivated across 259,356 hectares of land in the Indian Sundarbans. The annual production of Amman paddy reaches 613.61 thousand metric tons (B.A.E & S, 2013). In recent times, Boro (Rabi paddy) has also been introduced and is cultivated in specific areas of the Sundarbans, covering 28,276 hectares. Beyond paddy, the agricultural landscape includes the cultivation of pulses, wheat, various vegetables, sunflower, mustard, and betel vine, all of which contribute significantly to the agricultural diversity of the region.

3.19 Aquaculture and fishing

Aquaculture is a crucial component of the Sundarbans Biosphere Reserve's economy, serving as a significant supplement to traditional agricultural practices. The region's extensive network of tidal channels and waterways creates a distinctive environment that supports the growth and sustainability of aquaculture, making it an essential livelihood source for local communities.

Shrimp farming is a prominent aquaculture activity in the Sundarbans. The brackish water conditions, influenced by the mix of freshwater from rivers and saline water from the Bay of Bengal, create an ideal habitat for shrimp cultivation. The Sundarbans region is known for its production of both tiger shrimp (Penaeus monodon) and freshwater prawns.

In addition to shrimp, fish farming is also prevalent in the Sundarbans. Various indigenous fish species are cultivated in ponds and enclosures, contributing to the overall fish production of the region. The integration of aquaculture with traditional practices helps diversify livelihoods and ensures a more sustainable approach to resource utilization.

However, the expansion of aquaculture in the Sundarbans has raised environmental concerns, particularly regarding mangrove ecosystems and water quality. Balancing the economic benefits of aquaculture with the preservation of the delicate ecological balance in the Sundarbans is a critical challenge.

Efforts are being made to promote sustainable aquaculture practices, incorporating eco-friendly methods and community-based management. The aim is to ensure that aquaculture in the

Sundarbans Biosphere Reserve continues to contribute to the local economy while safeguarding the unique and fragile ecosystem of this UNESCO World Heritage Site.

3.20 Industry

The industrial landscape in the Indian Sundarbans remains relatively underdeveloped, positioning it as one of the industrially lagging regions in India. Challenges stemming from inadequate infrastructure, proximity to larger industrial centers such as Haldia, Falta, and Kolkata, and its remote geographical location have deterred the establishment of large-scale industries in the area. Instead, the primary industrial activities include brick kilns, sawmills, food processing units, handicrafts, and fish processing.

Jaynagar, within the Sundarbans, has carved out a niche for itself with its renowned sweet, "moa," which has become a branded product enjoying widespread popularity throughout Bengal. Despite the overall industrial limitations, Jaynagar's unique product exemplifies the potential for localized economic contributions and the preservation of traditional craftsmanship in the Sundarbans.

The Sundarbans, renowned for its rich biodiversity, also plays a crucial role in supplying raw materials for wood-based industries. In addition to conventional forest products like timber, fuelwood, and pulpwood, the region supports the large-scale collection of non-wood resources such as thatching materials, honey, beeswax, fish, crustaceans, and mollusks. Various industries, including newsprint mills, match factories, hardboard manufacturing, boat construction, and furniture production, depend on the raw materials derived from the Sundarbans ecosystem.

Furthermore, the Sundarbans has emerged as a hub for ecotourism, adding another dimension to its industrial profile. The diverse ecosystem and unique wildlife attract tourists, contributing to the development of the ecotourism industry in the region. Despite various challenges, the Sundarbans exemplify a harmonious integration of traditional livelihoods, industrial ventures, and sustainable initiatives. This dynamic interplay highlights the region’s ongoing efforts to balance economic growth with environmental conservation, ensuring the preservation of its unique ecosystem while supporting local communities.

3.21 Demography

The administrative jurisdiction of the Indian Sundarbans spans across 19 blocks, with 13 situated in South 24 Paraganas and the remaining 6 in North 24 Paraganas. According to the

2011 census, the population of the Indian Sundarbans stood at approximately 4.42 million, with a gender distribution of 51.15% male and 49.85% female. Notably, the average sex ratio of 955 and child sex ratio of 965 surpass the national averages. Canning-II recorded the highest sex ratio at 966.11, while Haroa reported the lowest at 930. Similarly, Sandeshkhali-II documented the highest child sex ratio at 997, while Haroa marked the lowest at 947 (Table 1).

Table 1 Demographic status of SBR Blocks

Blocks	Population	Sex Ratio	Sex Ratio (below 6)	Schedule Caste (%)	Schedule Tribe (%)	Literacy (%)	Male Literacy (%)	Female Literacy (%)	Working Population (%)	Working Female out of Working Population (%)	Main Workers (%)
Haroa	214401	930.2	947.1	23.6	5.9	63.8	68.2	59.0	34.2	14.1	79.0
Hasnabad	203262	954.1	965.7	25.2	3.7	62.7	67.0	58.1	39.4	23.6	82.1
Hingalganj	174545	962.6	973.5	66.0	7.3	68.5	75.2	61.6	42.7	28.7	54.6
Minakhan	199084	955.1	961.3	30.4	3.9	61.4	66.5	56.1	30.4	16.8	66.7
Sandeshkhali-I	144645	955.7	935.8	30.9	26.0	67.3	72.7	55.2	38.4	23.4	55.4
Sandeshkhali-II	160976	965.0	997.4	44.9	23.4	61.4	68.6	53.9	38.4	25.2	55.3
Basanti	336717	965.9	970.4	35.5	6.0	58.0	64.4	51.5	39.2	28.7	53.0
Canning-I	304724	964.4	942.9	47.6	1.2	60.5	66.8	53.9	35.7	22.6	67.7
Canning-II	252523	966.1	961.2	20.9	5.9	55.1	60.6	49.4	33.2	20.7	52.4
Gosaba	246598	958.6	950.6	62.7	9.5	70.1	76.8	63.1	45.0	31.7	45.9
Jaynagar-I	263151	954.8	954.8	39.0	0.0	63.1	69.1	56.8	33.9	18.7	70.0
Jaynagar-II	252164	956.9	977.6	33.9	0.4	59.0	65.7	52.0	37.0	25.5	59.2
Kakdwip	281963	956.5	975.6	34.7	0.7	68.3	74.1	62.4	35.7	18.8	59.2
Kultali	229053	976.7	976.7	45.5	2.5	65.9	66.9	49.8	38.3	26.3	55.9
Mathurapur-I	195104	980.3	983.0	35.2	2.1	63.4	69.3	57.2	32.9	16.9	56.7
Mathurapur-II	220839	940.1	948.8	28.2	2.1	68.5	75.0	61.6	36.6	19.3	61.8
Namkhana	182830	958.8	958.8	25.9	0.4	75.5	80.4	70.2	36.0	19.6	63.7
Patharpratima	331823	964.6	964.6	23.0	0.8	71.7	77.4	65.8	42.5	30.4	46.2
Sagar	212037	937.0	964.3	26.5	0.4	73.8	79.5	67.7	40.0	26.9	53.2
Average		**954.5**	**964.8**	**35.8**	**8.6**	**70.5**	**74.1**	**58.2**	**37.5**	**23.7**	**60.4**

Source: Census of India, 2011

Over time, the Indian Sundarbans have witnessed significant population growth, rising from 1.52 million in 1961 to 4.42 million in 2011. The population surge has been particularly notable since 1981, as illustrated in the figure depicting the combined population of undivided blocks (Canning, Mathurapur, Jaynagar, and Sandeshkhali) till that year. From 2001 to 2011, the decadal growth rate was 17.80%, with Kultali and Gosaba experiencing the highest and lowest growth rates at 21.84% and 10.67%, respectively. The average decadal growth for the entire

period from 1961 to 2011 was 23.82%, with Minakhan leading with a growth rate of 33.94% (Table 2). This demographic data reflects the dynamic population trends in the Indian Sundarbans over the past few decades.

Table 2 Decadal growth of Population in the SBR Blocks

Block	Decadal Growth 1961-1971	Decadal Growth 1971-1981	Decadal Growth 1981-1991	Decadal Growth 1991-2001	Decadal Growth 2001-2011	Average (1961-2011)
Haroa	21.37	31.84	12.64	20.8	17.47	20.82
Hasnabad	21.47	11.77	-5.12	17.47	14.5	12.02
Hingalganj	28.56	28.72	35.78	9.92	11.6	22.91
Minakhan	28.65	20.83	79.41	23.01	17.83	33.94
Sandeshkhali-I & II	29.9	18.43	25.31	15.6	17.58	21.36
Basanti	41.17	26.69	31.69	22.74	20.86	28.63
Canning-I & II	33.85	27.73	39.87	26.63	26.48	30.91
Gosaba	36.16	19.52	19.12	11.13	10.67	19.32
Jaynagar-I & II	23.7	17.4	42.49	18.1	20.33	24.4
Kakdwip	31.07	30.6	13.98	25.9	17.82	23.87
Kultali	47.46	22.82	6.32	20.16	21.84	23.72
Mathurapur-I & II	28.96	17.36	28.72	23.06	15.26	22.67
Namkhana	36.22	30.84	81.18	19.56	13.82	36.32
Patharpratima	41.92	23.17	24.24	17.42	15.06	24.36
Sagar	23.9	26.31	33.82	20.39	14.22	23.73
Indian Sundarbans	**31.17**	**22.58**	**28.48**	**19.09**	**17.8**	**23.82**

Source: Census of India

3.22 Culture:

The Sundarbans communities celebrate various festivals that reflect their cultural diversity and religious practices. Among these, the traditional Bengali festivals such as Durga Puja and Kali Puja are widely celebrated. These festivals bring the community together, fostering a sense of unity and shared identity.

Folk music and dance are important cultural expressions in the Sundarbans. Traditional songs, known as "Baul" and "Bhatiali," often depict the struggles and joys of daily life in the delta.

Dance forms like the "Jhumur" are also prevalent, adding vibrancy to social and religious occasions.

The Sundarbans region boasts a vibrant tradition of arts and crafts, with local artisans producing intricate handicrafts, including unique items crafted from the renowned Sundarbans honey. The artistry in this region is deeply influenced by its natural surroundings, often depicting mangrove forests, wildlife, and the close relationship between the local communities and their environment.

The Sundarbans are steeped in mythology and folklore, with stories of Bonbibi, a local deity believed to protect the inhabitants from the dangers of the forest, being particularly significant. These stories are not only a source of entertainment but also serve to impart important lessons about coexisting with nature.

3.23 Literacy

The cultural landscape of the Indian Sundarbans is intricately woven with the threads of its socio-economic fabric, and an examination of literacy rates provides insight into the educational dimensions of this unique region. According to the 2011 Census, the average literacy rate in the Indian Sundarbans stands at 64.45%, with a noticeable disparity between male and female literacy rates, recorded at 70.45% and 58.16%, respectively.

This level of literacy falls below the national average, reflecting the challenges faced by the communities in accessing educational opportunities. Among the various blocks within the Sundarbans, Namkhana emerges with the highest total literacy rate at 75.54%. Notably, Sagar, Patharpratima, and Gosaba also boast literacy rates exceeding 70%, with percentages of 73.80%, 71.71%, and 70.07%, respectively. These four blocks secure the top positions concerning both male and female literacy rates.

Conversely, Canning-II, Kultali, Basanti, and Jaynagar-II exhibit literacy rates below 60%, indicating educational disparities in these areas. The disparities underscore the need for targeted interventions and educational initiatives to uplift literacy levels in these blocks and ensure equitable access to education for both genders.

The literacy landscape of the Sundarbans reflects not only the challenges but also the potential for growth and development. Efforts to bridge the gender gap in literacy and enhance overall educational access can contribute significantly to the cultural and socio-economic advancement of the Sundarbans communities.

3.24 Cast

Within the intricate tapestry of the Indian Sundarbans, the demographic composition adds a layer of complexity, notably characterized by the prevalence of the Schedule Caste (SC) and Schedule Tribe (ST) communities. According to the 2011 Census, a significant 35.77% of the Sundarbans population identifies as Schedule Caste, while 5.56% falls under the Schedule Tribe category.

Delving into the nuances of caste distribution across blocks, Hingalganj stands out with the highest percentage of Schedule Caste population at 66.01%, emphasizing the substantial presence of this community. In contrast, Canning-II exhibits the lowest proportion at 20.93%, showcasing variations in caste demographics within the Sundarbans. Similarly, the Schedule Tribe population is most noticeable in Sandeshkhali-I, accounting for 25.94%, while Jaynagar-I registers the lowest at 0.03%.

The dominance of particular caste categories is a defining aspect of the Sundarbans cultural landscape. The Pods (Poundra Kshatriya) and Namasudras emerge as the prominent caste groups in this region, shaping social dynamics and cultural practices. Additionally, the Sundarbans is home to major tribes, including the Munda and Oraon communities. Historically, these tribes were relocated to the Sundarbans from Hazaribagh and Santhal Paraganas to facilitate forest clearance, road construction, and the development of railways and ports at Canning and Diamond Harbour (Pargiter, 1934).

The interplay of caste and tribal identities in the Sundarbans reflects a historical narrative of migration, settlement, and socio-economic roles within this dynamic ecosystem. Acknowledging and understanding these intricate social structures is essential for formulating inclusive development strategies that cater to the diverse needs of the Sundarbans communities.

3.25 Working population

The economic dynamics of the Sundarbans are intricately woven into the fabric of its workforce, with agriculture and fishing emerging as the predominant livelihoods. According to Mistri and Das (2020), a substantial 59% of workers engage in agriculture, while 33% are involved in fishing activities.

The workforce in the Indian Sundarbans comprises approximately 1.66 million individuals, constituting 37.48% of the total population. Within this workforce, 76.28% are male, totaling 1.27 million, while 23.72% are female, amounting to 0.39 million. Notably, out of the total

working population, 40.58% of the workforce in the region falls under the category of marginal workers, indicating that they have been employed for less than six months in a calendar year.

The dynamics of the workforce in the Sundarbans are closely tied to the seasonality of farming, as reflected in the fact that 54.68% of marginal workers are engaged in agriculture labor. The ebb and flow of agricultural demands dictate their employment opportunities, emphasizing the impact of seasonal variations on livelihoods.

However, the female workforce participation rate in the Sundarbans is marked at 23.72%, falling below the national average of 31.12%. This disparity highlights the need for targeted efforts to enhance opportunities for women in the workforce and address the factors hindering their participation in economic activities.

In summary, the Sundarbans' economic landscape is deeply rooted in agriculture and fishing, with a significant portion of the population engaged in these sectors. Understanding the intricacies of the workforce, including the prevalence of marginal workers and gender disparities, is crucial for formulating inclusive development plans that address the exclusive challenges faced by the communities in this region.

3.26 Pollutions

The Sundarbans, renowned for its unique ecological significance, faces significant challenges related to pollution, impacting its soil, air, and water quality. These environmental concerns pose threats to the delicate balance of the ecosystem and the communities that depend on it.

3.26.1 Soil Pollution:

Pesticide and Chemical Runoff: Intensive agriculture practices in and around the Sundarbans contribute to the runoff of pesticides and chemical fertilizers into the soil. This contamination can have adverse effects on both terrestrial and aquatic flora and fauna, disrupting the natural balance of the ecosystem.

Industrial Effluents: Industries in the vicinity may release pollutants into the soil, including heavy metals and toxic chemicals. Over time, these pollutants can build up in the soil, disrupting plant growth and posing a risk of entering the food chain, which may have broader ecological and health implications.

3.26.2 Air Pollution:

Deforestation and Biomass Burning: The clearing of land for agriculture and other human activities can lead to deforestation. The burning of biomass, such as wood and agricultural

residues, releases particulate matter and pollutants into the air, contributing to air quality degradation.

The close proximity of industrial zones contributes to the release of various pollutants into the atmosphere. Airborne contaminants, such as sulfur dioxide and nitrogen oxides, can have harmful effects on the environment, leading to air quality degradation, acid rain, and ecosystem imbalances. Additionally, prolonged exposure to these pollutants poses serious health risks, including respiratory issues and other chronic illnesses in humans.

3.26.3 Water Pollution

Oil Spills: The Sundarbans are susceptible to oil spills from maritime activities, which can have devastating consequences for aquatic life. Oil contamination affects the mangrove roots and can harm fish, crabs, and other aquatic species, disrupting the intricate food web.

Plastic Pollution: The increasing use of plastics, coupled with improper waste disposal practices, contributes to plastic pollution in the water. Mangrove ecosystems and aquatic life are adversely affected by the presence of non-biodegradable plastics.

3.27 Hazards

The Sundarbans, with its intricate mangrove ecosystem, faces a range of hazards that pose significant challenges to both the environment and the communities residing in this region. Several types of hazards have been identified, encompassing natural, anthropogenic, and ecological factors. Some of the prominent hazards in the Sundarbans include:

The Sundarbans, a unique and ecologically vital region, faces a myriad of hazards that collectively pose significant challenges to its ecosystems and communities. Prone to tropical cyclones, the area contends with strong winds and storm surges that result in widespread damage to mangrove forests, coastal erosion, and direct threats to human settlements. Climate change-induced sea level rise compounds the vulnerability of this deltaic region, leading to persistent hazards of inundation that endanger both human habitats and the intricate mangrove ecosystems.

Salinity intrusion, driven by changes in sea levels, emerges as a critical threat to the biodiversity of the Sundarbans. This intrusion of saline water into freshwater ecosystems adversely affects plant life, including the mangroves, and disrupts the availability of freshwater resources vital for local communities. Furthermore, soil erosion, exacerbated by intensive human activities and natural processes, contributes to habitat instability and compromises the overall health of the mangrove habitats. Deforestation, agricultural practices, and resource extraction accelerate this soil loss, impacting the region's ecological equilibrium.

The Sundarbans also grapple with pollution, stemming from industrial effluents, agricultural runoff, and oil spills. The resulting soil, air, and water pollution have detrimental effects on the ecosystem, affecting both flora and fauna. Additionally, human expansion into wildlife habitats leads to conflicts, particularly with tigers, posing risks to humans, livestock, and the endangered species themselves.

Unsustainable logging and resource extraction further jeopardize the mangrove ecosystem, as overharvesting of wood, honey, and other resources leads to habitat degradation. Disease outbreaks, both affecting humans and wildlife, are heightened by increased interactions and changing environmental conditions, contributing to the spread of diseases.

The Sundarbans' vulnerability extends to various socio-economic aspects, including limited access to resources, education, and healthcare. This amplifies the challenges faced by the population in adapting to environmental changes, particularly during natural disasters. As sea levels rise and climate patterns shift, there is a potential for climate-induced migration, leading to socio-economic challenges and placing additional stress on receiving areas.

Agricultural intensification, influenced by increased activities and the use of chemical fertilizers and pesticides, contributes to soil degradation. This increasing intensity presents a significant threat to the health of the mangrove ecosystem and the livelihoods of communities dependent on agriculture. The resulting environmental stress can disrupt ecological balance, reduce agricultural productivity, and negatively impact local food security and economic stability. The region's vulnerability to tsunamis, coupled with its geographical location, exposes it to potential devastation from seismic activities, impacting both human settlements and mangrove habitats.

Overfishing, habitat destruction, and changes in water salinity collectively contribute to a decline in fish stocks, jeopardizing the livelihoods of local communities heavily dependent on fisheries. Coastal erosion, driven by natural processes and human activities, accelerates the loss of shoreline stability, impacting both terrestrial and aquatic habitats.

Water scarcity, resulting from changes in precipitation patterns and increased salinity intrusion, poses challenges for both human populations and the mangrove ecosystem, which heavily relies on freshwater sources. Inadequate waste management practices, including plastic

pollution, further exacerbate environmental challenges, affecting biodiversity and human health.

Both legal and illegal extraction of resources, including timber, honey, and aquatic products, threaten the sustainability of the Sundarbans. Unregulated exploitation can lead to habitat destruction and loss of biodiversity. The region also lacks adequate climate-resilient infrastructure, including embankments, shelters, and early warning systems, leaving communities ill-prepared for cyclones, floods, and other climatic events.

The Sundarbans Biosphere Reserve, spanning international borders between India and Bangladesh, introduces geopolitical tensions that may hinder collaborative conservation efforts. Moreover, the growing tourism industry, while providing economic opportunities, poses hazards such as habitat disturbance, pollution, and increased stress on the fragile ecosystem. The Sundarbans Biosphere Reserve may also experience challenges related to limited access to education, inadequate flood control measures, and vulnerability to illegal activities such as poaching and illegal logging.

The high population density in some parts of the Sundarbans Biosphere Reserve exacerbates environmental stress, requiring strategic planning and sustainable development initiatives to balance conservation efforts with the needs of the local population. Inadequate research and monitoring efforts impede the understanding of the Sundarbans' dynamic ecosystem, hindering informed decision-making and effective conservation strategies.

The vulnerability of mangrove species to changes in salinity, temperature, and sea-level rise is a crucial concern, as the loss of these keystone species would have cascading effects on the entire ecosystem. Global economic pressures, such as fluctuations in commodity prices, further impact the livelihoods of communities in the Sundarbans Biosphere Reserve, affecting their resilience to environmental hazards.

In conclusion, the Sundarbans face a complex interplay of environmental, socio-economic, and geopolitical challenges that necessitate comprehensive and collaborative strategies for conservation and sustainable development.

The Sundarbans Biosphere Reserve, a marvel of biodiversity and a crucial ecological buffer, faces a multitude of interconnected hazards that underscore the fragility of this unique ecosystem. From climate-induced threats like cyclones, sea-level rise, and changing precipitation patterns to anthropogenic challenges like pollution, deforestation, and

unsustainable resource extraction, the hazards are diverse and complex. These environmental stressors not only endanger the rich biodiversity of the region but also pose significant risks to the livelihoods and well-being of the communities dwelling within and around the Sundarbans.

The compounding impact of these hazards requires a holistic and collaborative approach. It involves implementing sustainable development practices, strengthening climate resilience, promoting community engagement, and enhancing conservation efforts. Maintaining a balance between economic growth and environmental conservation is essential for ensuring the long-term sustainability of the Sundarbans Biosphere Reserve. A well-planned approach that integrates development with ecological preservation will help protect biodiversity, support local livelihoods, and safeguard this fragile ecosystem for future generations. Moreover, addressing the challenges outlined—ranging from inadequate infrastructure and healthcare access to geopolitical tensions and global economic pressures—demands a concerted effort from local stakeholders, governments, researchers, and the international community.

Preserving the Sundarbans is not merely an environmental imperative; it is a commitment to safeguarding the intricate tapestry of life, culture, and resilience that defines this remarkable biosphere. By recognizing and mitigating the manifold hazards, we can strive towards a harmonious coexistence between nature and human communities, ensuring the Sundarbans continues to thrive for generations to come.

Chapter-4

4. Methodology

4.1 Land use Methodology

4.1.1 Satellite data

Cloud-free Landsat 5 TM (Thematic Mapper) images from 2000 and 2010, along with OLI (Operational Land Imager) images from 2020, were utilized to classify the land use/land cover (LULC) of the SBR. These satellite images have a spatial resolution of 30 meters by 30 meters and were obtained from the USGS Earth Explorer website (https://earthexplorer.usgs.gov/). The study area was covered by two image scenes corresponding to path/row 138/44 and 138/45. To ensure seamless analysis, the two scenes were mosaicked for each year. The images were then projected using the Universal Transverse Mercator (UTM) system, specifically Zone 45, with the WGS 84 datum.

To minimize the impact of atmospheric and scattering effects, radiometric calibration and atmospheric correction were applied (Duggin & Robinove, 1990; Module, 2009; Sibanda & Ahmed, 2021; Sardar & Samadder, 2021). These scattering effects are particularly significant in Landsat data (Song et al., 2001). In this research, the visible and near-infrared (VNIR) bands of Landsat imagery underwent atmospheric correction. Additionally, radiometric calibration was performed to transform digital number (DN) values into top-of-atmosphere radiance (L_{TOA}) using the standard sensor calibration function (Chander et al., 2007). Further processing involved converting VNIR band radiance into surface reflectance through an image-based atmospheric correction model developed by Chavez (1996). The radiance (L_p), influenced by interactions with aerosols and atmospheric particles, was estimated based on the methodologies proposed by Song et al. (2001), Chavez (1996), and Sobrino et al. (2004).

4.1.2 Land use/land cover classification and accuracy assessment

A supervised classification approach employing the maximum likelihood classification technique was used to classify all images (Giri et al., 2007; Datta & Deb, 2012; Giri et al., 2021). A total of twelve land use/land cover (LULC) categories were identified, including rural and urban settlements, monocrop, double-crop, and triple-crop agricultural land, aquaculture, water bodies, mangroves, rivers/streams, creeks, barren land, and mudflats. Training samples were selected from satellite imagery using field observations and high-resolution Google Earth imagery to facilitate classification. To refine the results, a majority spatial filter with a 3 × 3 kernel size was applied to each classified image to eliminate isolated pixels. The classification

accuracy was evaluated for all three images, and transformation matrices were generated to assess LULC changes between 2000–2011 and 2011–2020.

4.1.3 Crop classification

In the SBR three times cropping such as Kharif (mid-July to end of November), Rabi (December to March), and Rabi summer (April to mid-June) are reported during different seasons. Of the three times cropping, Kharif cultivation is the most predominant due to the availability of irrigation water during the summer monsoon. However, two other cropping are also observed in some parts of the SBR where irrigation water is available. In order to classify the single-crop (only Kharif cultivation), double-crop (two times cropping), and triple-crop (three times cropping) agricultural lands, some other satellite data were considered in addition to the data used for LULC classification. Detail of the satellite data used for crop classification has been shown in Table 3**.** Atmospheric corrections and other processing of the satellite data followed the same methodology of LULC classification. Crop and non-crop areas were identified on Rabi and Rabi-summer images using the maximum-likelihood classification method. The classified crop images of rabi and rabi-summer were integrated on the LULC layer. It was considered that Kharif cultivation was common for all the agricultural lands as it could not be classified due to the unavailability of cloud-free satellite images during the summer monsoon.

Table 3 Data Used for crop classification

Kharif- (Mid-July to Mid-November)	**Rabi- (December to April)**	**Rabi Summer/Pre-monsoon- (End of March to Mid-June)**
6/09/2000	26/01/2000	17/05/2000
	11/02/2000	
	27/12/2000	
	12/01/2001	
	17/03/2001	26/04/2001(ETM+)
	26/12/2010	11/04/2010
	21/01/2010	10/6/2011
	24/01/2011	
	25/02/2011	
	13/03/2011	

	30/01/2019	6/05/2019
	30/3/2019	
	19/03/2019	
	01/01/2020	06/04/2020
	17/01/2020	
	02/02/2020	

4.1.4 Accuracy assessment

Accuracy assessment is a crucial step in evaluating the reliability of land use/land cover (LULC) classification, ensuring that classified results align with actual ground conditions. This study assesses the accuracy of LULC classifications derived from Landsat 5 TM (2000, 2011) and Landsat 8 OLI (2020) images, covering the Sundarbans Biosphere Reserve (SBR). The assessment was based on overall accuracy, producer's accuracy, user's accuracy, and kappa statistics, generated from error matrices for each classification year.

The accuracy metrics were derived from a confusion matrix, and the following equations were used:

$$\text{Producer Accuracy} = \frac{Number\ of\ correct\ plot\ in\ collumn}{Number\ of\ total\ plot\ in\ collumn} \times 100$$

$$\text{User Accuracy} = \frac{Number\ of\ correct\ plot\ in\ row}{Number\ of\ total\ plot\ in\ row} \times 100$$

$$\text{Total (Overall) Accuracy} = \frac{Number\ of\ correct\ plot}{Number\ of\ total\ plot} \times 100$$

$$K = \frac{N \sum_{i=1}^{r} x_{ii} - \sum_{i=1}^{r} (x_{i+} \times x_{+i})}{N^2 - \sum_{i=1}^{r} (x_{i+} \times x_{+i})}$$

Where, r = number of rows in cross classification table

x_{ii} = number of combinations along diagonal

x_{i+} = total observation in row i

x_{+i} = total observation in column i

N = total number of cells

4.1.5 Generation of Scenario-wise transition probability matrix:

For each of the four scenarios, four custom transition probability matrix were generated in accordance with the story-line. The default Markovian transition probability matrix generated by the model was used for the BAU scenario. For the other three custom scenario, Linear programming (LP) approach was taken to optimize land allocation of each land-use category and recalculate the transition probability matrix. Simplex LP in Solver, an extension of Microsoft Excel, was utilized for solving the optimization problem. For each of the three custom scenarios, hypothetical total land demand of each land-use category was calculated based on story-line. Then these values were optimized by solving linear programming (LP) problem. Linear programming (LP) is a mathematical technique to perform optimization and widely used for solving a decision-making problem. It helps to depict complex relationship through few simple linear assumptions. Linear Programming Problem is a system of finding the optimal value (maximum or minimum value) of a linear function (called objective function) of any variables, subject to the conditions that the variables are non-negative and satisfy a set of linear inequalities or equality defining limitations on decisions (called linear constraints). A typical LP problem can be denoted as Max or Min of objective function

$$f(x, y) = ax + by$$

subject to the conditions $x \geq 0, y \geq 0$ and where a, b represents the constraints. Though widely used in a number of business problems, there are fewer studies (Hashimoto et al. 2018, DasGupta et.al. 2019) where LP based approach has been used to calculate optimal transition probability matrix for custom scenario-based land-use projection.

The transition probability matrix, is simply a square matrix having the probability of conversion of land use categories from i to j. In this study Markov Chain Analysis module has been used to compute the transition probability matrix of BAU scenario which is in turn used for land change prediction. To compute the custom transition probability matrix according to each of the three scenario-based future projections, first the hypothetical total future land demand of each land-use category was defined proportionate with the story-line. For our problem, the objective function can be defined as,

$$f = \sum_{i=1}^{n} \sum_{j=1}^{n} x_{ij} w_{ij}$$

where x_{ij} is the amount of land (in sq. km.) to be transited from landuse category i to j and w_{ij} is an arbitrary weightage factor (unitless) that essentially dictates the suitability of conversion

of land use category from i to j. The weightage factors were decided for each of the three scenarios, based on existing land use conversion trends in the region, expert knowledge, stake-holder consultations, household survey and government policy decisions through brain-storming sessions, in accordance with the story-line. For each scenario, a weightage matrix (w_{ij}) were defined such that each of the land use transitions was given an arbitrary weightage factor ranging from 0 to 3, where '0' denotes an unsuitable/illogical land conversion and '3' denotes high suitable/favourable land conversion. For our problem, the linear constraint is defined by the fact that the total land area is conserved in both the time steps when subjectd to the hypothetical land allocation for each land use category.

Thus the objective function $f = \sum_{i=1}^{n} \sum_{j=1}^{n} x_{ij} w_{ij}$ was maximized in Excel-Solver using Simplex LP as solving method, subjected to $\sum_{j=1}^{n} x_{ij} = L_{i,200}$ for i = 1, 2,…, n and $\sum_{i=1}^{n} x_{ji} = L_{j,2030}$ for j = 1, 2,…, n, where L_i and L_j, denote the total area (sq. km) of land use category i and j. The optimized matrix thus derived were in turn converted to a new customized transition probability matrix for each scenario which were subsequently used for change allocation based on a multi-objective land allocation (MOLA) algorithm.

4.2 Land Use Change Allocation using Cellular Automata-Markov (CA-Markov) model

The CA-Markov model is a widely used technique for predicting future land use/land cover (LULC) patterns by analysing past spatiotemporal trends (Weng, 2002; Regmi et al., 2014; Nouri et al., 2014). It integrates the Cellular Automata (CA) technique with Markov chain analysis and the Multi-Criteria/Multi-Objective Land Allocation (MOLA) algorithm (Eastman et al., 1998). This model leverages the CA approach to capture spatial variations in complex systems while utilizing the Markov model's ability to forecast long-term transitions.

The Markov chain model represents a system where a given state, S = {S_0, S_1, S_2, …, S_n}, transitions from state S_i to state S_j in the next step based on transition probabilities (P_{ij}). The future state S(t+1) is determined from the previous state S(t) using the following equation (Mondal et al., 2017):

$$S(t+1) = S(t) \times P_{ij}$$

In this study, Markov chain analysis was conducted for two time periods: 2011–2020 and 2020–2030. This process generated a land use area transfer matrix and a transition probability matrix. Using these probabilities and suitability assessments for each pixel, the Multi-Criteria

Evaluation (MCE) method, in conjunction with MOLA, allocated land from existing categories to other classes until the demand for each LULC type was met.

The probability maps derived from Markov chain analysis were then utilized as inputs for the CA model to simulate future LULC distributions. The Cellular Automata component incorporated a kernel function that reduces the suitability of pixels farther from existing instances of a particular land cover type. This ensures that for a pixel to be selected for conversion, it must be both spatially suitable and in proximity to existing areas of that category.

The LULC prediction model was implemented using the TerrSet Geospatial Monitoring and Modelling System framework.

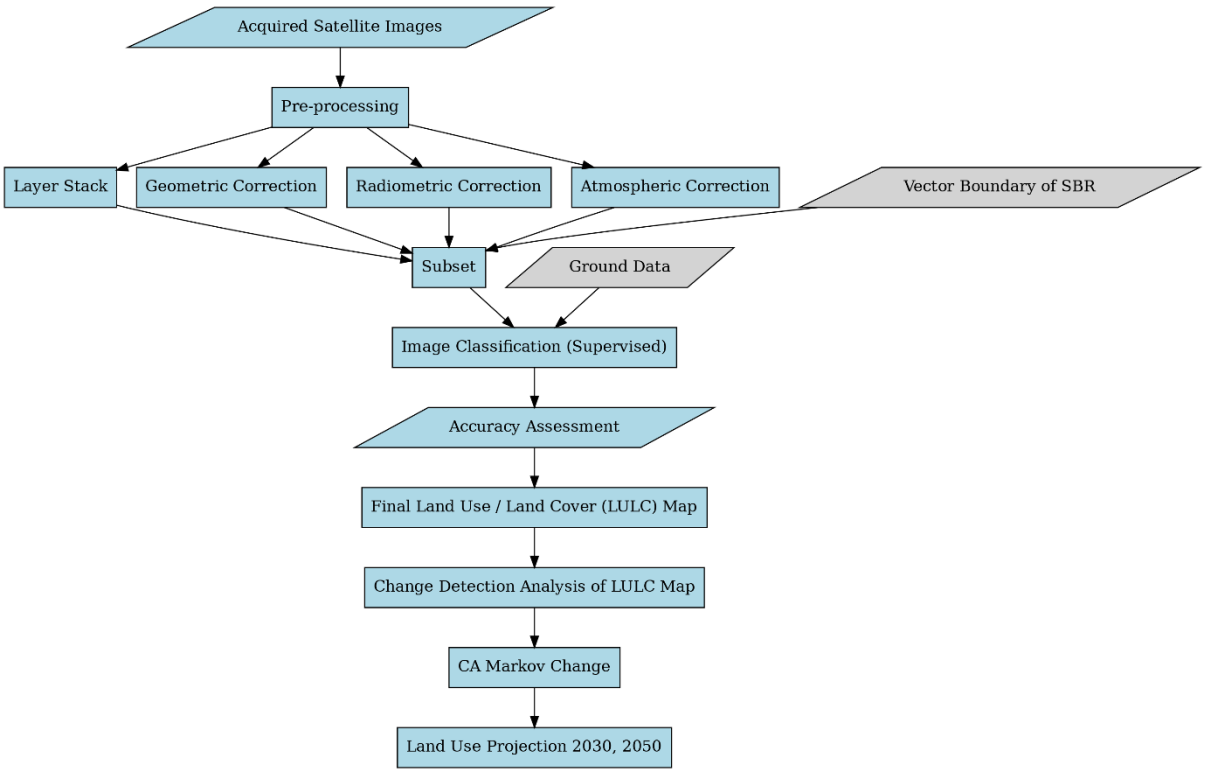

Figure 2 Methodology for land use / land cover change and LULC projection

4.3 Mangrove change Methodology

The analysis considers (1) mangrove extent and associated losses and gains, (2) mangrove species composition and (3) indicators of mangrove health. The details are explained below.

4.3.1 Mangrove extent

To assess the extent of mangroves, an initial classification was conducted based on key land cover categories using winter-season Landsat imagery. Landsat TM images with a 30-meter

resolution were used for the years 2000, 2005, and 2010, while Landsat 8 OLI images were analyzed for 2015 and 2020. These datasets were sourced from the USGS Earth Explorer platform (https://earthexplorer.usgs.gov/). The classification process focused on distinguishing mangroves and adjacent land cover types within the Sundarbans Biosphere Reserve (SBR). Four primary land use/land cover (LULC) classes were identified: river, mangrove, mudflat, and saline blanks. The study area was covered by two Landsat scenes, corresponding to path/row 138/44 and 138/45. To enhance data accuracy, radiometric calibration and atmospheric correction were applied to mitigate atmospheric distortions and scattering effects. The images were then classified using a maximum likelihood supervised classification technique. Training samples were carefully selected based on field observations and high-resolution Google Earth imagery to improve classification precision.

4.3.2 Mangrove Species Classification

Mangrove species classification was conducted using Landsat-5 imagery for the year 2000 and Landsat 8 OLI data for 2020. To correct atmospheric distortions and enhance image accuracy, radiometric calibration and atmospheric correction were applied using the FLAASH algorithm in ENVI. This algorithm utilizes the MODTRAN4 radiation transfer model to estimate radiance at the sensor based on surface reflectance (Wang et al., 2018).

For species classification, two Landsat 8 OLI scenes were mosaicked, and a subset was extracted using the mangrove class derived from the previously classified image. A maximum likelihood supervised classification (MLSC) method was employed for species identification. The MLSC algorithm applies the Bayesian equation to calculate the weighted distance or likelihood of an unknown measurement vector belonging to a specific class (Giri et al., 2014; Ghosh et al., 2016).

Training points for classification were selected based on field observations, prior knowledge of researchers, and existing literature (Manna & Raychaudhuri, 2020; Giri et al., 2014; Ghosh et al., 2016; Mitra & Karmakar, 2010; Kumar et al., 2019; Mukhopadhyay et al., 2018; Hati et al., 2021).

4.3.3 Mangrove Health Indicators

To assess mangrove health, datasets from both MODIS (250 m resolution) and Landsat TM (30 m resolution) were utilized. MODIS data were chosen for their higher temporal resolution (every 16 days, year-round), while Landsat images provided better spatial resolution. To ensure

continuous year-long data coverage, the Terra MODIS Vegetation Indices Version 6 (MOD13Q1) product was used (Didan, 2015; AppEEARS Team, 2020). This product includes two key vegetation index (VI) layers: Normalized Difference Vegetation Index (NDVI) and Enhanced Vegetation Index (EVI), generated at a 250-meter resolution with a 16-day temporal interval. MOD13Q1 data from 2000 to 2019 were downloaded, and the VI layers were filtered using the Pixel Reliability layer to retain only high-quality pixels.

Since year-round high-resolution multispectral data were unavailable, only winter-season data were used, as mangroves typically exhibit their best health during this period. Landsat TM, ETM+, and OLI imagery from 2000 to 2020 was radiometrically corrected in ENVI software using the FLAASH atmospheric correction tool. Cloud masking was performed using the Quality Assessment (QA) band provided by USGS in each Landsat product.

All NDVI and EVI raster datasets (Pastor-Guzman et al., 2018; Kovács & Gulácsi, 2019) were normalized, and a winter seasonal average was generated. To analyze temporal trends in vegetation indices, the Mann-Kendall statistical method was applied (Neeti & Eastman, 2011).

4.3.4 Temperature and Rainfall Estimation

Daily maximum and minimum temperature and rainfall data were obtained from the India Meteorological Department (IMD) for the period 2000–2019 (http://www.imdpune.gov.in/Clim_Pred_LRF_New/Grided_Data_Download.html). The gridded temperature data have a spatial resolution of 0.25 degrees, while the rainfall data are available at a 1.0-degree resolution.

4.3.5 Correlating Climatic variability with vegetation health

To facilitate analysis, climate data were resampled to match the 250 m spatial resolution of MODIS vegetation index (VI) data. A time series was then constructed by aggregating the 16-day VI dataset and daily climate variables into monthly and subsequently seasonal averages—classified as winter (DJF), summer (MAM), monsoon (JJA), and post-monsoon (SON). These aggregated datasets were used for trend analysis and linear modelling.

A pixel-based time-series trend analysis was conducted using the Mann-Kendall non-parametric test to identify increasing or decreasing trends in vegetation activity (Neeti & Eastman, 2011). The relationships between vegetation indices (VI) and climatic factors (maximum and minimum temperature and rainfall) were examined through multiple regression analysis at different time lags. In this context, Lag 0 indicates a direct comparison of dependent

and independent variables at the same time step, while a negative lag shifts the independent variable to an earlier time period, allowing an assessment of delayed climate impacts on vegetation health.

4.3.6 Estimating Cyclone Impact on Mangroves

4.3.6.1 Canopy density

To assess changes in forest canopy density before and after Cyclones Bulbul and Amphan, Landsat OLI images were analysed. Forest Canopy Density (FCD) serves as a key indicator of forest condition and is crucial for evaluating cyclone-induced damage and overall forest health deterioration. The FCD model is based on bio-spectral modelling and analysis, incorporating four indices: Advanced Vegetation Index (AVI), Bare Soil Index (BI), Shadow Index (SI/SSI), and Thermal Index (TI) (Sahana et al., 2015; Rikimaru, 2002). The percentage of canopy density was computed for each pixel using this method.

4.3.6.2 Enhanced Vegetation Index (EVI)

To further assess vegetation health changes, EVI was calculated using atmospherically corrected Landsat OLI images from pre- and post-cyclone periods. The calculation followed Huete et al. (2002) using the formula (Equation 1):

EVI = 2.5 * ((Band 5 – Band 4) / (Band 5 + 6 * Band 4 – 7.5 * Band 2 + 1))
……Equation 1

EVI values range from -1 to +1, where higher values indicate healthier vegetation. The pre- and post-cyclone EVI raster values were normalized and differenced to detect changes. The resulting image was classified into positive and negative values, with positive values indicating vegetation health improvement and negative values representing vegetation loss due to cyclone impact.

4.4 Mangrove Future

4.4.1 SLAMM overview

SLAMM version 6.7 (Warren Pinnacle Consulting, 2016) was chosen on account of its simplicity and minimal data requirements, while acknowledging its limited physical basis. SLAMM was first developed in the mid-1980s to simulate coastal habitat transitions and associated land loss due to SLR at broad spatial scales. It is essentially a kinematic model that neglects any constraint imposed by a sediment budget and simply considers the balance between inundation and vertical accretion in each cell of a raster digital elevation model

(DEM). A decision tree allows transitions to occur between habitat types, for example, if the elevation of a cell declines below a minimum required elevation for the existing habitat in that cell. Vertical accretion can be specified as a constant rate, or as a non-linear function of the cell elevation within the tidal frame (Clough et al., 2010, Li et al., 2015). Selected DEM cells can be masked to represent dry land or land that is protected from inundation by dikes. Land loss due to erosion can also be simulated for both fetch-limited and open coastal situations using algorithms of varying sophistication, depending on the availability of bathymetric and wind climate data and observational erosion data for calibration.

The principal model inputs are a DEM of suitable accuracy and spatial resolution and a set of similarly dimensioned raster layers describing the topographic slope, land cover and wetland habitat class (Figure 5). Wetland habitats are defined using the US National Wetlands Inventory (NWI) classification, which is developed for North America and requires some adjustment for application in the Sundarbans region. SLAMM also requires specification of the vertical tidal frame in terms of a Great Diurnal Tide Range (GDTR), and parameter values for the selected accretion and erosion sub-models.

4.4.2 Raster input layers

4.4.2.1 DEM and slope

A DEM with high vertical accuracy and spatial resolution is required to achieve meaningful results in SLAMM. Airborne lidar data are not presently available for the Sundarbans, and therefore, a range of satellite-derived DEM products (SRTM) (Farr et al., 2007), TanDEM (Rizzoli et al., 2017), CoastalDEM (Kulp and Strauss, 2018) were evaluated. These were compared to a ground surveyed DEM constructed from point-based elevation data (2276 points) acquired on Mousuni Island, West Bengal, using a micro-optic theodolite on a 100 x 100 m grid. Elevations were referenced to a Survey of India permanent benchmark at the former Collectorate building in the centre part of the island and GPS was used to determine the point locations. For comparison with the satellite-derived products, the surveyed DEM was interpolated to a resolution of 90 x 90 m using inverse distance weighting. CoastalDEM showed the best agreement to the survey elevation data (Figure 3) and was selected for the SLAMM analysis. The spatial resolution of CoastalDEM is 3 arc seconds (~90 m) and its vertical uncertainty is estimated as < 1 m. Figure 4 a, b shows the resulting DEM and a derived topographic slope raster layer generated using the slope tool in ArcGIS 10.5.

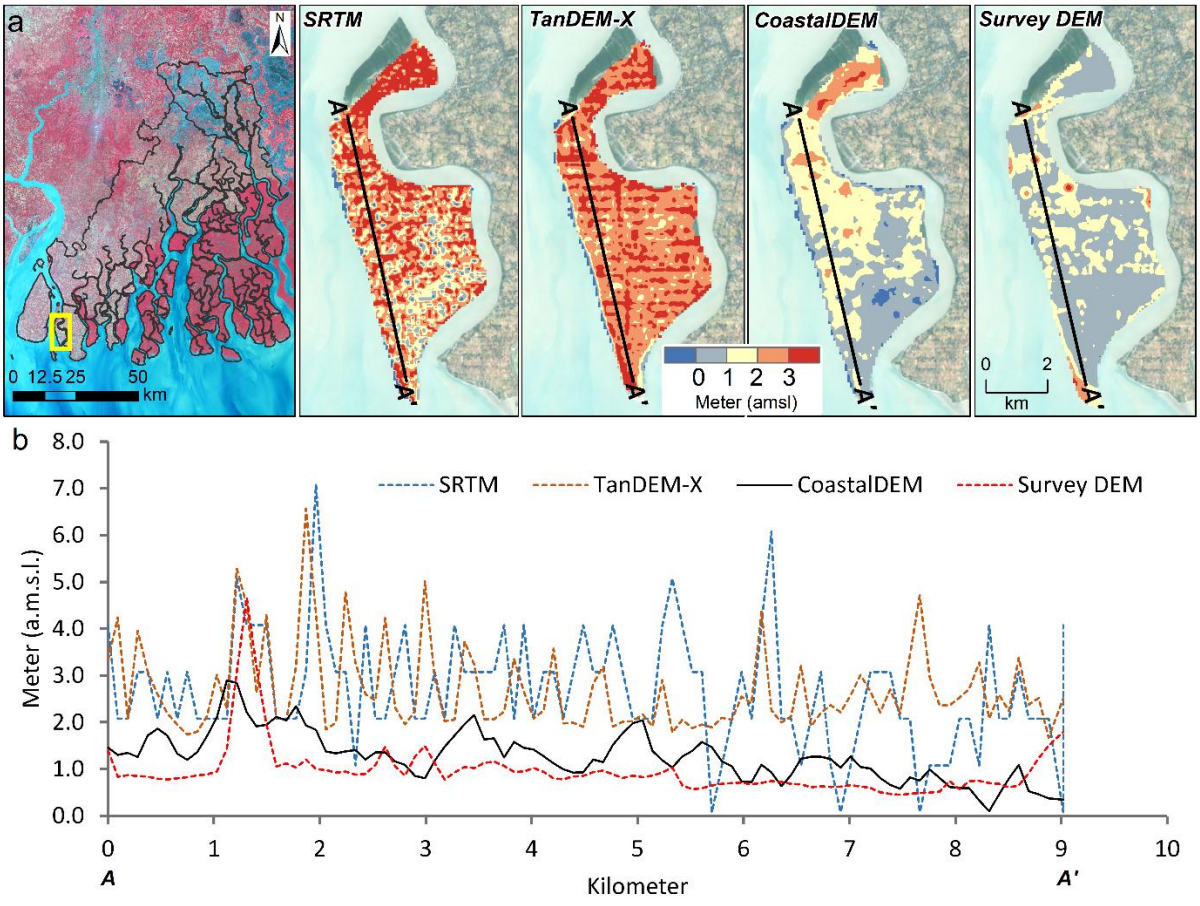

Figure 3 Comparison of ground-surveyed elevations with CoastalDEM, SRTM, and TanDEM datasets at Mousuni Island: a) A map indicating the survey transect location.b) An elevation comparison between surveyed data and DEM products along transect A-A'.

4.4.2.2 Wetland habitat layer

A land use/land cover (LULC) map was generated (Figure 4d) using Landsat-TM data from 2001. The US NWI classification is embedded within the SLAMM 6.7 program code and this is not directly applicable to the range of habitats found in the Sundarbans. Accordingly, LULC classes were adjusted to use the nearest NWI classes. For example, the 'urban settlement' class was assigned to 'developed dry land', rural settlement-crop and-barren land was assigned to undeveloped dry land, Aquaculture was assigned to transitional salt marsh, saline blank to regularly flooded marsh, water bodies to inland open water, and river and creek was represented by estuarine open water.

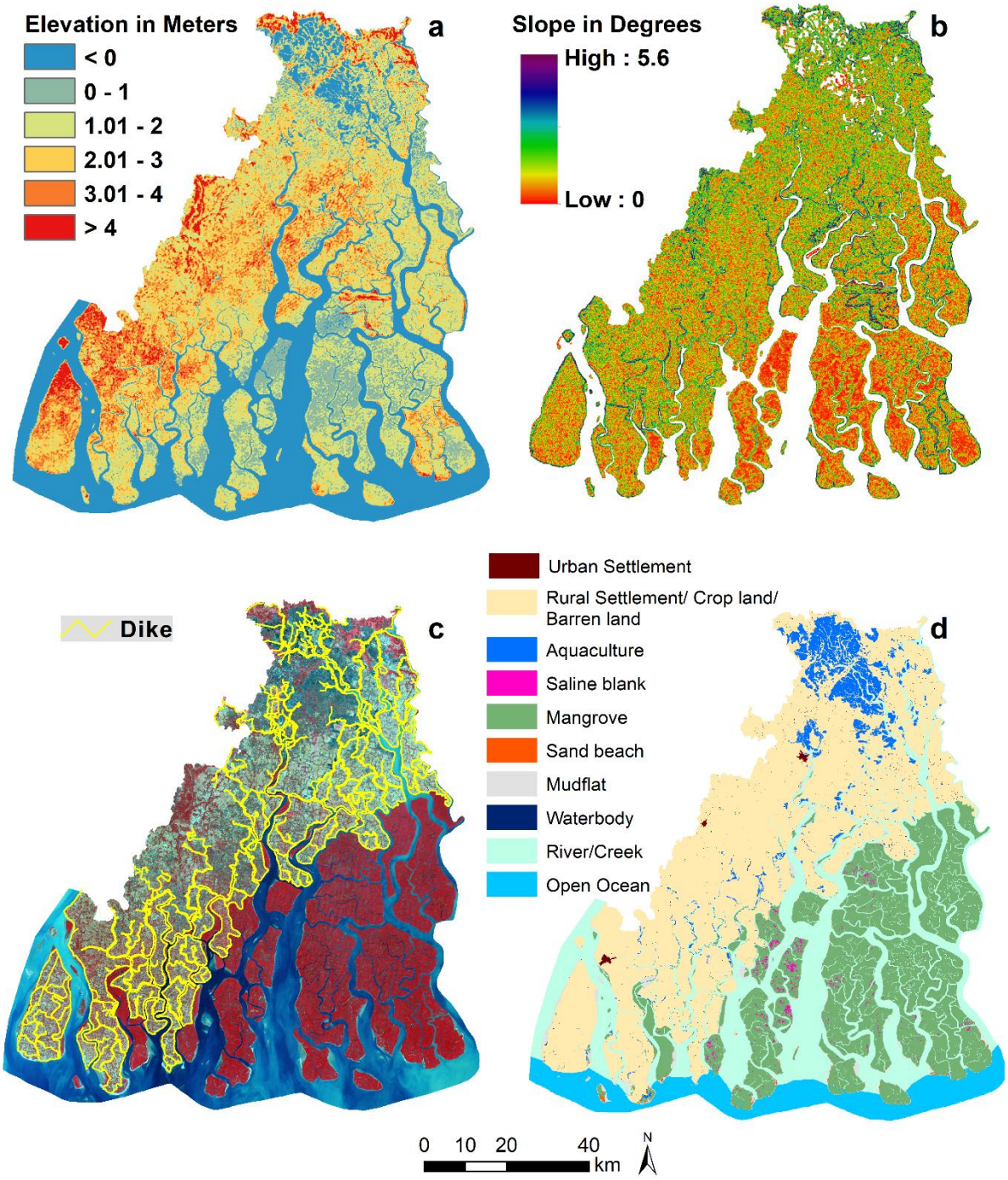

Figure 4 Key input layers for SLAMM simulations: a) Elevation derived from the CoastalDEM dataset.b) Topographic slope. c) Presence of dikes.d) Land use and land cover.

4.4.2.3 Subsidence layer

Stanley and Hait (2000) estimated a maximum subsidence of 5.0 mm yr-1 in the Indian Sundarbans based on geological evidence. Brown and Nicholls (2015) conducted a more systematic review of land subsidence rates across the Ganges–Brahmaputra–Meghna delta,

using 205 data points derived from a range of methods and timescales. The Sundarbans showed the lowest mean (2.8 mm yr-1) and median (2.0 mm yr-1) rates of net subsidence compared with other land uses in the delta. Payo et al. (2016) used a net subsidence rate of 2.5 mm yr-1 in their SLAMM simulations of the Bangladesh Sundarbans and made the reasonable assumption that subsidence is linear over short geological (decadal to centennial) timescales. In the present study we similarly use a uniform subsidence rate of 2.5 mm yr-1 for the entire SBR and assume that this remains constant to 2100.

4.4.2.4 Flood defence (dike) layer

The location of dikes and polders are key to understand where mangroves can or cannot exist. A flood defence (dike) layer (Figure 4c) was generated by on-screen digitization in Google Earth. The resulting KML file was converted to a raster of the same dimensions as all the other inputs. An arbitrary crest elevation of 5 m was assigned to all dike pixels to ensure that protected areas remained dry for all the SLR scenarios considered.

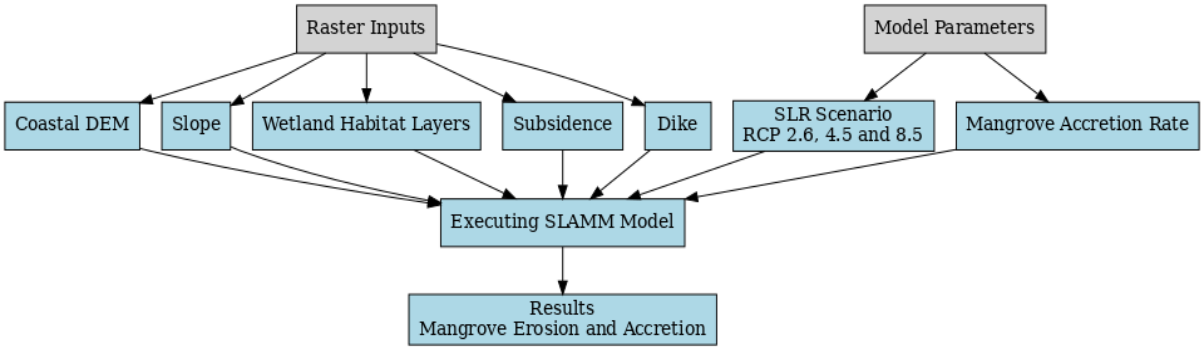

Figure 5 Methodology for SLAMM model

4.4.3 Model parameters

Tidal range varies at multiple time scales (including fortnightly spring-neap, seasonal, interannual and 18.6-year nodal tide variation) and spatially along and between the estuarine distributaries. SLAMM does not accommodate time-variation in the tidal range and tide gauges are too limited to define the spatial variation. Based on analysis of the available tidal records, a time- and space-average Great Diurnal Tidal Range (GDTR) of 3.5 m was therefore used in all simulations.

Vertical sediment accretion is an important process and there is a general consensus that tidal marshes and mangroves have some resilience to SLR such that increased inundation is at least partially compensated for by enhanced accretion (French, 2006; Woodroffe et al., 2016). Accretion, measured by sediment deposition above a surface (or near-surface marker), does not

translate directly into elevation gain since it is subject to various shallow subsidence/expansion processes (Cahoon and Lynch, 1997; Krauss et al, 2014). SLAMM does not resolve this level of detail and the term accretion is used here to refer to the net elevation change resulting from sedimentation. Insufficient data exist to define an empirical accretion model for the Sundarban mangroves. The sparse data that do exist come mainly from multi-decadal sediment cores. Banajee et al (2012) obtained accretion rates of 3.0 to 4.8 mm yr-1 from 210Pb-dated cores at three Sundarbans mangrove sites. These rates are broadly consistent with 14C based accretion of 2.0 to 5.0 mm yr-1 estimated by Stanley and Hait (2000). The implication is that over the last few centuries at least, mangrove elevations were able to keep pace with relative SLR that was probably dominated by delta subsidence and a slow eustatic rise.

Given that higher sedimentation rates are generally localised around estuary channel margins and interior rates tend to be lower, it is reasonable to use the lower end of reported ranges (i.e. around 3.0 mm yr-1) as a regional average. Modelling has demonstrated that wetland response to SLR is likely to be constrained by sediment supply (French, 2006; Kirwan et al 2010), and a global analysis by Saintilian et al. (2020) indicates that mangroves may be unable sustain their elevations when SLR exceeds about 6 mm yr-1. In the present study, we use a baseline mangrove accretion rate of 3.0 mm yr-1, which is consistent with the present evidence that mangrove elevations are currently not quite keeping pace with relative SLR (Samanta et al., 2021). We also simulate a higher rate of 6.0 mm yr-1 to approximate the upper threshold of Saintilian et al (2020) in the sediment-limited context of the Indian Sundarbans.

4.4.4 Data-driven modelling of coastal land loss due to erosion

The SLAMM 6.7 routines for fetch and depth limited wind wave erosion require too much data for application to the Sundarbans estuaries, and its prediction of open coast shoreline erosion routine based on the Bruun (1962) model in which retreat is fixed at 100 x SLR is too generic. Accordingly, a separate data-driven model was devised to predict shoreline retreat as a function of SLR. This uses the earlier results of Samanta et al. (2021), who analysed shoreline changes along the open coast and larger estuary mouth regions in relation to mean sea level variations for a series of 5-year time epochs between 1990 and 2020. Their results showed that, in the low-lying delta plain environment of the Sundarbans, SLR appears to drive much more rapid shoreline retreat (up to five times the standard Bruun approximation). By the end of 21st century, present retreat rates of up to about 38 m yr-1 are projected to increase to up to about 180 m yr-1.

4.4.5 SLR scenarios

Three realistic non-linear climate-induced SLR scenarios based on IPCC (2019) (Table 4) were adopted from Nicholls et al. (2021). The high end of the likely ranges for RCP2.6 (low), RCP4.5 (moderate) and RCP8.5 (high) emission scenarios are used, giving a eustatic SLR of 0.59 m, 0.72 m and 1.1 m by 2100.

Table 4 Climate-induced eustatic SLR scenarios used in this study (derived from Nicholls et al., 2021).

	RCP2.6(m)	**RCP4.5(m)**	**RCP8.5(m)**
1995	0.00	0.00	0.00
2025	0.15	0.15	0.15
2055	0.32	0.35	0.38
2085	0.50	0.59	0.82
2100	0.59	0.72	1.10

4.4.6 Management scenarios

Simulations were performed for two management scenarios - 'Continued Protection' and 'Managed Realignment' (table -5). In the Continued Protection scenario, it is assumed that all existing protective dikes are maintained (with any implied increases in crest elevation). This restricts the ability of mangroves to migrate inland over the inhabited areas within the Biosphere Reserve.

Under the 'Managed Realignment' scenario, it is assumed that all the existing protective dikes are removed, thereby creating additional accommodation space for the migration of mangrove inland. This would clearly affect presently inhabited areas, necessitating a relocation of people and activities which are also evaluated.

Table 2 summarises all of the model runs. Only a selection of the full range of outputs are visualised in the following Results section; the remaining results are provided in the Supplementary Materials for this paper.

Table 5 Summary of the model runs and the scenario assumptions.

Run ID	**SLR forcing scenario**	**Mangrove accretion rate (mm yr-1)**	**Land loss due to erosion**	**Management scenario**

1	RCP2.6	3	included	Continued Protection
2	RCP4.5	3	included	Continued Protection
3	RCP8.5	3	included	Continued Protection
4	RCP2.6	6	included	Continued Protection
5	RCP4.5	6	included	Continued Protection
6	RCP8.5	6	included	Continued Protection
7	RCP2.6	3	included	Realignment
8	RCP4.5	3	included	Realignment
9	RCP8.5	3	included	Realignment
10	RCP2.6	6	included	Realignment
11	RCP4.5	6	included	Realignment
12	RCP8.5	6	included	Realignment

Chapter-5

5. Results

5.1 Analysis of LULC transformation within the last two decades

5.1.1 Land use Change between 2000-2010:

The land-use analysis between 2000 and 2010 reveals significant shifts driven by agricultural intensification, urbanization, and environmental changes, with several categories showing notable increases or declines. Aquaculture grew by 8.6% (343.1 km^2 to 372.7 km^2), reflecting the rising demand for seafood, while brick kiln areas saw a sharp 195.2% increase (4.2 km^2 to 12.4 km^2), indicative of rapid urbanization and construction. Double cropping expanded by 47.7% (318.6 km^2 to 470.5 km^2), and triple cropping by 77.3% (29.9 km^2 to 53 km^2), suggesting a shift toward more intensive farming practices, while single crop areas decreased by 15.9% (2682.3 km^2 to 2254.8 km^2), likely due to land-use conversion or diversification into multi-cropping systems. Rural settlements grew by 38.4% (610.2 km^2 to 844.4 km^2), and urban settlements by 26.1% (9.2 km^2 to 11.6 km^2), driven by population growth and infrastructure expansion. Environmental degradation is evident from the 53% decline in mud flats (166.5 km^2 to 78.3 km^2), the 19% loss in wetlands (2.1 km^2 to 1.7 km^2), and the 3.4% decrease in mangrove areas (2072.4 km^2 to 2002.6 km^2). Meanwhile, saline blank areas increased by 121.4% (37.3 km^2 to 82.6 km^2), suggesting rising salinity issues, and waterbody coverage grew by 34.9% (21.2 km^2 to 28.6 km^2), likely reflecting improved water management. Barren land rose by 29.7% (9.1 km^2 to 11.8 km^2), and sandy areas increased by 20.3% (7.4 km^2 to 8.9 km^2), hinting at land-use shifts or environmental pressures. River/stream areas remained relatively stable with a 3.1% increase (2543.7 km^2 to 2623.4 km^2), reflecting effective conservation. These trends highlight a complex interplay between development, agricultural practices, and environmental changes, demonstrating a clear shift toward economic growth and agricultural optimization, but also signalling the need for sustainable land management to mitigate environmental degradation and ensure ecological resilience (Figure 6 and Table 6).

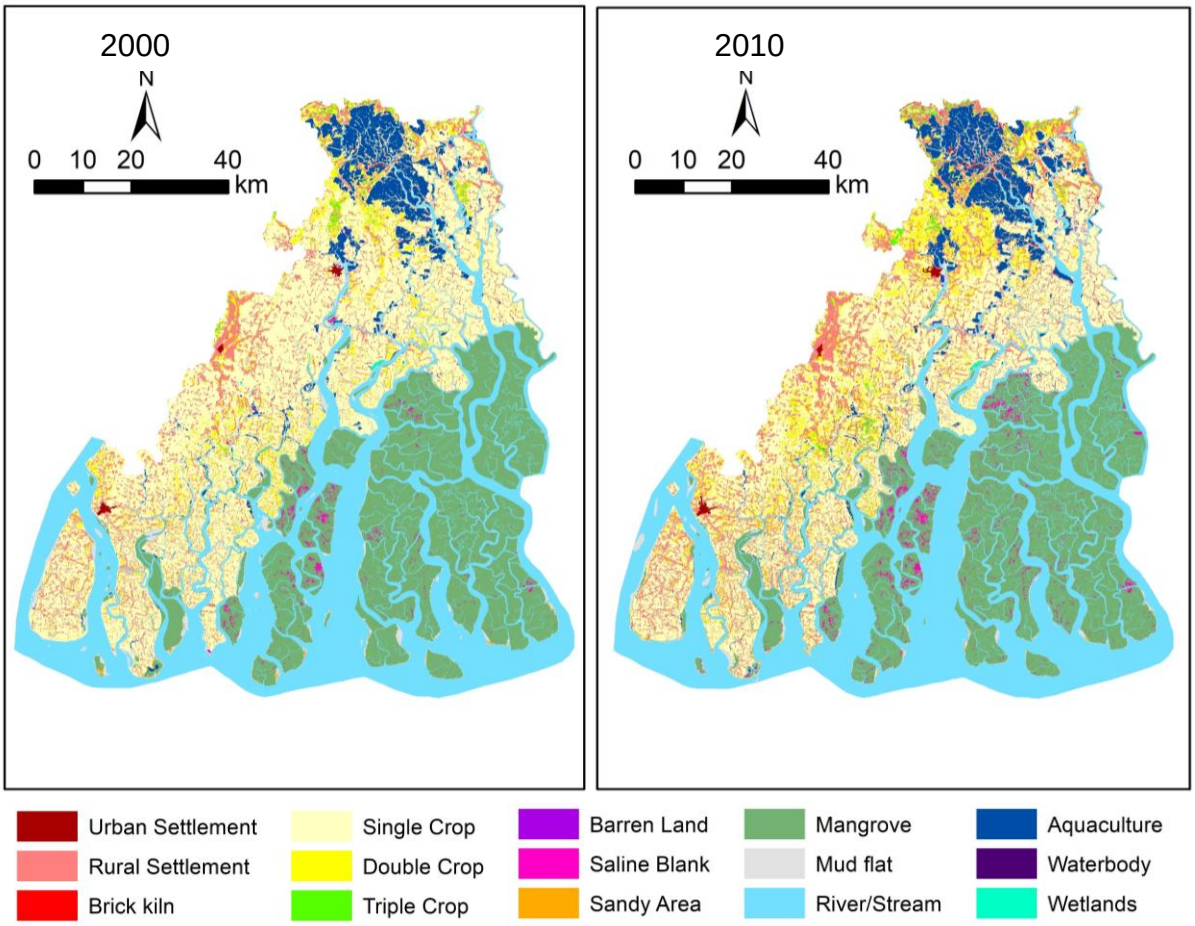

Figure 6 Land use / land cover change between 2000-2010 in Sundarbans Biosphere Reserve

5.1.2 Land use Change between 2010-2020:

The land-use analysis between 2010 and 2020 highlights significant changes driven by agricultural intensification, urbanization, and environmental shifts. Aquaculture expanded by 37.1% (372.7 km^2 to 510.8 km^2), reflecting growing market demand, while brick kiln areas increased by 57.3% (12.4 km^2 to 19.5 km^2), indicating continued urbanization and construction. Double-cropped areas grew by 28.3% (470.5 km^2 to 603.6 km^2), and rural settlements expanded by 36.1% (844.4 km^2 to 1149.2 km^2), reflecting population growth and agricultural development. In contrast, single-cropped areas declined by 28.2% (2254.8 km^2 to 1618.8 km^2), suggesting a shift toward diversified or intensive cropping. Urban settlements grew significantly by 64.7% (11.6 km^2 to 19.1km^2), driven by infrastructure expansion, while waterbody coverage increased by 15.7% (28.6 km^2 to 33.1 km^2), likely due to better water management. Environmental changes are evident, with mud flats increasing by 23.9% (78.3 km^2 to 97 km^2) and saline areas rising by 24.9% (82.6 km^2 to 103.2 km^2), potentially due to sediment changes or seawater intrusion. However, wetlands shrank by 47.1% (1.7 km^2 to 0.9 km^2), and mangrove areas experienced a slight decline of 0.5% (2002.6 km^2 to 1991.7 km^2),

indicating ecological degradation. Sandy areas decreased by 12.4% (8.9 km^2 to 7.8 km^2), likely due to land-use conversion. River and stream areas remained stable, with a marginal increase of 0.4% (2623.4 km^2 to 2633.3 km^2), reflecting consistent water flow. These trends suggest rapid development and agricultural optimization but highlight the need for sustainable practices to mitigate environmental degradation and promote ecological balance (Figure 7 and Table 7).

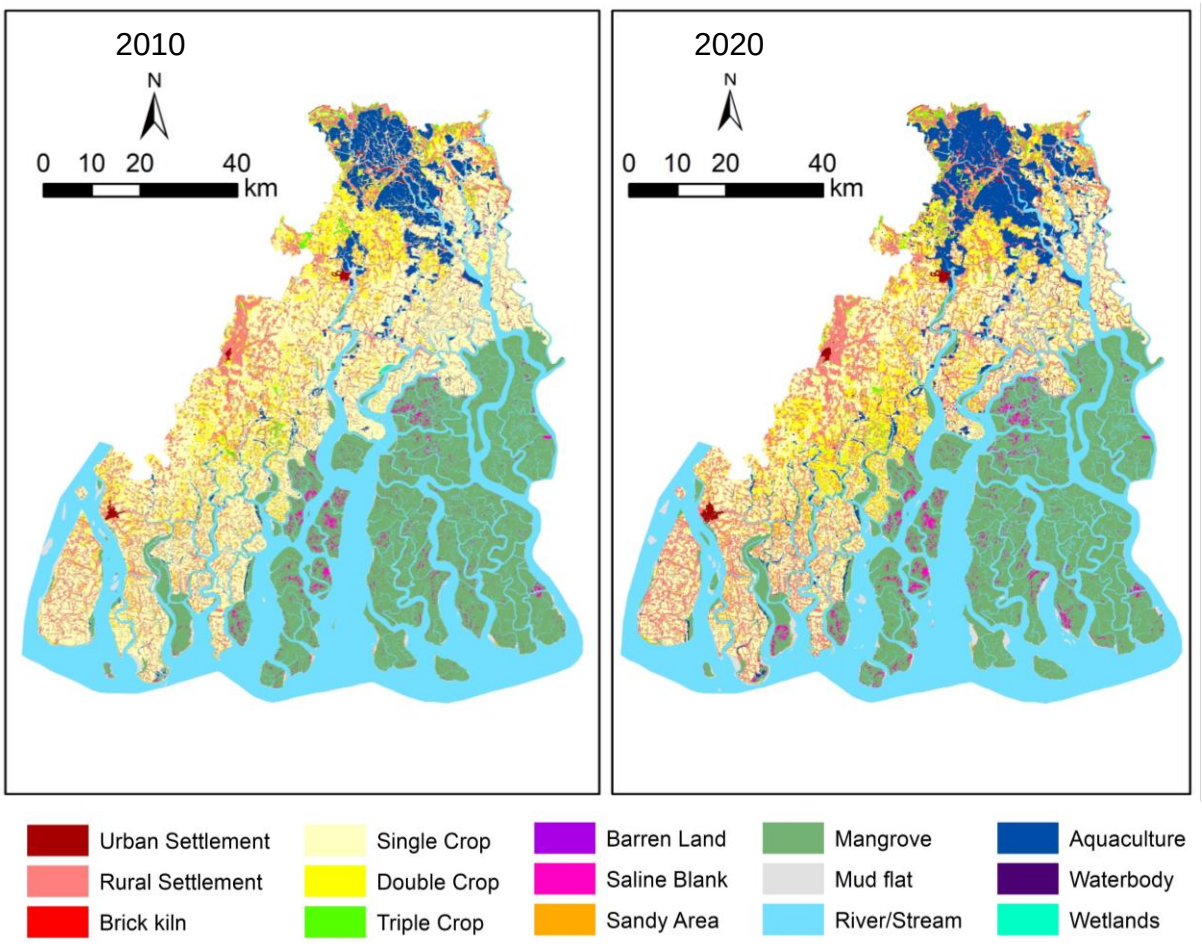

Figure 7 Land use and land cover change between 2010-2020 in Sundarbans Biosphere Reserve

The transformation among twelve LULC classes during the last two decades (2000 – 2010 and 2010 – 2020) has been portrayed in Tables 6 and 7, respectively. Of the twelve LULC classes, only single crop areas have been observed to get transformed to all other land use. The maximum transformation was observed to double-crop (322 km^2) followed by rural settlement (191 km^2), aquaculture (33 km^2), and triple crop (20 km^2) which account for 12.22%, 7.25%, 1.24%, and 0.75% of the total single crop area, respectively during 2000 to 2010. This transformation pattern was similar from 2010 to 2020; however, a noticeable amount of single crop areas (108 km^2) was also transformed into aquaculture. Overall, from 2000 to 2020, a total of 1010.6 km^2 (38.4% of total single crop area) single crop areas were transformed into other

land use classes. The aquaculture area in the SBR showed a steady increase from 343 km^2 in 2000 to 511 km^2 in 2020. However, the unprecedented growth of aquaculture (80.6% of the total increase) took place from 2010 to 2020. Apart from aquaculture, double-crop and triple-crop areas also increased by 274 km^2 and 24 km^2, respectively, during the last two decades (2000 – 2020). Due to the availability of irrigation water, many single croplands could be transformed into double and triple croplands, especially in the northern blocks of the SBR.

Table 6 Land use change Matrix 2000-2010 (area in sq. km)

Class	Aquaculture	Barren Land	Brick kiln	Double Crop	Mangrove	Mud flat	River/stream	Rural Settlement	Saline Blank	Sandy Area	Single Crop	Triple Crop	Urban Settlement	Waterbody	Wetlands	2000 Grand Total
Aquaculture	323.9	2.3	4.3	0.1	0.4	1.0	0.9	0.1	0.0	0.1	9.8	0.0		0.2	0.0	**343.1**
Barren Land	2.3	0.1	0.1	0.3			0.0	0.0		0.0	6.3			0.0		**9.1**
Brick kiln		0.0	4.0			0.0				0.0	0.1			0.0		**4.2**
Double Crop	2.1	1.0	0.3	117.6	0.4	0.0	0.5	29.4		0.2	145.0	21.9	0.0	0.5		**318.6**
Mangrove	0.4	0.0		0.6	1936.0	20.3	63.7	1.6	45.8	0.7	3.1	0.2	0.0	0.0		**2072.4**
Mud flat	2.0	0.1	0.2	0.5	24.6	30.5	66.2	2.2	0.9	2.4	36.4	0.1		0.3		**166.5**
River/Stream	2.1	0.1	0.3	0.0	29.3	19.1	2470.6	1.7	3.5	0.6	16.0	0.0	0.0	0.2		**2543.7**
Rural Settlement				0.1		0.0	0.0	607.4			0.3	0.1	2.2	0.0		**610.2**
Saline Blank					4.1	0.6	0.7		31.9	0.0						**37.3**
Sandy Area	0.0				0.4	2.9	2.8		0.3	0.8	0.2					**7.4**
Single Crop	39.8	8.1	3.2	343.2	7.3	3.9	17.9	197.0	0.1	4.0	2027.1	21.5	0.5	8.8	0.0	**2682.3**
Triple Crop	0.0	0.0	0.0	8.0	0.1	0.0	0.1	4.5			8.3	8.9		0.0		**29.9**
Urban Settlement		0.0		0.0			0.0	0.1		0.0	0.1	0.0	8.9	0.1		**9.2**
Waterbody	0.1	0.0	0.0	0.2	0.0	0.0	0.0	0.3		0.1	1.7	0.3	0.0	18.5		**21.2**
Wetlands	0.0	0.0		0.0							0.4				1.7	**2.1**
2010 Grand Total	**372.7**	**11.8**	**12.4**	**470.5**	**2002.6**	**78.3**	**2623.4**	**844.4**	**82.6**	**8.9**	**2254.8**	**53.0**	**11.6**	**28.6**	**1.7**	**8857.3**

Conversely, many double crops (148.9 km2 during 2000 – 2010 and 161.1 km2 during 2010 – 2020) and triple crops (12.0 km^2 during 2000 – 2010 and 6.0 km^2 during 2010 – 2020) land also exhibited reverse transformation to single cropland due to paucity of irrigation water. A huge amount of mudflat (169.6 km^2) was observed in 2000 that subsequently got transformed into single croplands (68.2 km^2) followed by fringe mangrove forest (32 km^2) from 2000 to 2010. However, from 2010 to 2020 this conversion of mudflat to a single crop was least evident and only 29.7 sq. km of mudflat turned into the fringe mangrove forest. To accommodate the huge population, increase, rural settlement area has remarkably increased to 1160.4 km^2 in 2020 from 620.4 km^2 in 2000 mainly at the expense of single cropland followed by double cropland. Unlike rural settlement, urban settlement increased only 8.8 km^2 within the last two decades. Fringe mangrove forest was observed to increase almost at the same rate per decade (35.5 km^2 during 2000 – 2010 and 37.3 km^2 during 2010 – 2020) (Table 6 and Table 7). The natural transformation of some single croplands into rivers indicates the erosional loss, but that did not get reflected in the overall increase in river area during the last two decades, because this erosional loss was compensated by the accretional formation of mudflat in some other parts of the SBR.

Table 7 Land use change Matrix 2010-2020 (area in sq.km)

Class	Aquaculture	Barren Land	Brick kiln	Double Crop	Mangrove	Mud flat	River/stream	Rural Settlement	Saline Blank	Sandy Area	Single Crop	Triple Crop	Urban Settlement	Waterbody	Wetlands	2010Grand Total
Aquaculture	354.3	0.1	4.7	0.0	0.9	0.5	3.0	4.6	0.0	0.0	4.4	0.1	0.0	0.2	0.0	**372.8**
Barren Land	2.7	0.2	1.1	1.1	0.0	0.0	0.1	0.5		0.0	5.8	0.3	0.0	0.0		**11.8**
Brick kiln	0.3		11.4	0.0	0.0	0.0	0.3	0.1		0.0	0.2	0.0		0.0		**12.4**
Double Crop	26.5	0.7	0.2	210.0	1.4	0.1	0.4	42.9	0.0	0.0	170.0	16.9	0.7	0.6	0.0	**470.5**
Mangrove	1.4	0.0		4.2	1894.2	6.6	43.2	2.9	45.0	0.2	3.4	1.4		0.1	0.1	**2002.6**
Mud flat	2.1		0.0	0.2	21.2	24.5	22.4	0.7	3.0	1.5	2.2	0.0	0.1	0.1	0.3	**78.3**
River/Stream	2.4	0.0	0.0	1.4	32.0	52.2	2523.6	1.4	2.1	1.7	6.2	0.1	0.0	0.2	0.0	**2623.4**
Rural Settlement	0.4	0.0	0.0	0.1	0.3	0.0	0.5	837.8	0.0	0.0	0.2	0.0	4.9	0.2		**844.4**
Saline Blank				0.0	22.7	0.5	6.9	0.0	52.4	0.1	0.0	0.0				**82.6**
Sandy Area	0.1	0.0	0.1	0.2	1.0	1.8	2.2	0.2	0.3	1.9	0.9	0.0	0.0	0.1		**8.9**
Single Crop	117.6	12.2	1.8	362.9	17.4	10.5	30.1	254.8	0.4	2.3	1417.7	18.2	2.1	6.5	0.3	**2254.8**
Triple Crop	0.7	0.0	0.0	23.2	0.3	0.0	0.1	2.5		0.0	6.3	19.2	0.2	0.4		**53.0**
Urban Settlement			0.0	0.1		0.1	0.1	0.2			0.1	0.0	11.1	0.0		**11.6**
Waterbody	0.9		0.0	0.3	0.2	0.1	0.4	0.5	0.0	0.0	1.2	0.1	0.0	24.8		**28.6**
Wetlands	1.4			0.0	0.0		0.0	0.0			0.1			0.0	0.2	**1.7**
2020 Grand Total	**510.8**	**13.1**	**19.5**	**603.6**	**1991.7**	**97.0**	**2633.3**	**1149.2**	**103.2**	**7.8**	**1618.8**	**56.3**	**19.1**	**33.1**	**0.9**	**8857.3**

5.2 Accuracy results:

The accuracy assessment of land use/land cover (LULC) classification for the years 2000, 2010, and 2020 provides valuable insights into classification reliability and improvements over time. The assessment focused on four key metrics: Producer's Accuracy (PA), User's Accuracy (UA), Overall Accuracy (OA), and the Kappa Coefficient (K), derived from confusion matrices using 50 validation points per land use class. The results indicate a significant improvement in classification accuracy over the years. In 2000, the overall accuracy was 88.4%, with a kappa coefficient of 0.81, indicating moderate agreement between classified and reference data. The producer's accuracy averaged 85.6%, reflecting classification errors primarily in urban settlements, saline blanks, and aquaculture areas. The user's accuracy was 83.2%, suggesting some misclassification between Barren Land, Waterbody, and Mud Flats due to spectral similarity (Table 8).

By 2011, classification accuracy improved significantly, with an overall accuracy of 90.7% and a kappa coefficient of 0.85, indicating strong agreement. The producer's accuracy rose to 91.2%, showing better classification of Mangrove, Single Crop, and Urban Settlement. User's accuracy also improved to 87.9%, reducing confusion between agricultural areas and water bodies. The 2020 classification exhibited the highest accuracy, with an overall accuracy of 92.3% and a kappa coefficient of 0.88, reflecting very strong agreement. The producer's accuracy peaked at 96.1%, demonstrating precise classification across all land use classes, particularly Aquaculture, Triple Crop, and Wetlands. The user's accuracy reached 91.4%, indicating highly reliable classification outputs (table 8).

The increasing accuracy over the years can be attributed to several factors, including advancements in satellite sensor technology, improved classification algorithms, and enhanced ground truth validation. The transition from Landsat 5 TM (2000, 2010) to Landsat 8 OLI (2020) provided higher spectral resolution and better radiometric capabilities, enabling finer differentiation between land cover types. Additionally, the application of radiometric calibration and atmospheric correction reduced spectral distortions, improving classification performance. The adoption of machine learning and object-based classification approaches also contributed to higher accuracy levels, minimizing errors compared to traditional classification

methods. Furthermore, ground truth data collection efforts, including WWF surveys and GPS-based field validation, played a crucial role in improving classification reliability.

Overall, the accuracy assessment confirms continuous improvements in LULC classification for the Sundarbans over time. The increasing Overall Accuracy, Producer's Accuracy, and User's Accuracy demonstrate the effectiveness of sensor advancements, refined classification techniques, and better field data collection methods. The rising Kappa Coefficient from 0.81 in 2000 to 0.88 in 2020 further underscores the growing reliability of classification outputs. Moving forward, future research should explore multi-sensor integration, deep learning classification techniques, and expanded field validation datasets to further enhance the precision and consistency of LULC classification in dynamic and ecologically sensitive regions like the Sundarbans.

Table 8 Accuracy assessment results

Year	Overall Accuracy (%)	Kappa Coefficient	Average Producer's Accuracy (%)	Average User's Accuracy (%)
2000	88.4	0.81	85.6	83.2
2011	90.7	0.85	91.2	87.9
2020	92.3	0.88	96.1	91.4

5.3 Driver of Land use changes:

The factors driving LULC changes are as follows (Table 9):

Table 9 Drivers of land use/ land cover change

Factors	**Land use Drivers**	**Cause**	**Scale**	**Potential Impacts on LULC Change**
Socio-economic	Over Population	High birth rate and population growth, in-migration	Regional	Conversion of agricultural land into settlements, food security demand can shift from monocropping to double and triple cropping, and illegal clearing of forest land.

	Agriculture land conversion	Market driven conversion, Population driven change to settlement, Expansion of commercial agriculture	Regional	Conversion of agricultural land to aquaculture, transformation of aquaculture and agricultural land to non-productive brick kilns/housing, expansion of rural and peri-urban settlements, loss of fertile land due to infrastructure development, reduction in biodiversity, increased soil degradation, and water resource depletion.
Climatic	Cyclone and storm surge	High wind speed, and high-water level, extreme rainfall	Regional	Loss of mangrove forest, increased coastal erosion, changes in the periphery of islands, saltwater intrusion leading to the conversion of agricultural land into fallow land or wetlands, destruction of infrastructure and human settlements, loss of biodiversity, displacement of communities, and reduced freshwater availability.
	Relative Sea level rise and surge	Climatic induced sea level rise by thermal expansion and glacial melt, deltaic subsidence	Global and Regional	Rising sea levels cause increased coastal flooding and storm surges, leading to island boundary erosion, loss of agricultural land, and displacement of settlements. Saltwater intrusion degrades soil quality, converting fertile land into fallow land or wetlands. Changes in hydrology impact freshwater availability, threatening local livelihoods and biodiversity.
	Temperature Rise	Continuous warming of land and atmospheric temperatures due to climate change and greenhouse gas emissions	Global and Regional	Decline in agricultural productivity, shifts in cropping patterns, increased soil evaporation leading to drought like conditions, adverse impact on mangrove growth and seed germination, changes in ecosystem composition, reduced biodiversity, and increased vulnerability to heat stress in both flora and fauna.

	Diminishing Rainfall	Seasonal rainfall changes, shifting monsoon patterns, and climate change effects	Global and Regional	Irregular rainfall patterns reduce agricultural productivity, leading to land-use shifts such as the conversion of farmland into fallow land or brackish water aquaculture s. Increased drought like conditions contribute to soil degradation, reduced groundwater recharge, and alterations in wetland ecosystems.
Hybrid	Salinisation	Sea water ingress, excess fertiliser, over withdrawal of ground water	Regional	Saltwater intrusion and excessive chemical fertilizer use degrade soil quality, making agricultural land unproductive. This leads to the conversion of farmland into fallow land, barren land, or aquaculture. Long-term salinization on surface and subsurface reduces crop diversity and threatens freshwater availability.

5.4 Land use/ land cover future projection

5.4.1 Land use change between 2020-2030:

Between 2020 and 2030, significant land use changes are projected across all categories. Aquaculture will expand by 25.4%, growing from 510.8 sq. km to 640.4 sq. km, primarily at the expense of wetlands and agricultural land. Urban settlements will witness the sharpest increase, rising by 113.6% from 19.1 sq. km to 40.8 sq. km, driven by population growth and infrastructure needs. Single-cropped land will decline by 28.4%, shrinking from 1618.8 sq. km to 1159.7 sq. km, while double-cropped land will decrease by 7.8% from 603.6 sq. km to 556.4 sq. km due to urbanization and aquaculture expansion. Mangroves will experience a moderate decline of 2.5%, reducing from 1991.7 sq. km to 1942.5 sq. km, and waterbodies will shrink by 37.5%, falling from 33.1 sq. km to 20.7 sq. km. Wetlands will decline by 11.1%, from 0.9 sq. km to 0.8 sq. km, highlighting their vulnerability to conversion into aquaculture and settlements. Barren land will reduce by 40.5%, from 13.1 sq. km to 7.8 sq. km, while brick kilns will expand by 24.1%, increasing from 19.5 sq. km to 24.2 sq. km due to industrial growth. Saline blanks will rise by 53.2%, from 103.2 sq. km to 158.1 sq. km, likely due to soil salinization, and mudflats will grow significantly by 71.3%, from 97.0 sq. km to 166.2 sq. km, driven by sediment deposition. Sandy areas will expand slightly by 23.1%, growing from 7.8

sq. km to 9.6 sq. km, while triple-cropped land will see a minor decline of 1.8%, reducing from 56.3 sq. km to 55.3 sq. km (Figure 8 and Table 10). These changes reflect a clear trend toward aquaculture, urbanization, and industrial growth, occurring at the cost of agricultural land, wetlands, and natural ecosystems, emphasizing the urgent need for sustainable land use policies to balance development with ecological preservation.

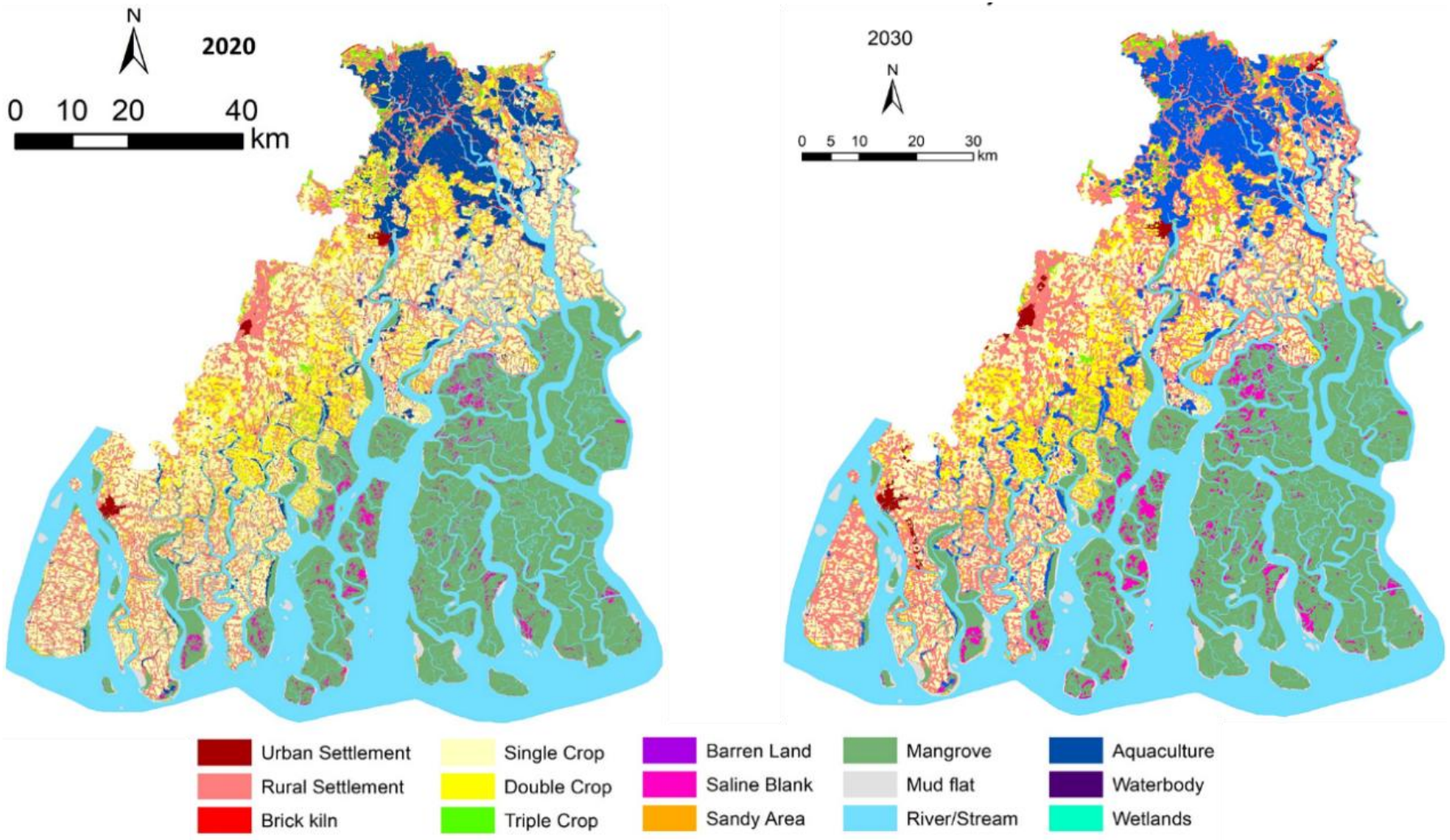

Figure 8 Land use/ Land Cover change (2020-2030)

Table 10 Land use change matrix 2020-2030 (area sq. km)

Class	Aquaculture	Barren Land	Brick kiln	Double Crop	Mangrove	Mud flat	River/stream	Rural Settlement	Saline Blank	Sandy Area	Single Crop	Triple Crop	Urban Settlement	Waterbody	Wetlands	2020Grand Total
Aquaculture	510.0	0.0	0.5	0.0	0.0	0.0	0.1	0.2	0.0	0.0	0.0	0.0	0.0	0.0	0.0	**510.8**
Barren Land	0.4	5.4	4.5	0.2	0.0	0.0	0.1	0.6	0.0	0.0	1.9	0.0	0.0	0.0	0.0	**13.1**
Brick kiln	0.1	0.0	18.7	0.0	0.0	0.0	0.6	0.0	0.0	0.0	0.1	0.0	0.0	0.0	0.0	**19.5**
Double Crop	36.8	0.0	0.0	438.1	0.0	0.1	0.5	71.8	0.0	0.0	48.9	7.3	0.0	0.0	0.0	**603.6**
Mangrove	0.0	0.0	0.0	1.6	1918.1	0.4	13.4	0.2	57.8	0.0	0.0	0.0	0.0	0.0	0.0	**1991.7**
Mud flat	0.7	0.0	0.0	0.0	5.3	82.2	3.3	0.1	2.5	1.8	0.4	0.0	0.0	0.0	0.7	**97.0**
River/Stream	0.1	0.0	0.1	0.0	13.6	80.7	2537.4	0.6	0.6	0.1	0.1	0.0	0.0	0.0	0.0	**2633.3**
Rural Settlement	0.5	0.0	0.0	2.5	0.2	0.1	0.4	1121.6	0.0	0.0	1.7	0.7	21.3	0.2	0.0	**1149.2**
Saline Blank	0.0	0.0	0.0	0.0	4.3	0.0	1.8	0.0	97.0	0.0	0.0	0.0	0.0	0.0	0.0	**103.2**
Sandy Area	0.0	0.0	0.0	0.0	0.0	0.1	0.1	0.1	0.2	7.3	0.0	0.0	0.0	0.0	0.0	**7.8**
Single Crop	89.7	2.4	0.3	104.8	0.7	2.6	26.2	281.7	0.0	0.4	1104.3	5.1	0.1	0.4	0.0	**1618.8**
Triple Crop	0.7	0.0	0.0	8.8	0.0	0.0	0.0	3.9	0.0	0.0	0.5	42.2	0.0	0.2	0.0	**56.3**
Urban Settlement	0.0	0.0	0.0	0.0	0.0	0.0	0.1	0.0	0.0	0.0	0.0	0.0	18.8	0.0	0.0	**19.1**
Waterbody	0.7	0.0	0.0	0.2	0.1	0.0	0.2	9.9	0.0	0.0	1.7	0.0	0.5	19.9	0.0	**33.1**
Wetlands	0.8	0.0	0.0	0.0	0.0	0.0	0.0	0.0	0.0	0.0	0.0	0.0	0.0	0.0	0.1	**0.9**
2030 Grand Total	**640.4**	**7.8**	**24.2**	**556.4**	**1942.5**	**166.2**	**2584.1**	**1490.7**	**158.1**	**9.6**	**1159.7**	**55.3**	**40.8**	**20.7**	**0.8**	**8857.3**

5.4.2 Land use change between 2030-2050:

Between 2030 and 2050, significant land use changes are projected across all categories, driven by urbanization, industrial growth, and environmental changes. Aquaculture will decline slightly by 4.4%, from 640.4 sq. km to 612.4 sq. km, due to competition for land and environmental regulations. Barren land will experience a drastic reduction of 71.8%, shrinking from 7.8 sq. km to 2.2 sq. km, primarily converting into brick kilns, rural settlements, and agricultural fields. Brick kilns will decline marginally by 8.7%, from 24.2 sq. km to 22.1 sq. km, reflecting industrial stabilization. Double-cropped land will face a significant decline of 29.7%, reducing from 556.4 sq. km to 391.1 sq. km, driven by urban expansion and soil degradation. Mangrove cover will decrease by 9.7%, from 1942.5 sq. km to 1753.8 sq. km, as encroachment for settlements and saline blanks continues. Mudflats will expand by 3.7%, increasing from 166.2 sq. km to 172.3 sq. km, reflecting sediment deposition and coastal dynamics. River and stream areas will shrink slightly by 1.8%, from 2584.1 sq. km to 2537.4 sq. km, due to land reclamation. Rural settlements will remain stable at 1490.7 sq. km, absorbing land from agriculture and barren areas. Saline blanks will expand by 9.0%, from 158.1 sq. km to 172.3 sq. km, driven by rising salinity and soil degradation. Sandy areas, single-cropped land, and triple-cropped land will remain stable at 9.6 sq. km, 1159.7 sq. km, and 55.3 sq. km, respectively, reflecting limited changes in these categories. Urban settlements will see the sharpest increase, growing by 155.9%, from 40.8 sq. km to 104.4 sq. km, as population growth and infrastructure needs drive land conversion. Waterbodies will decline by 20.8%, reducing from 20.7 sq. km to 16.4 sq. km, as they are converted into aquaculture and reclaimed land. Wetlands will remain critically low at 0.8 sq. km, highlighting ongoing environmental pressures (Figure 9 and Table 11). These projections underscore rapid urbanization, declining agricultural areas, and continued pressures on natural ecosystems like mangroves, wetlands, and waterbodies, emphasizing the urgent need for sustainable land use planning and environmental conservation.

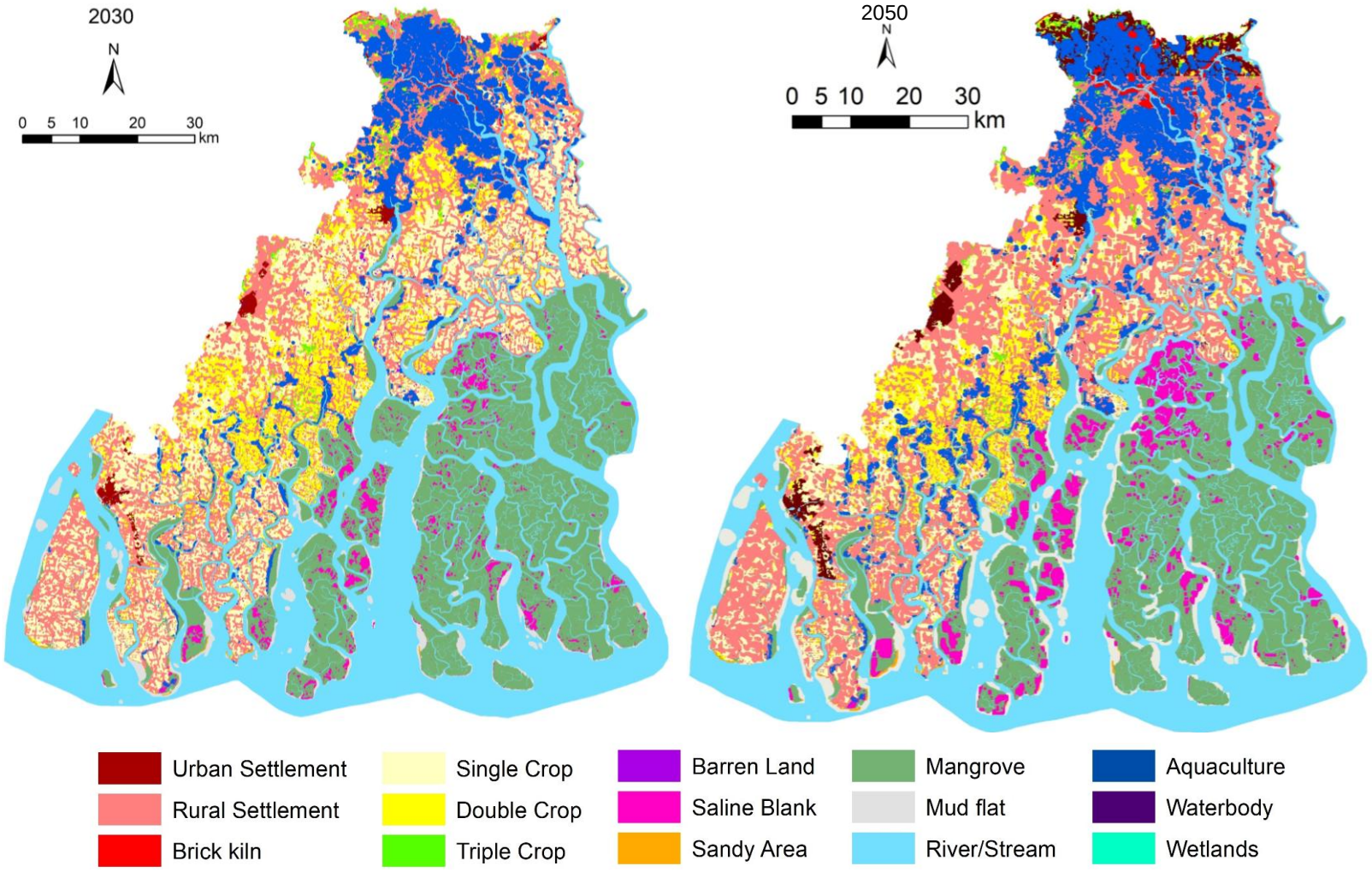

Figure 9 Land use / Land cover prediction 2030-2050

Table 11 Land use change matrix 2030-2050 (area sq. km)

Class	Aquaculture	Barren Land	Brick kiln	Double Crop	Mangrove	Mud flat	River/stream	Rural Settlement	Saline Blank	Sandy Area	Single Crop	Triple Crop	Urban Settlement	Waterbody	Wetlands	2030Grand Total
Aquaculture	612.4		27.2				0.7									640.4
Barren Land	0.0	2.2	5.2				0.1	0.3								7.8
Brick kiln			22.1				2.1									24.2
Double Crop	60.9			391.1				104.4								556.4
Mangrove					1753.8		16.4		172.3							1942.5
Mud flat	2.9				15.0	132.9	0.1		8.1	5.4	0.1				1.8	166.2
River/Stream						242.5	2341.3								0.3	2584.1
Rural Settlement								1368.9					121.8			1490.7
Saline Blank							6.3		151.8							158.1
Sandy Area									0.6	9.1						9.6
Single Crop	108.8	0.1		38.8			35.6	347.5			629.0	0.0				1159.7
Triple Crop	0.4			2.1				5.0				47.7		0.1		55.3
Urban Settlement				0.0		0.0	1.8				0.0		38.9			40.8
Waterbody	0.9							4.1			0.0			15.6		20.7
Wetlands	0.8														0.0	0.8
2050 Grand Total	787.0	2.3	54.5	432.0	1768.8	375.3	2404.4	1830.2	332.7	14.5	629.1	47.7	160.7	15.7	2.2	**8857.3**

5.5 Mangrove status of last two decade

5.5.1 Change in mangrove forest area

A multi-temporal analysis of Landsat data from 2000 to 2020 revealed significant erosion in both the core and buffer zones of the mangrove forest, along with an expansion of transitional areas near human settlements (Figure 10). Over this period, approximately 110 km² of mangroves were lost, while 81 km² were gained within the Sundarbans Biosphere Reserve (SBR). This corresponds to an average annual loss of 5.5 km² and a gain of 4.1 km² per year. The core forest area experienced a reduction of 58 km² (averaging 2.9 km²/year). The buffer zone lost 52 km² (2.6 km²/year). The transition zone outside the contiguous mangrove region saw an increase of 81 km² (4.1 km²/year).

Although mangrove plantation and regeneration efforts contributed to forest gains, these newly formed areas were fragmented and unable to sustain large fauna such as tigers, thereby failing to compensate for the loss of continuous mangrove cover.

The rate of mangrove change varied over time. The highest erosion rates were recorded between 2000 and 2005, with an annual loss of 4.5 km² in the core area and 3.4 km² in the buffer zone. Conversely, the greatest mangrove expansion occurred between 2015 and 2020, with an accretion rate of 7.7 km²/year.

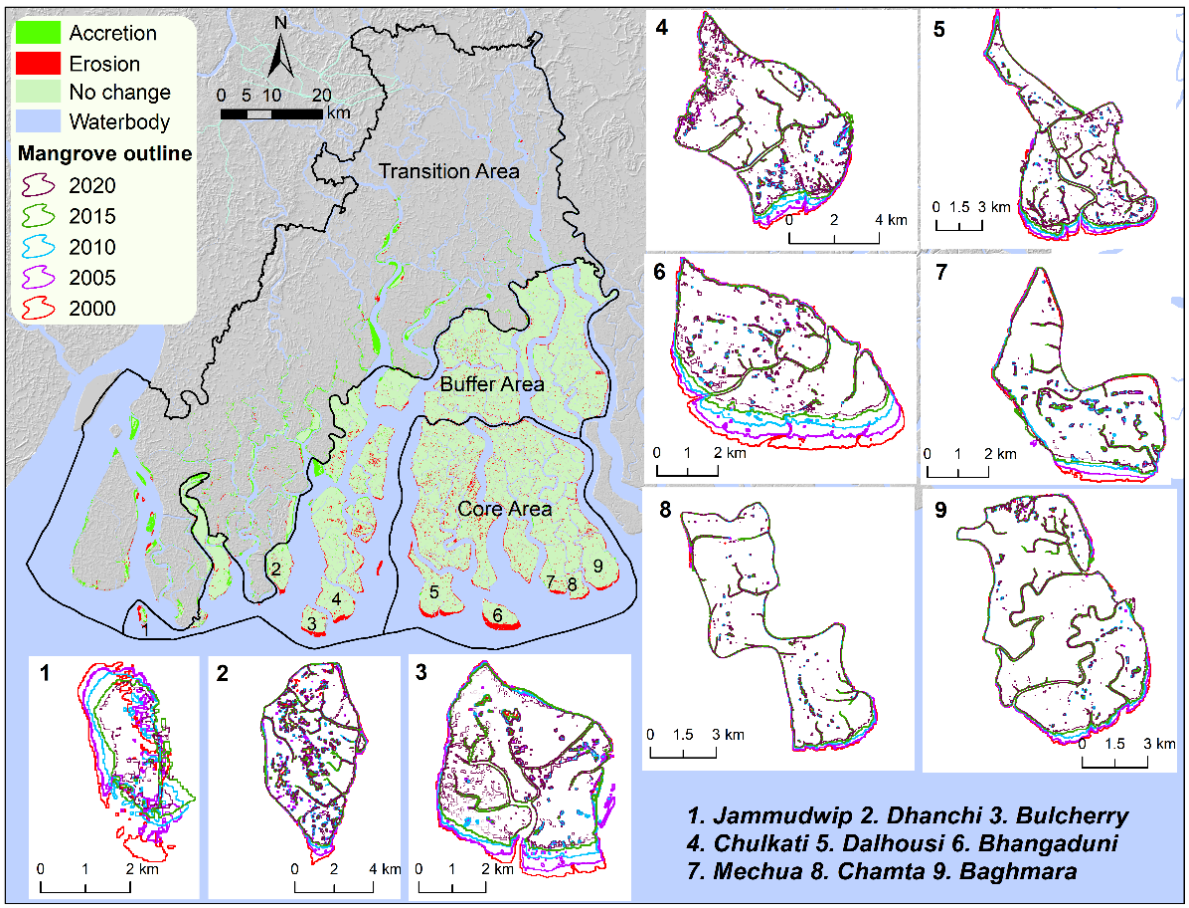

Figure 10 Mangrove area loss/gain in the sea-facing islands (numbers 1 to 9).

A detailed shoreline analysis of nine sea-facing islands—where erosion was most concentrated—was conducted (Figure 10, Table 12). Between 2000 and 2020, land loss on these islands ranged from 1.3 km² (130 hectares) on Jammudwip Island to 11.6 km² (1,160 hectares) on Dalhousie Island. In total, 49 km² of land was lost from these islands, all of which—except Jammudwip—serve as habitat for tigers.

Table 12. The Indian Sundarbans mangrove forest area over time. Numbers in parenthesis show average annual change over the proceeding five years, with negative indicating loss and positive indicating gain.

Year	Core Area (km^2)	Buffer Area (km^2)	Transition Area (km^2)	Total Area (km^2)
2000	903.2	1084.7	86.2	2074.1
2005	880.9 (-4.5)	1067.6 (-3.4)	100.3 (+2.8)	2048.8
2010	869.9(-2.2)	1053.2(-2.9)	109.5 (+1.8)	2032.6

2015	855.9 (-2.8)	1046.6 (-1.3)	128.7 (+3.8)	2031.2
2020	845.2 (-2.2)	1032.9 (-2.7)	167.4 (+7.7)	2045.4
2000 to 2020 (% change)	-6.42%	-4.78%	+94.20%	-1.38%

5.5.2 Change in Mangrove Species Composition

Mangrove community composition maps were developed at the genus level for the years 2000 and 2020 (Figure 11). The analysis (summarized in Table 13) indicates an increase in salt-tolerant mangrove species and a decline in species favouring lower salinity conditions.

Among the expanding mangrove genera: Ceriops sp.-dominated assemblages showed the highest increase (4.2%), Avicennia sp. increased by 1.8%, Excoecaria sp. expanded by 1.4%, and Phoenix sp.-dominated assemblages grew by 0.4%. Conversely, the following assemblages experienced a decline: Mixed mangrove class shrank by 5.7%, Sonneratia- declined by 0.6%. The increase in Avicennia sp. is likely due to plantation efforts along riverbanks and the natural colonization of newly formed char/mudflat areas in transitional zones.

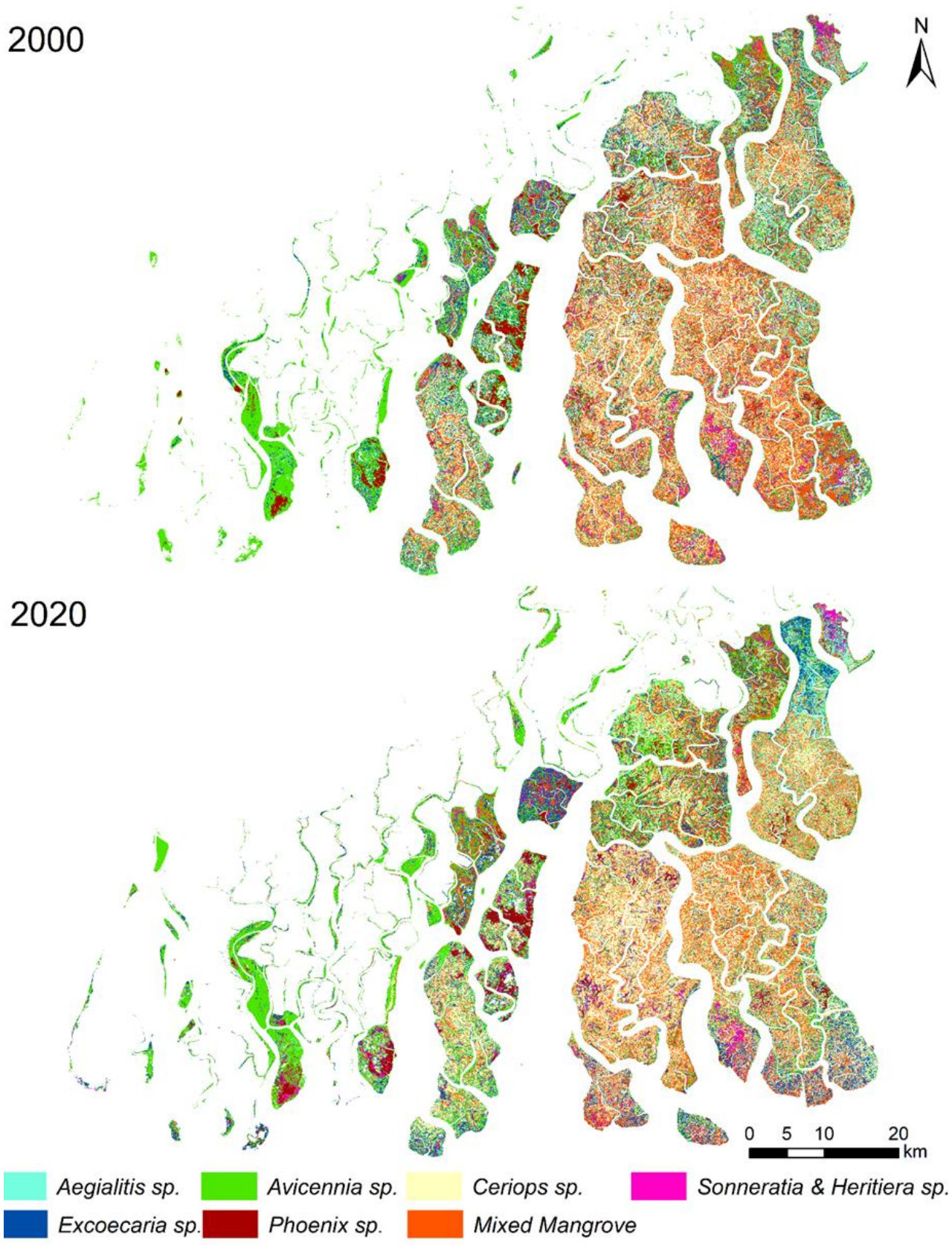

Figure 11 Distribution of dominant mangrove communities of the Indian Sundarbans in 2000 and 2020.

Table 13 Area (and percentage area) of principal mangrove genera in 2000 and 2020.

Mangrove Genus	Area (km^2)		% Area	
	2000	2020	2000	2020
Aegialitis sp.	159.4	144.3	7.7	7.1
Avicennia sp.	425.9	456.5	20.5	22.3
Ceriops sp.	459.3	537.4	22.1	26.3
Excoecaria sp.	253.0	278.2	12.2	13.6
Phoenix sp.	60.1	67.8	2.9	3.3
Excoecaria & Ceriops sp.	536.6	427.7	25.9	20.9
Sonneratia & Heritiera sp.	109.2	78.9	5.3	3.9
Mixed Mangrove	70.9	54.5	3.4	2.7

5.5.3 Change in mangrove health indicators

A long-term analysis of Landsat and MODIS image sequences (2000–2020) revealed a progressive decline in mangrove health, as indicated by decreasing NDVI and EVI values. Due to the limited availability of cloud-free Landsat images, the Mann-Kendall (MK) test was conducted for the winter season, while monthly trends were analyzed using MODIS data. The Landsat-based winter analysis showed that 23% of NDVI pixels and 40% of EVI pixels had a negative trend, whereas the MODIS monthly analysis revealed a much higher decline, with 73% of NDVI pixels and 81% of EVI pixels showing negative trends. Spatially, the most significant degradation was observed in sea-facing islands and the central, eastern, and northeastern parts of the forest, while localized improvements in NDVI and EVI were detected along western and some northern island margins (Figure 12), possibly due to plantation efforts or natural regeneration. Overall, the findings indicate widespread mangrove deterioration, particularly in coastal and interior areas, raising concerns about the ecosystem's resilience to environmental and anthropogenic stressors.

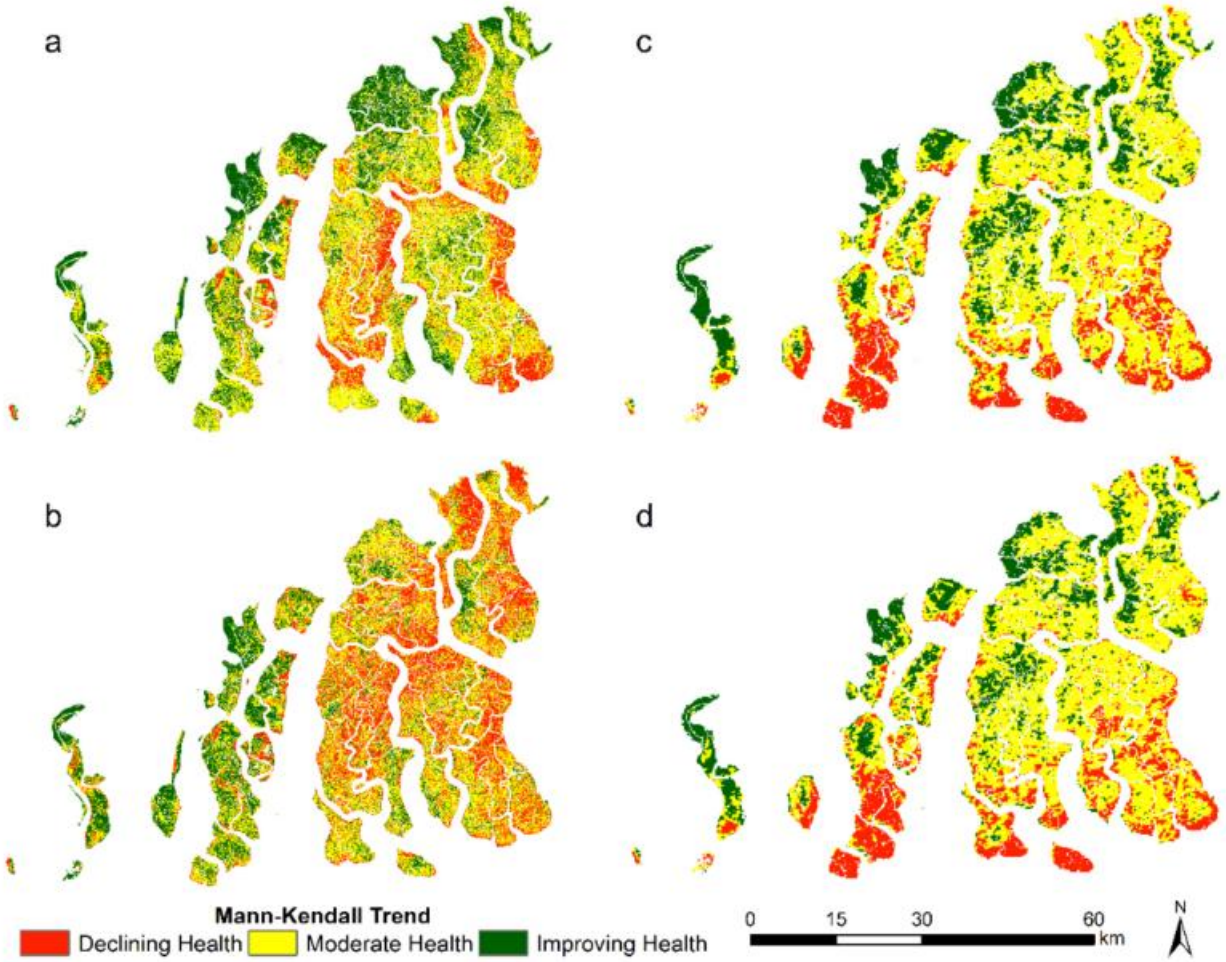

Figure 12 Trends in vegetation indices in terms of improving health and declining health from 2000 to 2020 using the Mann–Kendall test on EVI and NDVI, derived from Landsat and Modis data ((a)—Landsat NDVI MK test; (b)—Landsat EVI MK test; (c)—MODIS NDVI MK test; (d)—MODIS EVI MK test).

5.6 Drivers of change

There is major six driver have been identified for mangrove changes under three broad category (i.e. legacy drivers, progressive drivers and periodic shocks drivers) (Table 14).

Table 14 Drivers of change for mangroves in the Indian Sundarbans. Driver types: L—legacy; C—contemporary; S—shock. (Samanta et al. 2021)

Driver (and Type)	Cause	Scale and Duration	Potential Impact on the Mangroves	Strength of Evidence
Declining sediment supply (L)	Avulsion of river courses eastward with a consequent reduction in freshwater flow and sediment supply to the SBR	Regional, Centuries	Reduced resilience of mangrove to relative sea-level rise and increased coastal erosion	High based on greater losses in the Indian Sundarbans versus the Bangladesh Sundarbans
Salinization (L, C)	Avulsion of river courses eastward with a consequent reduction in freshwater inflow to the SBR, and increasing marine influence due to sea-level rise	Regional, Centuries	Salinity stress, loss/decline of low salinity mangroves, stunted growth and mangrove health deterioration,	High, based on an observed shift in mangrove community composition towards more salt-tolerant varieties
Relative sea-level rise (L, C)	Climate-induced sea-level rise and deltaic subsidence	Global and regional, decadal and longer	Loss of mangroves due to erosion and inundation	High based on tide gauge measurements across the region
Temperature rise (C)	Continuing warming of land and Sea	Global and regional, decadal and longer	Stress on mangrove germination and propagation, with potential adverse impacts on ecosystem functions	Hypothesized globally; insufficient observations in south Asia to confirm a causal relationship with mangrove health/loss
Change in rainfall (C)	Seasonal rainfall change and variability including in the monsoon	Regional, decadal and longer	Stress on germination and propagation, and potential for stress on established mangrove forest	Hypothesized globally; insufficient observations in south Asia to confirm a causal relationship with mangrove health/loss
Cyclones and Storm surges (S)	High wind speeds and extreme water levels	Local, Days to years	Abrupt loss of mangrove canopy cover, reduced leaf area, death along river margins due to storm/surge thrust	High, based on studies of past cyclones in the Sundarbans and also the remote sensing analysis presented in this paper

5.6.1 Salinity rise

The increasing salinity in the estuaries of the Sundarbans is a major environmental stressor, negatively affecting mangrove health, ecosystem services, and local livelihoods. The disconnection of major freshwater distributaries such as Adi Ganga, Matla, Jamuna, Bidyadhari, and Ichamati over the past century has led to a significant salinity ingress in the estuary. Eleven such major disconnections, caused by both natural and anthropogenic factors, have been identified through field and remote sensing studies. While salinity levels in the Hugli River were stabilized following the restoration of freshwater supply via the Farka Feeder Canal, salinity has increased significantly in the Sitamarhi-Matla-Thakuran and Thakur an estuary, which encompass the Sundarbans mangrove forest.

A synthesis of salinity measurements from the Hugli-Sitamarhi-Matla-Thakuran-Raimangal estuaries (Mitra et al.) revealed an acute freshwater scarcity in the core Sundarbans area. Salinity levels remain as high as 13 ppt even during monsoon, rising to 21 ppt in the post-monsoon period and reaching 28 ppt during the pre-monsoon dry season. The persistent salt

stress has led to stunted growth, poor physiological functioning, and widespread degradation of mangrove cover. As a result, freshwater-dependent mangrove species such as Heritiera fomes, Nypa fruticans, Xylocarpus, and Sonneratia caseolaris are in decline, being replaced by more salt-tolerant species like Ceriops, Avicennia, and Excoecaria, causing a loss in species diversity.

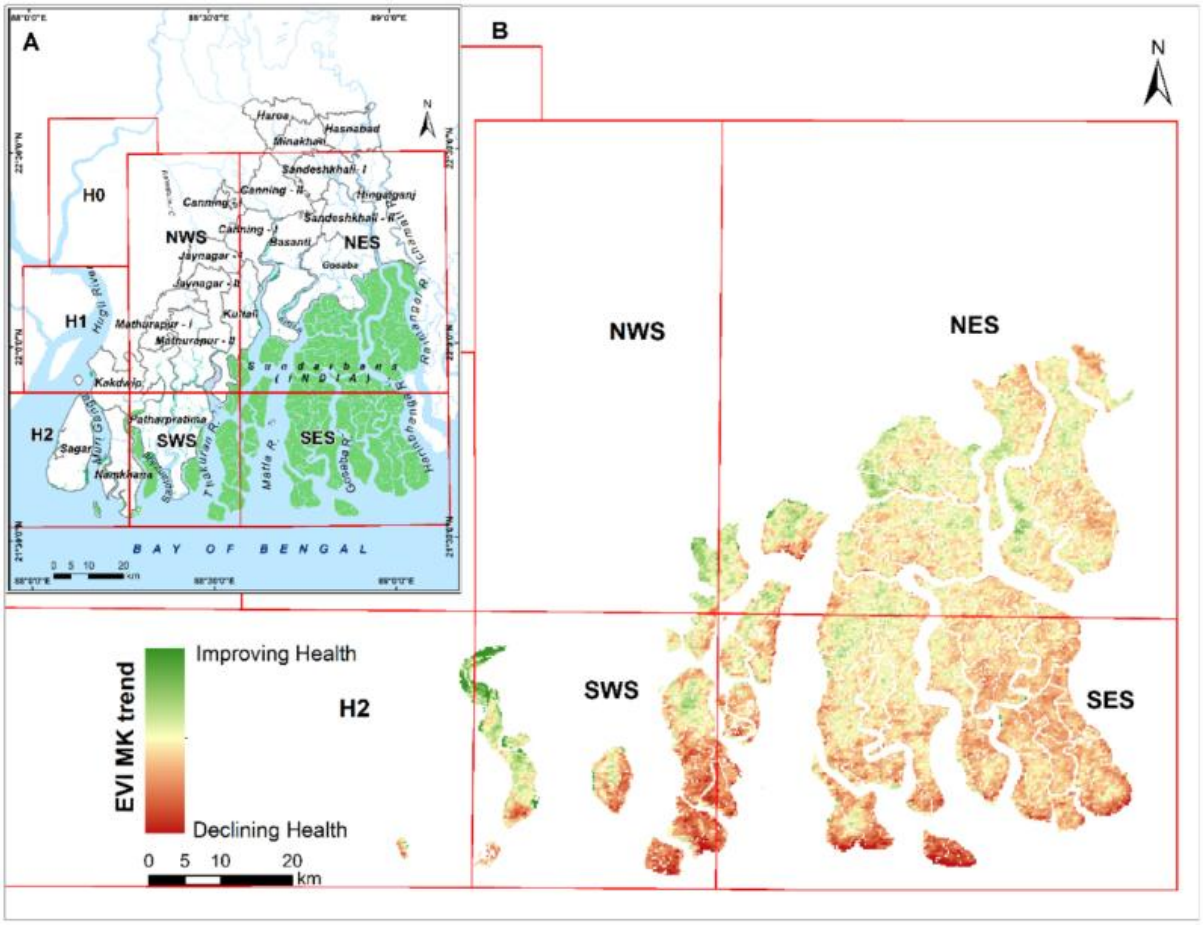

Figure 13 Comparison between salinity zones and mangrove health (MODIS EVI MK test). (A) the inset map showing the different salinity zones in SBR and (B) the spatial variability of EVI MK.

A review of water salinity measurements across the Sundarbans Biosphere Reserve (Mitra et al.) identified seven zones of salinity variation (Figure 13). In the sea-facing southwestern (SWS) and southeastern (SES) zones, which include the core and buffer areas, MODIS-based Mann-Kendall trend analysis indicates significant mangrove health deterioration. Salinity in these zones reaches 27–28 ppt in the pre-monsoon period and 17–21 ppt in the post-monsoon period, showing an increasing trend. In contrast, the northeastern Sundarbans (NES) near the Bangladesh border, despite experiencing high salinity, shows moderate mangrove health decline, attributed to occasional freshwater influx from the Ichamati River. Similarly, in the western Sundarbans, mangrove health is comparatively better, benefiting from freshwater inputs from the Hugli estuary through the Saptamukhi River. These findings underscore the

critical role of freshwater availability in sustaining mangrove ecosystems and highlight the threat posed by rising salinity levels to the region's biodiversity.

5.6.2 Relative sea-level rise

Over the past two decades, both absolute and relative sea levels have been rising in the northern Bay of Bengal, posing a significant threat to coastal ecosystems, including the Sundarbans. Analyzing sea surface height, halosteric height, and thermosteric height using Saral-Altika, GRACE, and Argo Float Data, Ghosh et al. estimated an absolute sea-level rise of 4.36 ±1.45 mm/year with 95% confidence. However, relative sea-level rise observed at the Diamond Harbour tide gauge was significantly higher, recorded at 5.7 mm/year, partially attributed to land subsidence at a rate of 4 mm/year (Brown et al. 2018).

According to data presented in the Indian Parliament by the Ministry of Earth Sciences, the average sea-level rise along India's coasts over the past 40–50 years has been estimated at 1.3 mm/year. However, at Diamond Harbour, the rate was much higher, measured at 5.16 mm/year between 1948 and 2005. A long-term estimate of relative sea-level rise at Diamond Harbour indicates a rise of 3.7 mm/year between 1948 and 2020 (Figure 14), but a much steeper increase of 12 mm/year between 2006 and 2014 (Hazra et al. 2016). These findings suggest that regional sea-level rise is accelerating, intensifying coastal erosion, saltwater intrusion, and habitat loss, further threatening the Sundarbans' fragile ecosystem.

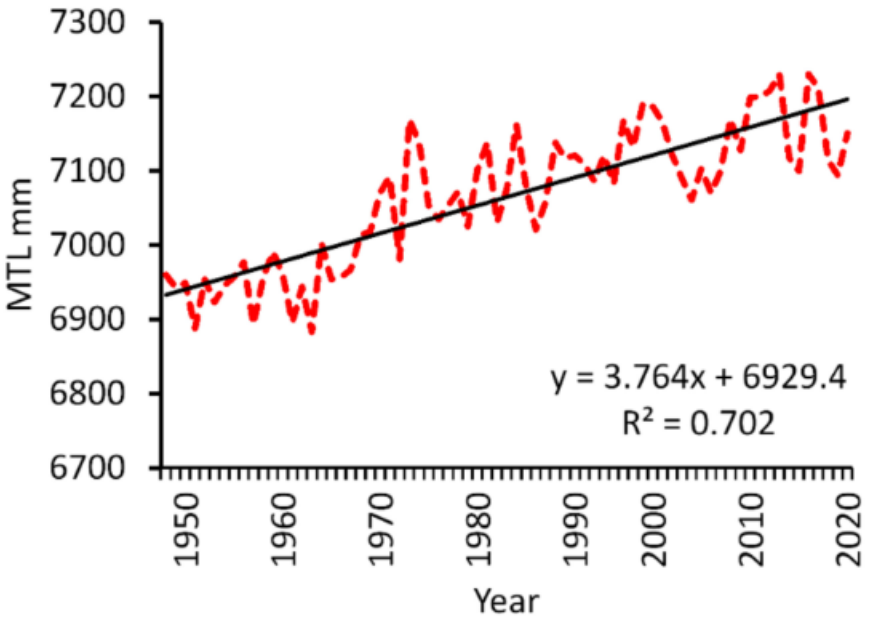

Figure 14 Mean sea-level rise at Diamond Harbor. MTL stands for mean tide level (source: Permanent Service for Mean Sea Level (https://www.psmsl.org/data/obtaining/stations/417.phpaccessed on 21 January 2021) and Kolkata Port Trust).

The estimation of sea-level rise in the Sundarbans Delta using tide gauge data is influenced by three key factors: (a) the rate of land subsidence or uplift, which is poorly documented but estimated to range between 2.5 mm/year to 4 mm/year in the delta (Brown et al. 2018), (b) the period of measurement, and (c) the position of the tide gauge (whether located on the open coast or within an estuary). When considering the 18.5-year lunar cycle, the observed sea-level rise shows a consistent trend of 6 mm/year. However, for assessing coastal impacts such as erosion (Figure 15) and inundation, the focus should be on local relative sea-level rise—which measures sea-level changes relative to land subsidence or uplift—rather than the absolute global rate of sea-level rise, as relative sea-level rise directly affects coastal stability and ecosystem resilience in the Sundarbans.

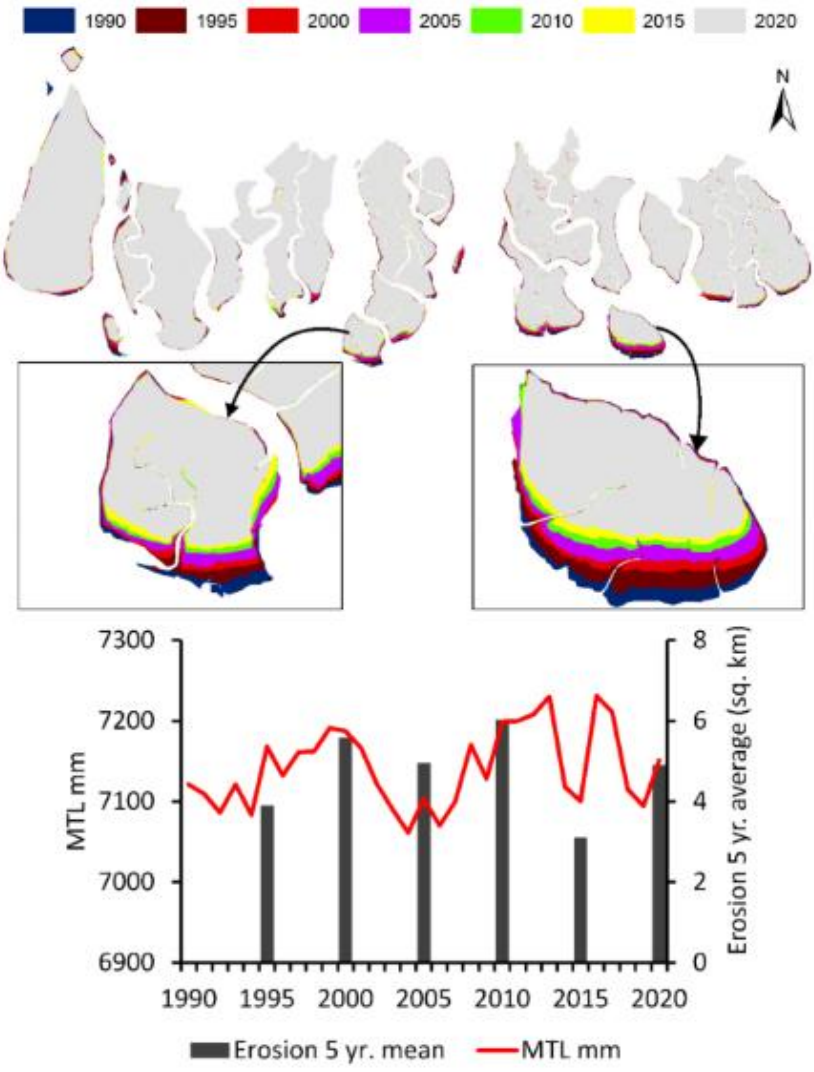

Figure 15 Relationship between sea-level rise and loss of mangrove island area due to erosion. MTL stands for mean tide level.

5.6.3 Temperature Rise

To assess the impact of rising temperatures on mangrove health, seasonal temperature trends over the Sundarbans were analyzed. Findings at higher spatial resolution align with stakeholder observations within the Sundarbans Biosphere Reserve (SBR). The maximum temperature during summer (March–May), monsoon (June–August), and post-monsoon (September–November) has shown a significant increasing trend (Figure 16), posing threats to mangrove ecosystems. Higher temperatures lead to increased evaporation, drying, and temperature shocks, particularly during the germination and propagation period (July–September) for mangrove seeds. If this warming trend persists, the region could experience a temperature rise exceeding 2°C, severely affecting mangrove health, ecosystem stability, and species composition.

Additionally, sea surface temperature (SST) anomalies recorded during El Niño years (2005, 2009–10, and 2015) indicate that Pacific warm events, coupled with the Indian Ocean Dipole, significantly influence climatic variability over the Indian Sundarbans Delta. These climatic shifts could exacerbate thermal stress on mangroves, further altering growth patterns, regeneration rates, and overall ecosystem resilience.

5.6.4 Changes in Rainfall

The Sundarbans Delta receives 70–80% of its annual rainfall during the summer monsoon (southwest monsoon), leading to high river discharge ranging between 2,952 and 11,897 m^3/s. However, during non-monsoon months, river discharge declines significantly, varying between 900 and 1,500 m^3/s (Mukhopadhyay et al. 2006). Rainfall variability and the resulting spatial and temporal fluctuations in salinity have profound implications for mangrove health and the livelihoods of forest-dependent communities.

Analysis over the past two decades reveals a consistent decline in summer and post-monsoon rainfall, whereas monsoon rainfall has remained relatively stable, and winter rainfall has shown a slight increase (Figure 16). The reduction in summer and post-monsoon rainfall is particularly concerning, as it negatively affects mangrove ecosystems, increasing salinity stress and reducing freshwater availability.

A partial correlation analysis between EVI (Enhanced Vegetation Index) and rainfall showed a strong negative correlation at lag-0 and lag-1, indicating an immediate adverse response of mangroves to rainfall reduction. However, a weaker positive correlation was observed at lag-2

and lag-3, suggesting that rainfall influences mangrove health over a delayed period of 2–3 months (Figure 17). Additionally, a strong combined correlation (R^2 = 0.7) between rising temperatures, rainfall variability, and declining EVI trends suggests that changing climatic patterns—particularly reduced pre-monsoon and post-monsoon rainfall—along with increasing salinity and sea-level rise, are major contributors to mangrove degradation.

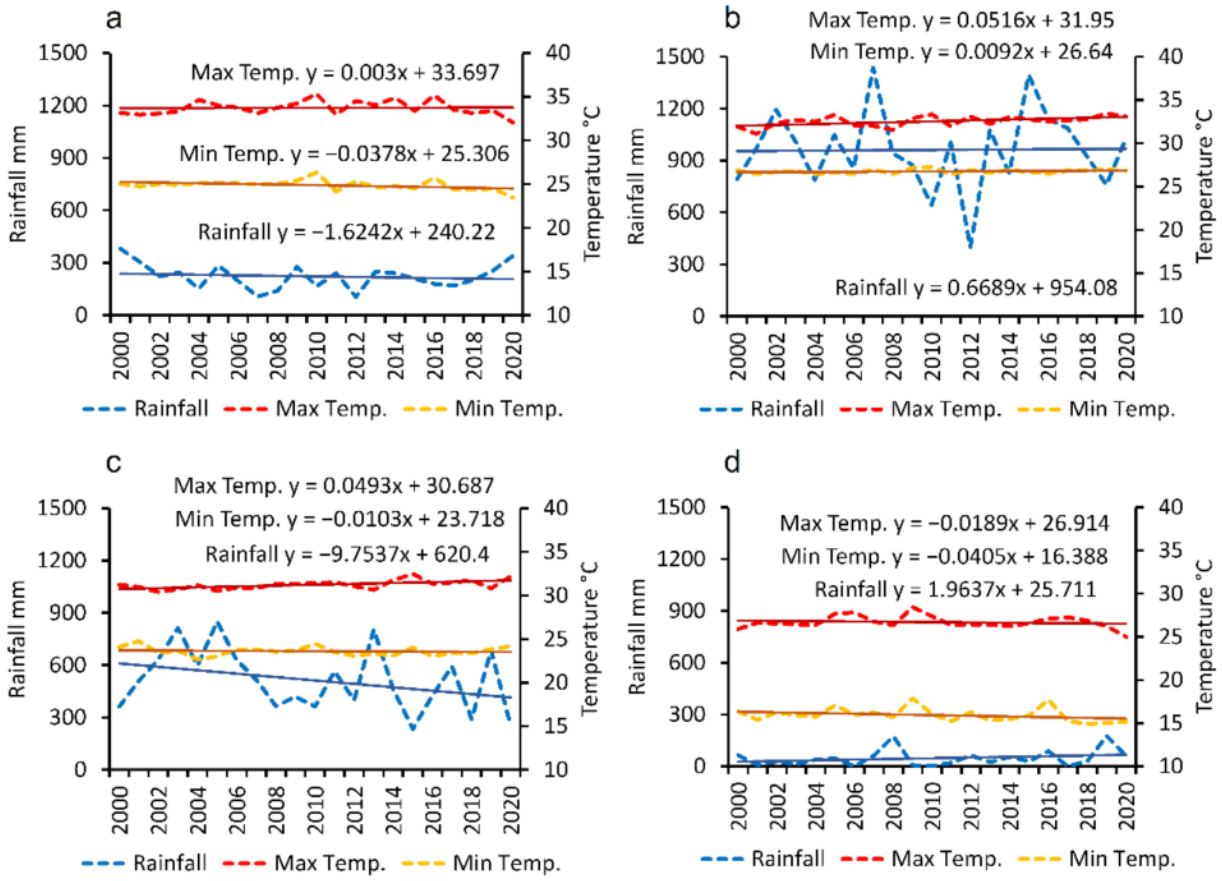

Figure 16 Annual rainfall, maximum temperature and minimum temperature variability in (a) summer, (b) monsoon, (c) post-monsoon, and (d) winter season during 2000–2020 in the SBR.

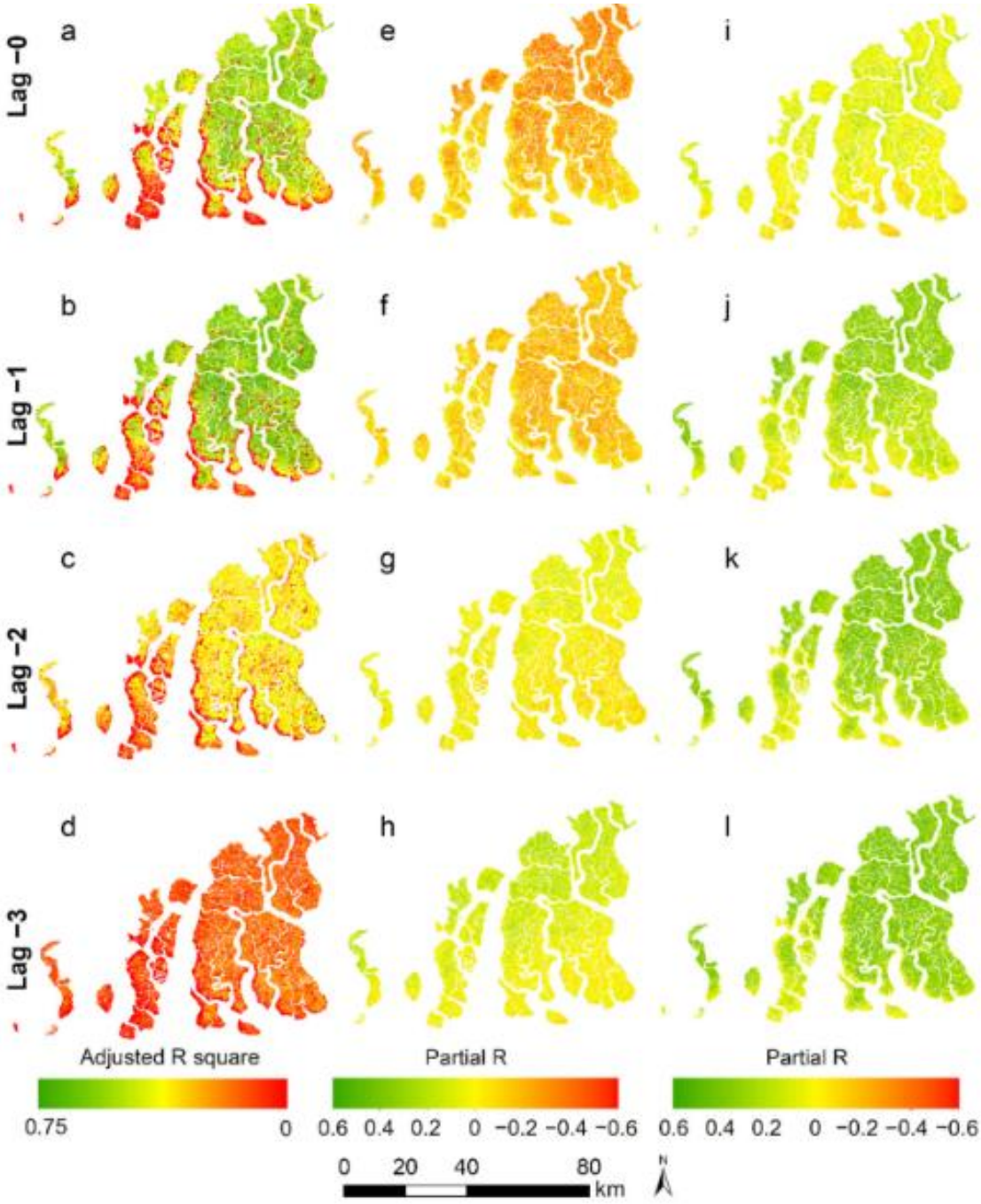

Figure 17 Adjusted R square (a–d), partial R EVI-rainfall (e–h), and EVI-maximum temperature (i–l).

5.6.5 Short term degradation due to cyclones

Frequent cyclones and the resulting coastal flooding from storm surges pose significant natural hazards to the Sundarbans delta, alongside ongoing sea-level rise and climate variability. The Bay of Bengal is responsible for approximately 7% of the world's most intense cyclonic events. Over the past 120 years, the occurrence of very severe cyclonic storms in the northern Bay of Bengal has risen by 26%, with a notable escalation in both their frequency and intensity over the past two decades.

During the early 21st century, increased sea surface temperatures (SSTs) contributed to the development of multiple cyclonic storms, such as Mala (2006), Sadr (2007), Bijli (2009), and Aila (2009), which collectively affected extensive areas of the Sundarbans region. In the following decade (2011–2020), several severe cyclones, including Roanu (2016), Titli (2018), Fani (2019), Bulbul (2019), and Amphan (2020), caused widespread destruction, while the Sundarbans narrowly escaped the impact of Phailin (2013) and Hudhud (2014).

This study particularly examined the effects of Cyclone Bulbul (9 November 2019) and Cyclone Amphan (20 May 2020), which struck the region within a six-month interval, on mangrove forest health. To reduce the influence of seasonal mangrove phenology, Landsat 8 and Sentinel-2 satellite imagery were utilized to assess variations in forest canopy density (FCD) before and after the cyclones. Vegetation health was assessed using remote sensing indices such as the Advanced Vegetation Index (AVI), Bareness Index (BI), Shadow Index (SI), and Thermal Index (TI).

Findings indicate a notable decline in FCD, particularly within the 80–100% canopy density range. Following Cyclone Bulbul, around 780 km² of mangrove forest transitioned from very high (80–100%) to high canopy density (60–80%), while a smaller area moved from high to moderate canopy density (40–60%) between 2018 and 2019. Similarly, post-Cyclone Amphan, 261 km² of mangrove cover shifted from very high to high density, while 142 km² transitioned from high to moderate canopy density between 2019 and 2020 (Figure 18). These results highlight the significant impact of extreme climatic events on the mangrove ecosystem, emphasizing the need for long-term monitoring, conservation efforts, and climate adaptation strategies to protect the fragile Sundarbans Biosphere Reserve.

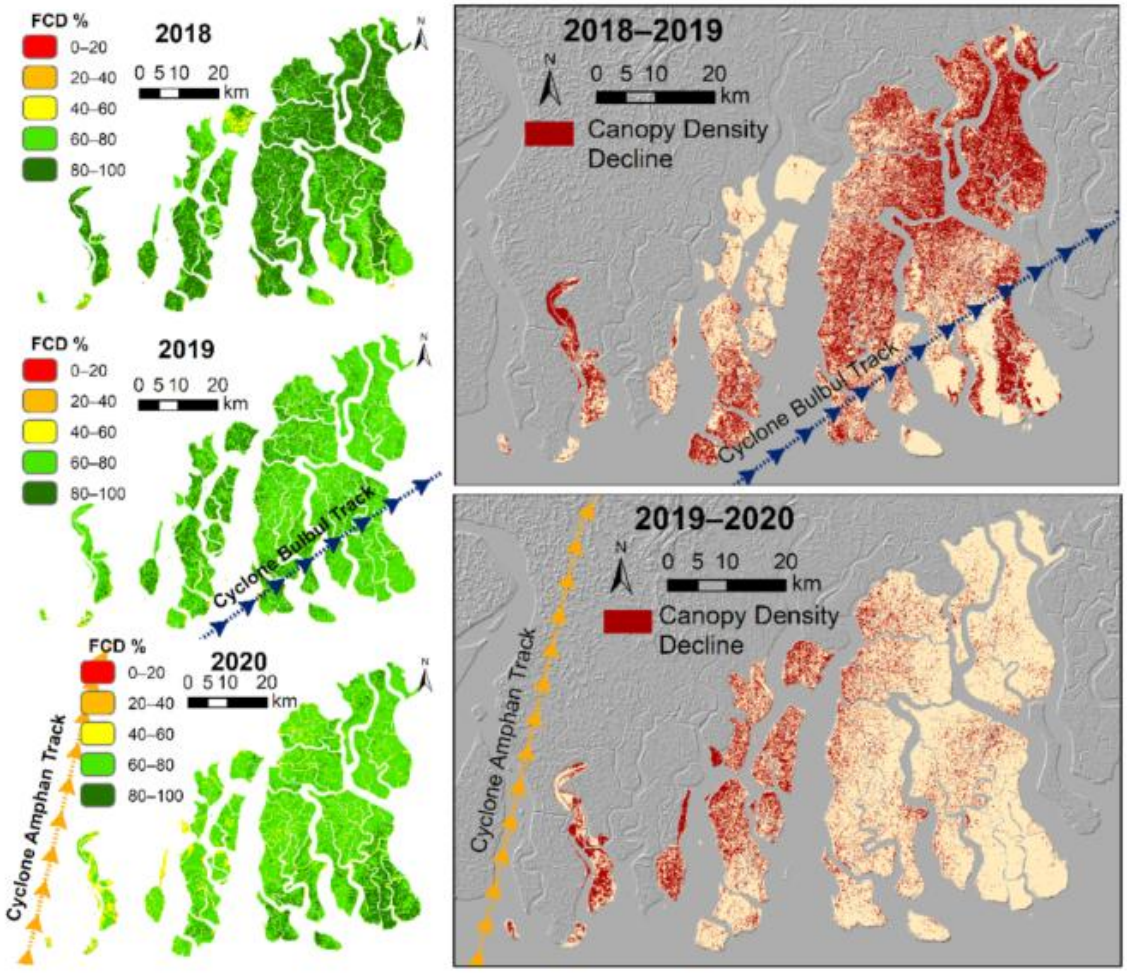

Figure 18 Change in the forest canopy density (FCD) of the mangroves after cyclones Bulbul (2019) and Amphan (2020).

Further analysis using the Enhanced Vegetation Index (EVI) (Figure 19) revealed a considerable decline in mangrove health along the cyclone tracks. Following Cyclone Bulbul, 14.6% (303.6 km²) of the mangrove area experienced high loss, and 45.8% (950.7 km²) suffered low loss. Similar trends were observed after Cyclone Amphan, with 14% (287 km²) experiencing high loss and 51% (1064 km²) showing low loss. Cumulatively, across both cyclones, 13.3% (277 km²) of the area exhibited high loss, while 57.4% (1190 km²) experienced low loss.

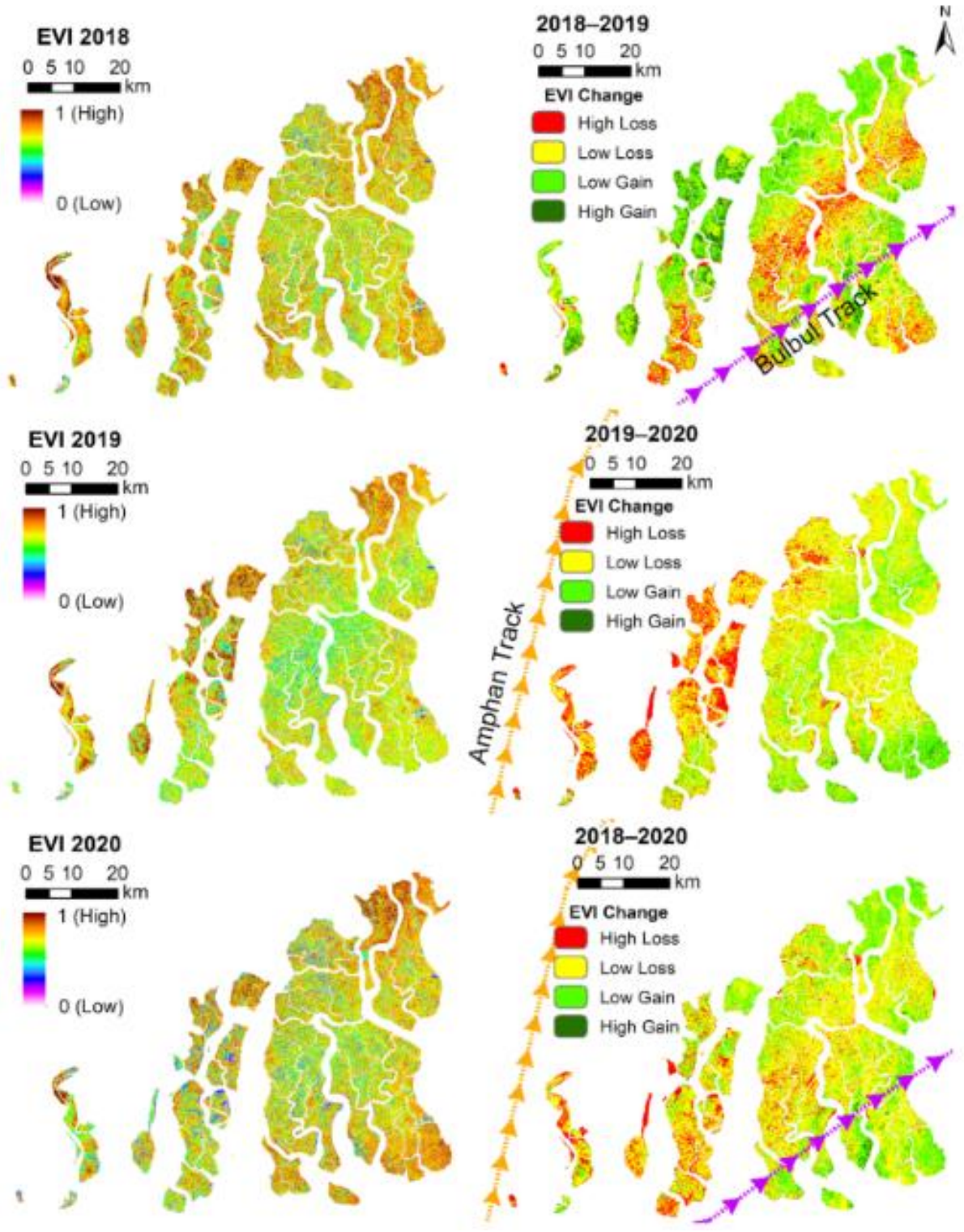

Figure 19 Change in the enhanced vegetation index (EVI) of the mangroves after two consecutive cyclones in 2019 and 2020.

These findings highlight the severe and cumulative impacts of consecutive high-intensity cyclones on the mangrove canopy, with limited recovery time between events. The increased frequency of intense cyclones in the Bay of Bengal poses a significant threat to mangrove

health, leading to canopy degradation and reduced resilience to further climatic and environmental stressors.

5.7 Mangrove Future

5.7.1 Impact of Sea-Level Rise on Sundarbans Mangrove Extent

The simulations using the Sea Level Affecting Marshes Model (SLAMM) coupled with an empirical shoreline erosion model indicate that the Indian Sundarbans are highly vulnerable to sea-level rise (SLR) under all Representative Concentration Pathway (RCP) scenarios. The results, based on Table 15, provide detailed projections for mangrove area changes under various scenarios:

Under the **Continued Protection scenario with Baseline Vertical Accretion (3 mm/year)**, the projections across all RCP scenarios reveal a gradual increase in mangrove area gains; however, these gains are consistently overshadowed by significant losses over time.

For RCP2.6, mangrove area gains are estimated at 1,755 hectares (1%) while losses reach 21,616 hectares (10%) by 2030, followed by gains rising to 4,534 hectares (2%) alongside losses of 38,876 hectares (18%) by 2050, and further increasing to gains of 15,340 hectares (7%) with losses amounting to 87,823 hectares (42%) by 2100.

Table 15 Summary of changes in mangrove area for the combined SLAMM and empirical shoreline erosion model simulations for the various SLR, accretion and management scenarios.

Baseline vertical mangrove accretion 3 mm yr^{-1}													
Continued protection	Run 1 RCP2.6					Run 2 RCP4.5					Run 3 RCP8.5			
	Gain (ha)	%	Loss (ha)	%		Gain (ha)	%	Loss (ha)	%		Gain (ha)	%	Loss (ha)	%
2030	1755	1	21,616	10	2030	1801	1	22,195	11	2030	1842	1	22,759	11
2050	4534	2	38,876	18	2050	5240	2	42,202	20	2050	5754	3	45,708	22
2100	15,340	7	87,823	42	2100	20,220	10	109,010	52	2100	44,651	21	168,421	80

Higher vertical mangrove accretion 6 mm yr^{-1}													
Continued protection	Run 4 RCP2.6					Run 5 RCP4.5					Run 6 RCP8.5			
	Gain	%	Loss	%		Gain	%	Loss	%		Gain	%	Loss	%
2030	1756	1	12,624	6	2030	1801	1	13,078	6	2030	1843	1	13,666	6
2050	4549	2	22,047	10	2050	5343	3	24,524	12	2050	6019	3	27,236	13
2100	18,291	9	45,808	22	2100	20,487	10	62,942	30	2100	44,081	21	122,401	58

Baseline vertical mangrove accretion 3 mm yr^{-1}													
Managed realignment	Run 7 RCP2.6					Run 8 RCP4.5					Run 9 RCP8.5			
	Gain	%	Loss	%		Gain	%	Loss	%		Gain	%	Loss	%
2030	19,360	9	21,640	10	2030	19,858	9	22,215	11	2030	20,398	10	22,782	11
2050	37,683	18	38,909	18	2050	39,785	19	42,239	20	2050	40,804	19	45,749	22
2100	54,329	26	87,992	42	2100	66,752	32	109,294	52	2100	113,855	54	168,782	80

Higher vertical mangrove accretion 6 mm yr^{-1}													
Managed realignment	Run 10 RCP2.6					Run 11 RCP4.5					Run 12 RCP8.5			
	Gain	%	Loss	%		Gain	%	Loss	%		Gain	%	Loss	%
2030	19,359	9	12,624	6	2030	19,855	9	13,080	6	2030	20,397	10	13,669	6
2050	37,693	18	22,058	10	2050	40,819	19	24,535	12	2050	43,921	21	27,251	13
2100	85,063	40	45,831	22	2100	71,729	34	63,030	30	2100	111,149	53	122,707	58

Under RCP4.5, the trend continues with gains of 1,801 hectares (1%) and losses of 22,195 hectares (11%) in 2030, increasing to gains of 5,240 hectares (2%) coupled with losses of 42,202 hectares (20%) by 2050, and reaching gains of 20,220 hectares (10%) while losses escalate to 109,010 hectares (52%) by 2100.

The RCP8.5 scenario demonstrates the most pronounced impacts, with mangrove gains of 1,842 hectares (1%) and losses totalling 22,759 hectares (11%) by 2030, progressing to gains of 5,754 hectares (3%) accompanied by losses of 45,708 hectares (22%) by 2050, and culminating in gains of 44,651 hectares (21%) while losses soar to 168,421 hectares (80%) by 2100 (Figure 20 and Table 15).

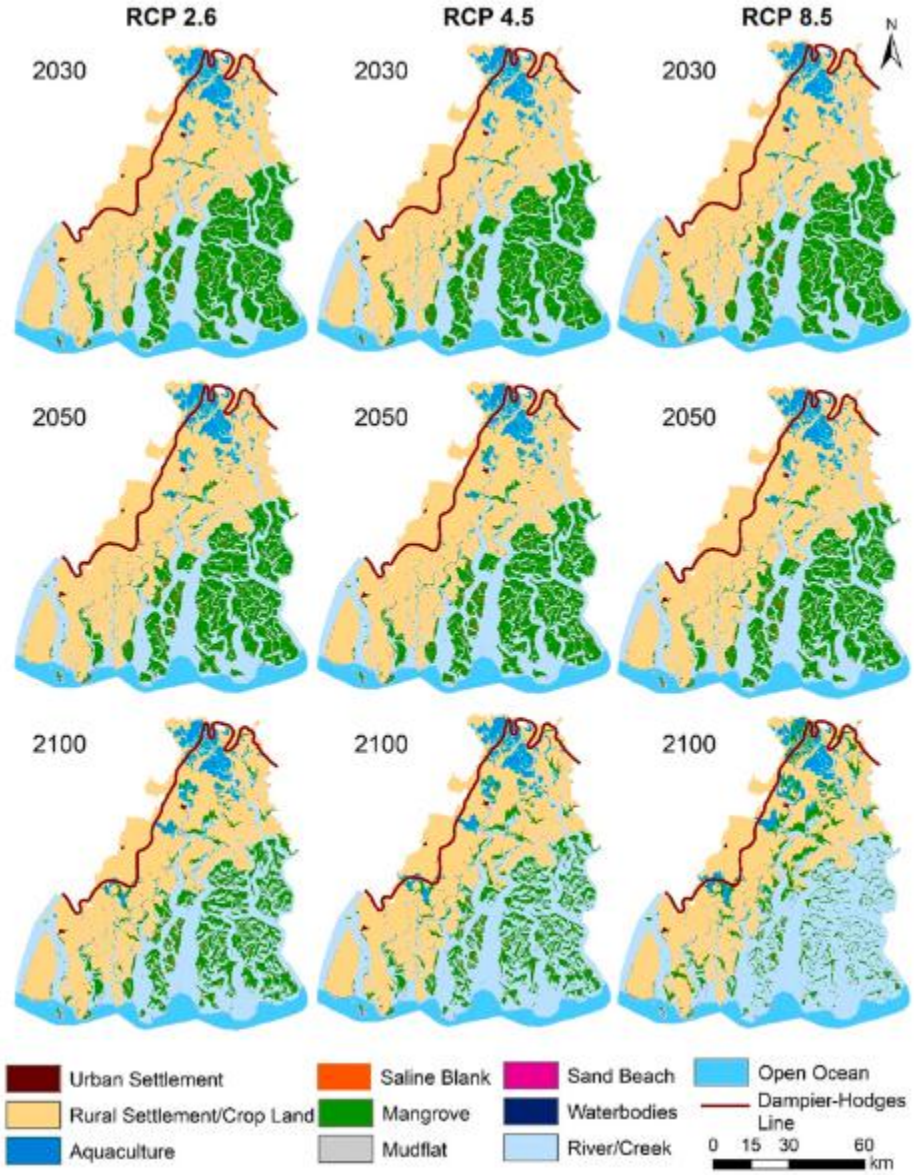

Figure 20 Simulated mangrove area changes due to the net effect of accretion and erosion for RCP2.6 (Run 1), RCP4.5 (Run 2) and RCP8.5 (Run 3) SLR scenarios using a baseline vertical mangrove accretion rate of 3 mm yr-[1] and assuming the Continued Protection scenario

Under the **Continued Protection scenario with Enhanced Vertical Accretion (6 mm/year),** the projections across all RCP scenarios demonstrate improved mangrove area gains compared to baseline accretion, though losses remain considerable.

For RCP2.6, mangrove gains are estimated at 1,756 hectares (1%) alongside losses of 12,624 hectares (6%) by 2030, increasing to gains of 4,549 hectares (2%) with losses of 22,047 hectares (10%) by 2050, and further reaching gains of 18,291 hectares (9%) accompanied by losses of 45,808 hectares (22%) by 2100 (Figure 21 and Table 15).

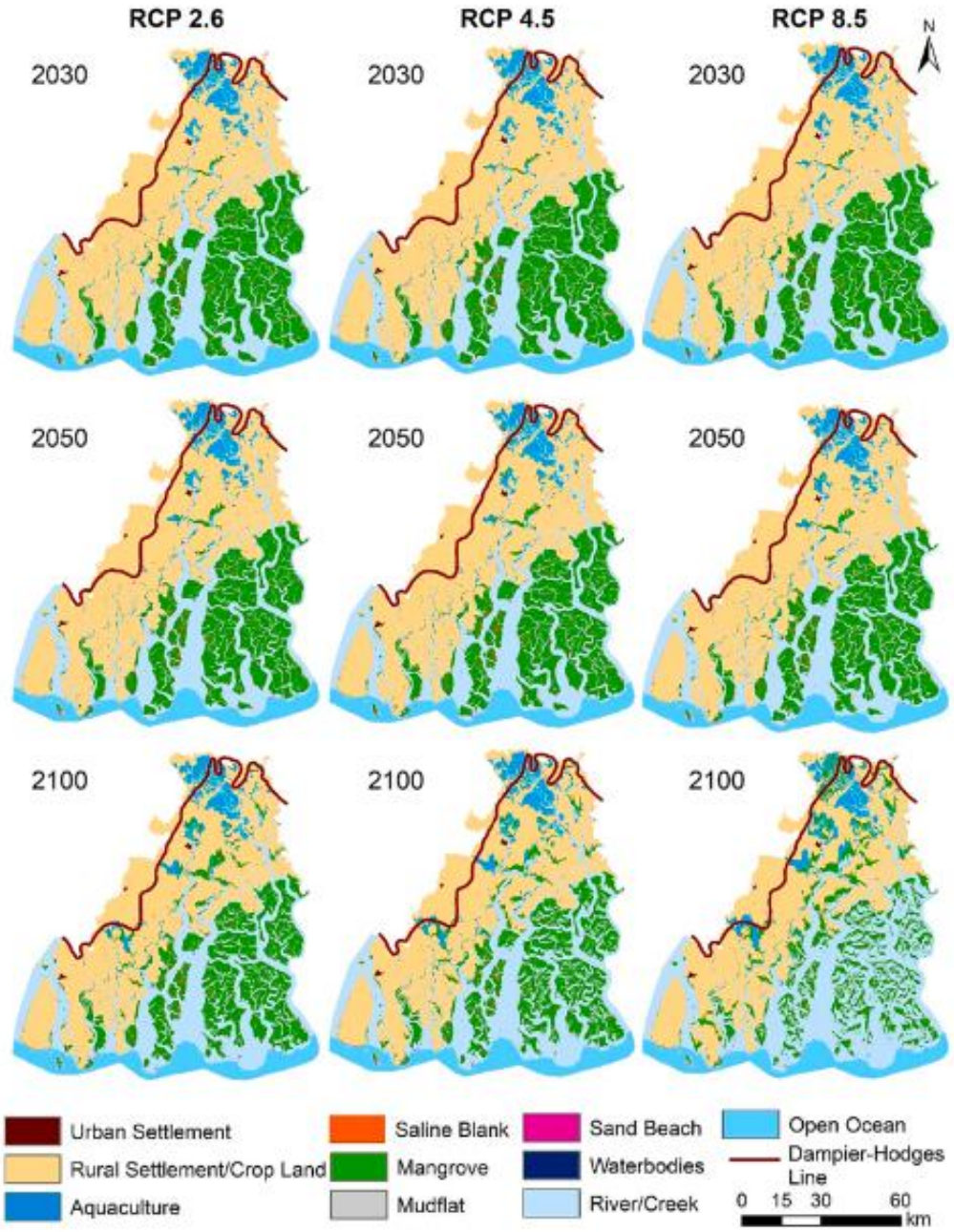

Figure 21 Simulated mangrove loss gains for RCP2.6 (Run 4), RCP4.5 (Run 5) and RCP8.5 (Run 6) scenarios, for a vertical mangrove accretion rate of 6 mm yr^{-1} to represent a plausible threshold for mangrove response to SLR, and assuming the Continued Protection scenario.

In the case of RCP4.5, gains amount to 1,801 hectares (1%) and losses total 13,078 hectares (6%) by 2030, followed by gains of 5,343 hectares (3%) and losses of 24,524 hectares (12%) by 2050, culminating in gains of 20,487 hectares (10%) with losses increasing to 62,942 hectares (30%) by 2100.

Under the RCP8.5 scenario, mangrove area gains rise to 1,843 hectares (1%) while losses reach 13,666 hectares (6%) by 2030, progressing to gains of 6,019 hectares (3%) alongside losses of 27,236 hectares (13%) by 2050, and finally achieving gains of 44,081 hectares (21%) with substantial losses of 122,401 hectares (58%) by 2100.

Under the **Managed Realignment scenario with Baseline Vertical Accretion (3 mm/year)**, projections across all RCP scenarios indicate substantial improvements in mangrove area gains compared to the continued protection scenarios, although losses remain significant. For RCP2.6, mangrove area gains are estimated at 19,360 hectares (9%) with losses of 21,640 hectares (10%) by 2030, increasing to gains of 37,683 hectares (18%) alongside losses of 38,909 hectares (18%) by 2050, and further rising to gains of 54,329 hectares (26%) with losses reaching 87,992 hectares (42%) by 2100.

Under RCP4.5, gains are projected to reach 19,858 hectares (9%) while losses total 22,215 hectares (11%) in 2030, followed by gains increasing to 39,785 hectares (19%) with losses of 42,239 hectares (20%) by 2050, and further expanding to gains of 66,752 hectares (32%) with losses amounting to 109,294 hectares (52%) by 2100.

The RCP8.5 scenario reveals the most significant gains, with mangrove areas increasing by 20,398 hectares (10%) alongside losses of 22,782 hectares (11%) by 2030, rising to gains of 40,804 hectares (19%) and losses of 45,749 hectares (22%) by 2050, and culminating in gains of 113,855 hectares (54%) while losses escalate to 168,782 hectares (80%) by 2100 (Figure 22 and Table 15).

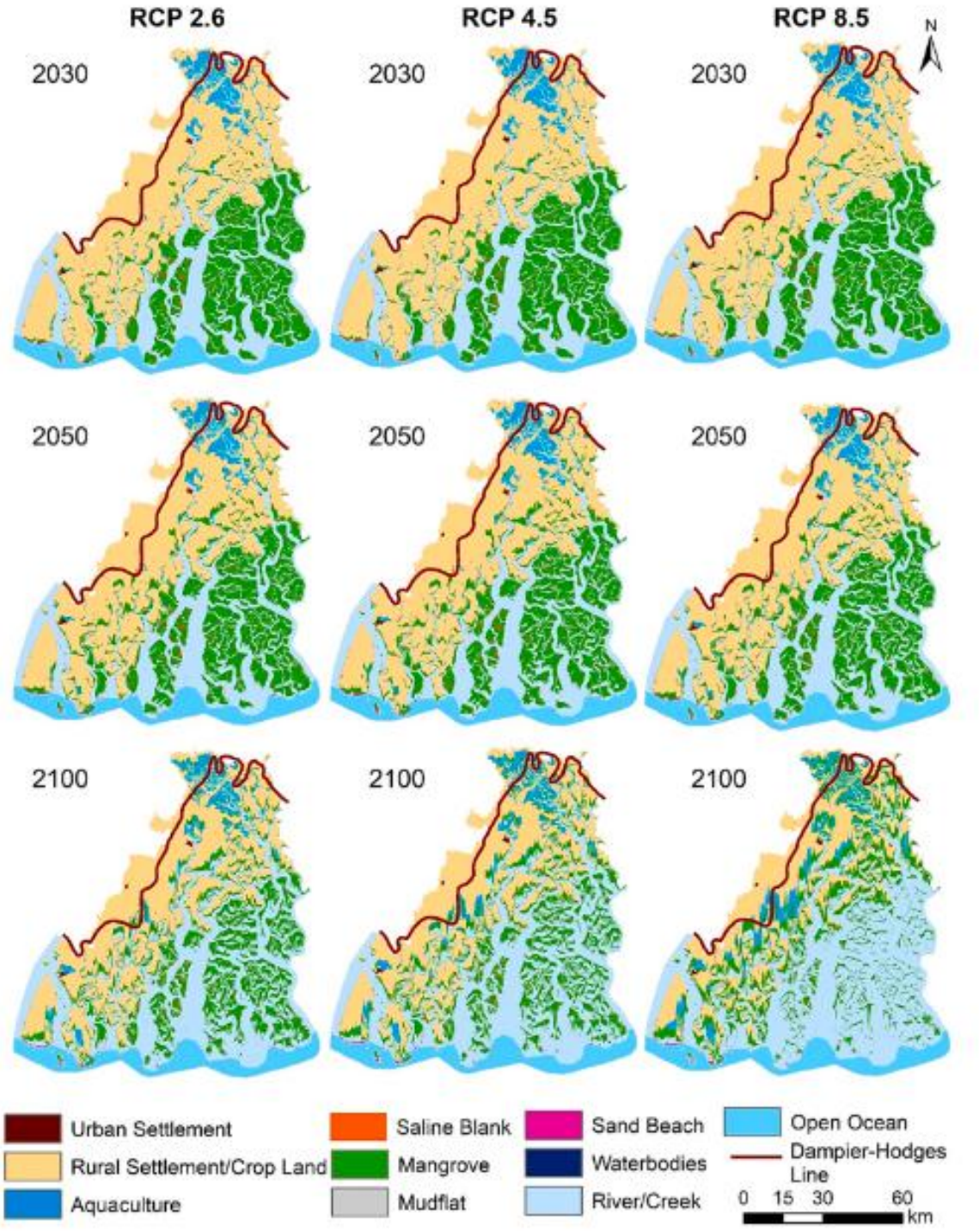

Figure 22 Simulated mangrove loss/gain for RCP2.6 (Run 7), RCP4.5 (Run 8) and RCP8.5 (Run 9) SLR scenarios using a baseline vertical mangrove accretion rate of 3 mm yr^{-1} and assuming the Managed Realignment scenario (inland migration of mangroves allowed).

Under the **Managed Realignment scenario with Enhanced Vertical Accretion (6 mm/year)**, the projections demonstrate significant mangrove area gains while reducing losses compared to baseline accretion, particularly under higher emission scenarios.

For RCP2.6, mangrove gains are projected at 19,359 hectares (9%) with losses of 12,624 hectares (6%) by 2030, increasing to gains of 37,693 hectares (18%) and losses of 22,058 hectares (10%) by 2050, and further expanding to gains of 85,063 hectares (40%) alongside losses of 45,831 hectares (22%) by 2100 (Figure 23 and Table 15).

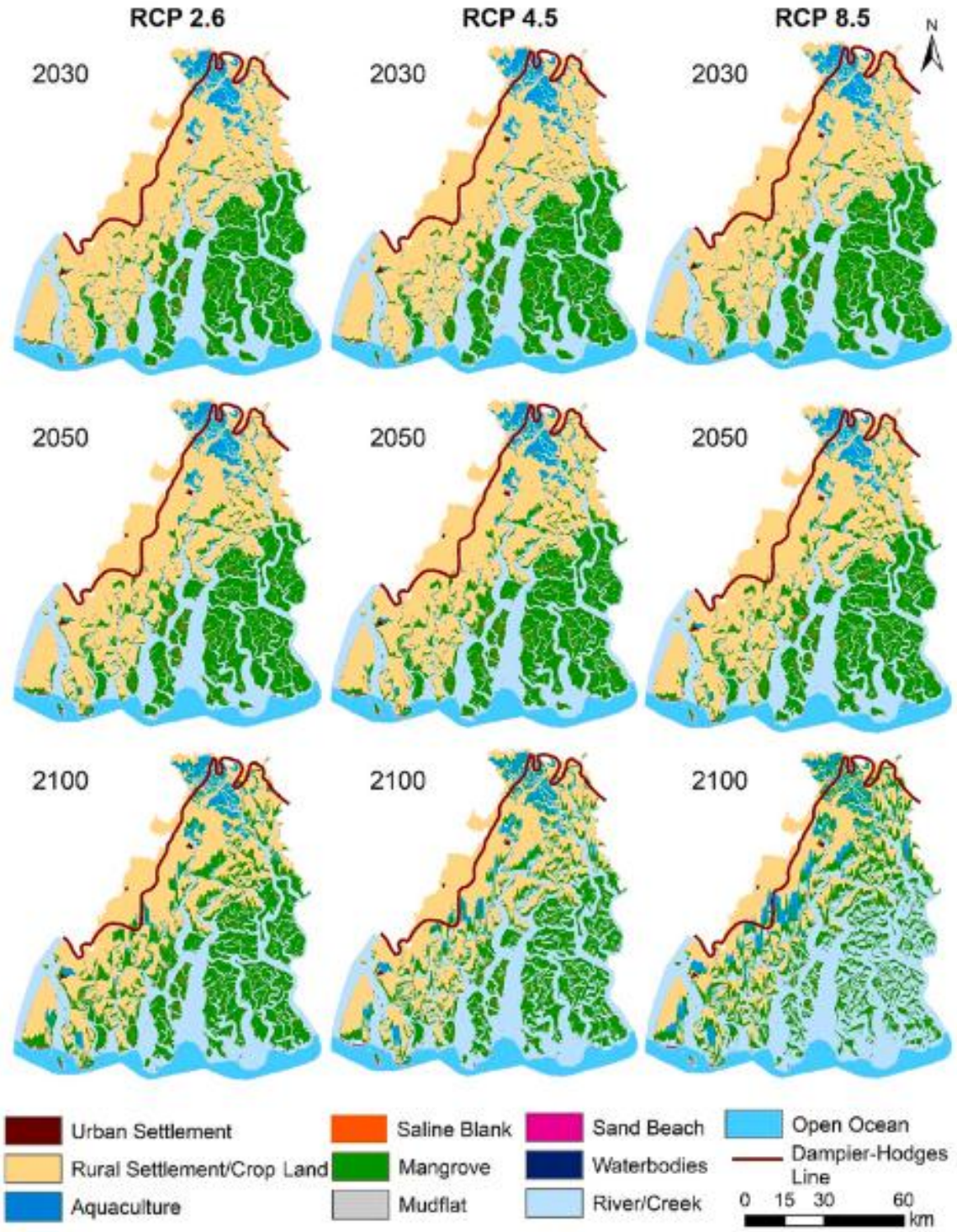

Figure 23 Simulated mangrove loss/gain for RCP2.6 (Run 10), RCP4.5 (Run 11) and RCP8.5 (Run 12) SLR scenarios using a baseline vertical accretion rate of 6 mm yr^{-1} and assuming the Managed Realignment scenario (inland migration of mangroves allowed).

Under RCP4.5, gains are estimated at 19,855 hectares (9%) with losses of 13,080 hectares (6%) by 2030, rising to gains of 40,819 hectares (19%) and losses of 24,535 hectares (12%) by 2050, and reaching 71,729 hectares (34%) with losses of 63,030 hectares (30%) by 2100.

The RCP8.5 scenario reveals the most substantial improvements, with mangrove area gains of 20,397 hectares (10%) and losses of 13,669 hectares (6%) by 2030, followed by gains of 43,921 hectares (21%) and losses of 27,251 hectares (13%) by 2050, and culminating in gains of 111,149 hectares (53%) while losses amount to 122,707 hectares (58%) by 2100.

These results collectively highlight the severe vulnerability of the Indian Sundarbans to sea-level rise (SLR) and emphasize the need for robust adaptive management strategies under varying vertical accretion scenarios. The findings reveal that baseline vertical accretion alone has limited effectiveness in offsetting mangrove losses, even under the most optimistic emissions pathway (RCP2.6), as losses consistently outweigh gains. Enhanced vertical accretion significantly improves outcomes by reducing the rate of mangrove losses and enabling moderate gains; however, under high-emission scenarios like RCP8.5, the scale of losses remains substantial, underscoring the critical need for additional adaptive measures. Projections further demonstrate that managed realignment, even with baseline accretion, provides substantial improvements in mangrove gains compared to continued protection strategies. Notably, Managed Realignment with Enhanced Vertical Accretion emerges as the most effective approach to mitigate mangrove losses and enhance gains. Nevertheless, significant losses persist under high emissions, highlighting the urgent need for emissions reduction and targeted management interventions to safeguard the Sundarbans' mangrove ecosystems from the accelerating impacts of SLR.

Chapter-6

6. Discussions

6.1 Land use dynamics

The Sundarbans, a dynamic deltaic ecosystem, has undergone significant land use and land cover (LULC) changes between 2001 and 2020, driven by a complex interplay of natural forces, human activities, and socio-economic factors. Over the two decades, agricultural practices intensified, urbanization expanded, and environmental changes altered the region's landscape. Double-cropping areas increased by 47.7% between 2001 and 2011 and by another 28.3% from 2011 to 2020, reflecting a shift toward intensive farming. Meanwhile, single-cropping areas saw a steep decline of 38.4%, with over 1,010 km² converted to other uses, including aquaculture and settlements. The rapid expansion of aquaculture, which grew by 8.6% in the first decade and by 37.1% in the second, underscores its economic importance. Rural settlements expanded by 84.4% over two decades, replacing agricultural lands, while urban settlements grew by 64.7%, highlighting infrastructure development and population pressures. Environmental transformations were equally significant, with mudflats decreasing by 53% from 2001 to 2011 and then increasing by 23.9% from 2011 to 2020 due to sedimentary shifts. Wetlands halved during this period, reflecting ecological degradation, while mangroves experienced minor declines, signalling both resilience and vulnerability.

The driving factors behind these changes are diverse. Biophysical drivers such as climate change, rising sea levels, and increased cyclone frequency have profoundly impacted land use. Saltwater intrusion, a consequence of sea-level rise, has rendered agricultural lands unsuitable, while cyclones like Amphan and Bulbul have caused widespread destruction of vegetation and settlements. Terrain characteristics, including elevation and soil salinity, have further dictated the suitability of land for agriculture and settlements. Socio-economic factors have also played a crucial role. Population growth and market demand have driven agricultural expansion, aquaculture growth, and settlement development. The Sundarbans' proximity to urban centres has intensified land conversion for infrastructure and commercial purposes. Institutional policies, including subsidies and conservation regulations, have influenced land use patterns, although enforcement remains a challenge.

The implications of these land use changes are profound. The loss of wetlands and mangroves has degraded biodiversity and increased the region's vulnerability to coastal erosion and storm surges. Soil salinization has reduced agricultural productivity, while mudflat dynamics have altered sedimentation processes, impacting riverine and coastal ecosystems. On the socio-

economic front, the expansion of aquaculture and multi-cropping has bolstered local economies but has also increased dependency on market-driven practices, reducing subsistence resilience. Displacement of natural ecosystems for settlements and infrastructure poses long-term sustainability challenges. Reduced mangrove cover and wetland loss have diminished the region's capacity to mitigate storm surges and absorb carbon, exacerbating climate change impacts.

Addressing these challenges requires a comprehensive, multidisciplinary approach. Ecosystem-based management, including mangrove restoration with salt-tolerant species and wetland conservation, is essential to enhance resilience. Sustainable agricultural practices, such as promoting climate-resilient crops and improving irrigation systems, are necessary to adapt to changing environmental conditions. Integrated planning and policies, such as transboundary water management with Bangladesh and enforcing zoning regulations, can balance development with conservation. Community-based resource management should be strengthened to align conservation goals with local needs, while technological innovations like GIS monitoring and precision agriculture can optimize resource use and reduce environmental impact.

The Sundarbans' land use trajectory reflects a fragile balance between economic development and environmental sustainability. Immediate action is needed to address the socio-economic and ecological drivers of change. This study highlights the importance of integrating ecological, agricultural, and socio-economic data into adaptive management strategies to protect this unique biosphere reserve. A holistic, inclusive approach is essential to ensure the long-term resilience and prosperity of the Sundarbans and its communities.

6.2 Land Use/Land Cover Changes and Future Projections discussion

The projected land use and land cover (LULC) changes in the Sundarbans between 2020 and 2050 underscore the growing tension between economic development and ecological preservation. These changes, driven by urbanization, industrial growth, and environmental pressures, have significant implications for biodiversity, ecosystem services, and regional sustainability. Between 2020 and 2030, urban settlements are expected to increase sharply by 113.6%, driven by population growth and infrastructure needs, primarily at the expense of single-cropped and double-cropped lands, which are projected to decline by 28.4% and 7.8%, respectively. Aquaculture is forecast to grow by 25.4%, expanding from 510.8 km² to 640.4

km², further encroaching on agricultural land and wetlands. Natural ecosystems will experience continued degradation, with mangrove cover declining by 2.5%, waterbodies shrinking by 37.5%, and wetlands reducing by 11.1%. Saline blanks and mudflats are projected to expand by 53.2% and 71.3%, respectively, driven by soil salinization and sediment deposition. Brick kilns will increase by 24.1%, reflecting industrial growth, while barren land will decrease by 40.5%, transitioning into industrial, agricultural, and settlement areas.

From 2030 to 2050, the trend toward urbanization intensifies, with urban settlements projected to increase by another 155.9%. However, aquaculture is expected to decline slightly by 4.4%, likely due to competition for land and environmental regulations. Mangrove cover is anticipated to experience a more significant reduction of 9.7%, as encroachment for settlements and saline blanks continues. Double-cropped land will face a steep decline of 29.7%, primarily due to urban expansion and soil degradation. Saline blanks are expected to grow by 9.0%, reflecting ongoing soil salinization, while mudflats will expand modestly by 3.7%. Wetlands and waterbodies will remain critically low, highlighting their continued vulnerability to land conversion.

These projected LULC changes indicate a clear shift toward urbanization, industrialization, and aquaculture expansion, occurring at the expense of agricultural land, wetlands, and natural ecosystems. Such transformations pose significant challenges for biodiversity conservation, carbon sequestration, and coastal resilience. The loss of mangroves and wetlands will exacerbate vulnerabilities to climate change, including rising sea levels, increased storm surges, and soil salinization. Declining agricultural areas threaten food security and local livelihoods, while the expansion of urban settlements and industrial land intensifies habitat fragmentation and environmental degradation. Although the slight decline in aquaculture post-2030 suggests some regulatory intervention, the continued pressure on natural ecosystems underscores the urgency of sustainable land use planning.

To mitigate these challenges, integrated and adaptive management strategies are essential. Conservation of mangroves and wetlands should be prioritized through restoration efforts and strict protection measures. Sustainable urban planning, incorporating zoning regulations and green infrastructure, is critical to minimizing the ecological footprint of expanding settlements. Climate-resilient agriculture, including agroforestry and crop diversification, can help adapt to soil salinization and reduce dependency on single-cropping systems. Cleaner technologies in

industrial sectors like brick kilns can reduce environmental degradation. Strengthening community-based resource management and leveraging remote sensing and GIS tools for monitoring will be key to aligning conservation goals with socio-economic needs.

The LULC changes projected between 2020 and 2050 highlight the critical need for sustainable development strategies that balance economic growth with ecological preservation. Without proactive measures, the Sundarbans' unique ecosystems face irreversible damage, jeopardizing biodiversity, climate resilience, and regional livelihoods. Future research should focus on scenario-based modelling and stakeholder-driven planning to ensure long-term sustainability and align conservation efforts with socio-economic development goals. These actions are essential to safeguarding this vital region for future generations.

6.3 Mangrove Change discussion

The current study reveals that approximately 110 km² of mangrove forest area was lost in the Indian Sundarbans between 2000 and 2020. A detailed spatial analysis of this loss indicates that the majority occurred within the core regions of the National Park and tiger reserve. In contrast, a gain of 81 km² of mangroves was observed in the fringe areas outside the contiguous forest, primarily through plantation and regeneration efforts. This raises critical questions about whether these compensatory gains can adequately replace the ecological services, such as habitat preservation and blue carbon storage, lost due to mangrove degradation.

To estimate the blue carbon loss over the last two decades, this study utilized the biomass estimates provided by Ray et al. (39.93 ± 14.05 t C ha^{-1} for aboveground and 9.61 ± 3.37 t C ha^{-1} for belowground carbon stores). Based on these values, the loss of mangrove cover is estimated to have resulted in the depletion of 0.29×10^6 t C from aboveground and 0.072×10^6 t C from belowground stores, amounting to a total loss of approximately 0.36×10^6 t C. Additional losses from eroded mangrove soils and carbon trapped in sediments are challenging to quantify due to high spatial variability in soil sediment carbon, but these figures provide a first-order estimate of the carbon that must be restored through future plantation and regeneration efforts.

This study is the first to correlate mangrove health degradation in the Sundarbans with rising maximum air temperatures and declining post-monsoon rainfall. Furthermore, it analyzes the impact of repeated cyclones, noting that two of the four major cyclones occurring within a 24-month period (at six-month intervals) caused severe damage. Historical observations, such as the six-to-seven-year recovery period for mangroves following Cyclone Sidr in Bangladesh,

emphasize the long-term impacts of such events. The combination of rising temperatures, decreased rainfall, and an increased frequency of high-intensity cyclones has significantly impaired mangrove health in the region.

High soil and estuarine salinity have further compounded these challenges, promoting stunted growth, reduced aboveground biomass, and health deterioration. Freshwater-loving mangrove species like Heritiera, Nypa, and Sonneratia are now virtually absent from the Indian Sundarbans. While correlations between soil salinity and mangrove health cannot yet be definitively established due to the lack of time-series data, observations suggest that healthier mangroves are found in buffer zones with some freshwater inputs from rivers like Hugli and Ichamati, compared to more degraded mangroves in saline, sea-facing locations. This warrants further investigation.

The research identifies two major contributors to mangrove degradation in the Sundarbans. The first is the high rate of relative sea-level rise combined with insufficient sediment supply, which has driven significant area losses. The second is the declining health of the remaining mangroves due to reduced freshwater availability, increasing salinity (further exacerbated by sea-level rise), and climatic factors such as rainfall variability and rising temperatures. These stressors have not only led to habitat loss for iconic species like the Bengal tiger but also diminished the region's blue carbon stock. The continuation and potential acceleration of these trends necessitate immediate action from planners and policymakers.

Despite these challenges, one promising finding from this study is the observed growth of fringe mangroves around inhabited islands within inner estuaries. This growth, facilitated by government agencies, NGOs, and local community efforts, highlights the potential of targeted plantation and restoration programs. Regenerating mangroves with salinity-tolerant species in available areas, such as mudflats around estuarine islands, is a viable short-term option. Supporting these efforts with measures like submerged oyster reefs or breakwaters to reduce erosion and offshore sediment loss could further enhance their effectiveness, as evidenced by their success on Kutubdia Island in Bangladesh.

For long-term ecosystem regeneration, addressing salinity increases and nutrient deficiencies is critical, particularly in the context of ongoing climate change. Earlier studies suggest that restoring moribund river channels and implementing intra-basin water transfer to provide approximately 500 $m^3 s^{-1}$ of freshwater could mitigate salinity and support mangrove recovery. However, achieving this will likely require transboundary collaboration between India and

Bangladesh, emphasizing the need for a shared management approach to conserve this globally significant ecosystem.

6.4 Mangrove Future discussion

This study evaluates the vulnerability of the Sundarbans mangrove forests under various sea-level rise (SLR) scenarios, considering the interplay of natural and anthropogenic factors. Using the hybrid Sea Level Affecting Marshes Model (SLAMM) combined with empirical shoreline erosion models, the findings reveal that under business-as-usual scenarios, mangrove losses could range from 42% to 80% by 2100. However, adopting managed realignment strategies, which allow mangroves to migrate inland, could mitigate these losses to some extent. The results emphasize that while SLR is a critical driver of mangrove loss, other factors such as sediment supply, delta subsidence, and coastal management policies significantly influence the ecosystem's resilience. These insights align with earlier global projections, such as those by Spencer et al. (2016), which predicted up to a 78% loss in global coastal wetlands under high SLR scenarios.

Recent research contributions have expanded the understanding of managing and preserving mangrove ecosystems under SLR impacts. For instance, Kanan et al. (2023) explored land cover interactions in the Sundarbans and emphasized the pivotal role of sediment dynamics and human activities in determining mangrove resilience. Their study highlighted that sufficient sediment deposition is crucial for mangroves to keep pace with rising sea levels, suggesting upstream river basin management as a strategy to enhance sediment supply. Additionally, Schuerch et al. (2022) underscored the importance of integrating scientific research with community engagement for managed realignment projects. Their approach, which prioritizes stakeholder involvement, is particularly relevant for the Sundarbans, where over four million people reside in the transition zone. In another study, Kiesel et al. (2022) examined the role of vegetation management in storm surge attenuation, demonstrating that well-designed managed realignment projects with sufficient vegetation cover could reduce storm surge impacts significantly. Applying these principles to the Sundarbans could serve the dual purpose of preserving mangroves and protecting coastal communities from cyclone risks.

The combined insights from this study and recent literature underline the need for an integrated, adaptive management framework for the Sundarbans. Strengthening sediment management through upstream interventions could help mangroves sustain vertical growth relative to rising sea levels, as advocated by Rahman et al. (2022). Managed realignment, while effective in

reducing mangrove losses, requires careful planning, particularly when it involves relocating human populations. Incorporating community-driven approaches, as suggested by Schuerch et al. (2022), could navigate socio-political challenges and enhance acceptance of such strategies. Leveraging nature-based solutions for coastal protection, such as vegetation-rich managed realignment sites, could further bolster resilience against cyclones, as emphasized by Kiesel et al. (2022).

The study identifies several future research directions, including the development of dynamic erosion models that account for localized geomorphological processes, expanding empirical data on sediment deposition rates to refine accretion modelling, and conducting detailed socio-economic impact assessments of managed realignment strategies. These areas of inquiry are crucial for advancing sustainable management practices.

Chapter-7

7. Conclusions

7.1 Land use change in the transition zone and the future projection

The Sundarbans, globally recognized as a critical ecological and socio-economic hotspot, has undergone significant transformations in land use and land cover (LULC) over the past two decades. These changes reflect the intricate interplay of natural forces, human activities, and socio-economic drivers, fundamentally reshaping the region's landscape. This study meticulously analyzed these LULC dynamics and projected future transformations up to 2050, providing essential insights into the challenges facing the region and potential pathways for sustainable management.

Between 2001 and 2020, the Sundarbans witnessed significant shifts in land use patterns. Agricultural intensification, urbanization, and aquaculture expansion dominated the landscape, with rural settlements increasing by 84.4% and urban settlements by 64.7%. These shifts were driven by population pressures, infrastructure development, and economic opportunities associated with aquaculture. Single-cropped lands declined by 38.4%, with over 1,000 km² converted into aquaculture or other uses, while double- and triple-cropping areas expanded to maximize agricultural yields. However, natural ecosystems bore the brunt of these changes. Wetlands declined by 50%, mangroves by 4%, and waterbodies by significant margins, reflecting the degradation of critical ecological assets. These losses, compounded by biophysical challenges such as sea-level rise, increasing soil salinization, and sediment deposition dynamics, have significantly reduced the region’s capacity to mitigate storm surges, sequester carbon, and support biodiversity, with far-reaching implications for climate resilience.

Projections for 2020–2050 indicate that these pressures will intensify. By 2030, urban settlements are expected to increase by 113.6%, and aquaculture by 25.4%, predominantly at the expense of agricultural land, mangroves, and wetlands. Single-cropped land is anticipated to shrink by 28.4%, and mangrove cover may decline by 2.5%. Looking further to 2050, urban settlements are projected to expand by 155.9%, driven by population growth and infrastructure demands, while mangrove cover could decline by an additional 9.7%. The continued growth of saline blanks and mudflats highlights the ongoing impacts of sea-level rise and sediment deposition, further compromising agricultural productivity and ecosystem stability. While aquaculture expansion may stabilize after 2030, its long-term sustainability could be challenged by environmental regulations and competition for land.

The drivers of these transformations are multifaceted, encompassing biophysical, socio-economic, and institutional factors. Climate change, with its associated impacts of rising sea levels, altered sediment dynamics, and increased cyclone frequency, poses a significant threat to the region. Socio-economic drivers, including population growth, market-driven aquaculture expansion, and tourism development, have reshaped land use patterns, often at the expense of ecological integrity. Institutional challenges, including fragmented policy frameworks and inadequate enforcement of conservation measures, have further exacerbated these issues.

The implications of these LULC changes are profound. The loss of wetlands, mangroves, and other natural ecosystems diminishes the region's capacity for carbon sequestration, coastal protection, and biodiversity conservation. Soil salinization and the decline of agricultural lands threaten food security and livelihoods, particularly for marginalized communities dependent on subsistence farming and natural resources. The rapid expansion of urban settlements and industrial activities intensifies habitat fragmentation, resource conflicts, and environmental degradation, jeopardizing the region's ecological and socio-economic stability.

Addressing these challenges requires a comprehensive, integrated, and adaptive management approach. Conservation of mangroves and wetlands must be prioritized through the restoration of degraded mangroves using salt-tolerant species and the enforcement of conservation policies to protect existing wetlands. Sustainable urban and industrial planning, including zoning regulations, green infrastructure, and cleaner technologies in industrial sectors such as brick kilns, is critical to minimizing development's ecological footprint. Climate-resilient agricultural practices, including agroforestry, crop diversification, and sustainable aquaculture, are essential to adapt to soil salinization and ensure food security. Strengthening community-based resource management can align conservation goals with local socio-economic needs, while leveraging remote sensing and GIS tools for real-time monitoring will support informed decision-making. Regional collaboration between India and Bangladesh to manage shared resources and address transboundary challenges is also vital.

Thus, the Sundarbans is at a critical juncture, facing mounting pressures from economic development and environmental challenges. The findings of this study underscore the urgency of adopting sustainable land use strategies that integrate ecological preservation with socio-economic growth. Without proactive measures, the region risks irreversible degradation, with severe consequences for biodiversity, climate resilience, and the well-being of millions who depend on its resources. This research highlights the need for coordinated efforts involving

scientific research, innovative technologies, and stakeholder engagement to ensure the long-term sustainability of the Sundarbans. By prioritizing ecosystem restoration, sustainable land use, and adaptive management, it is possible to protect this invaluable region while supporting its ecological and socio-economic functions. The future of the Sundarbans depends on collective commitment to balancing development with conservation, ensuring its legacy for generations to come.

7.2 Changes in the mangrove forest

This study provides a comprehensive assessment of the dynamics of mangrove forest change in the Indian Sundarbans between 2000 and 2020, revealing critical insights into their decline and underlying drivers. Approximately 110 km² of mangrove forests were lost over the two decades, primarily in the core and buffer zones of the forest. These losses, driven by a combination of shoreline erosion, reduced sediment supply, increasing salinity, and climatic variability, have far-reaching implications for the resilience of this globally significant ecosystem. While 81 km² of mangroves were gained through plantation and regeneration in transition zones, these gains do not adequately compensate for the ecological and carbon sequestration services lost due to the degradation of the contiguous mangrove cover.

Shoreline erosion, influenced by sea-level rise and sediment starvation, emerged as a primary driver of mangrove loss. Upstream river interventions, such as the Farakka Barrage, significantly disrupted sediment flow to the delta, exacerbating erosion and salinization. Rising salinity and reduced freshwater inflows caused a shift in mangrove species composition, with salt-tolerant genera like Avicennia and Ceriops increasingly replacing freshwater-dependent species such as Heritiera fomes and Sonneratia caseolaris. Climatic stressors, including rising air temperatures and declining post-monsoon rainfall, further weakened mangrove health, as evidenced by declining vegetation indices (EVI and NDVI) over the study period. High-intensity cyclones, such as Bulbul (2019) and Amphan (2020), caused severe canopy loss and hampered the natural regeneration process. Consecutive cyclone events within short intervals exacerbated the damage.

The degradation of mangroves has led to a significant decline in their capacity for carbon sequestration, with an estimated 0.36×10^6 t C lost from mangrove biomass during the study period. The fragmentation and reduction of mangrove forests have compromised their ability to act as a buffer against storm surges and tidal impacts, increasing the vulnerability of adjacent coastal communities. Additionally, habitat loss poses a threat to the biodiversity of the

Sundarbans, including iconic species such as the Bengal tiger. These changes highlight the importance of mangroves not only as a critical ecological asset but also as a key component of the region's socio-economic resilience.

Looking ahead, continued sea-level rise, salinity intrusion, and increasing cyclone frequency are expected to accelerate mangrove degradation unless effective mitigation measures are implemented. Restoration efforts focusing on reforestation with salt-tolerant mangrove species, combined with improved freshwater management, are essential for maintaining the ecological integrity of the Sundarbans. To safeguard this critical ecosystem, an integrated approach is needed, addressing both ecological and socio-economic challenges. Ecosystem-based management must prioritize mangrove restoration and the protection of existing forests. Sediment and freshwater management strategies, such as restoring river channels and negotiating transboundary water-sharing agreements with Bangladesh, are critical to enhancing mangrove resilience. Furthermore, engaging local communities in conservation efforts and developing adaptive strategies to mitigate the impacts of climate change are crucial for ensuring the long-term sustainability of the Sundarbans.

This study underscores the urgency of proactive, science-based interventions to preserve the Sundarbans, a critical ecosystem of global ecological and socio-economic importance. By addressing the root causes of mangrove degradation and implementing sustainable land use and conservation strategies, it is possible to secure the future of the Sundarbans for the benefit of both biodiversity and human well-being.

7.3 Future of the Mangrove Forest:

This study employs a hybrid modelling approach, combining the Sea Level Affecting Marshes Model (SLAMM) and empirical shoreline erosion data, to explore the potential impacts of sea-level rise (SLR) on the Indian Sundarbans mangrove forest up to 2100. The results underscore the grave threats posed by SLR, exacerbated by sediment deficits, delta subsidence, and the constraints imposed by flood defences that limit inland migration of mangroves. Under the "business-as-usual" scenario, mangrove loss is projected to range between 10% and 60%, with the higher losses associated with more severe SLR scenarios like RCP8.5.

The study highlights that sediment supply and vertical accretion rates are crucial in determining mangrove resilience. A sediment accretion rate of 6 mm/year could mitigate some losses, but it is unlikely to completely offset the impacts under severe SLR scenarios. Managed realignment, which allows for inland migration of mangroves, emerges as a promising

mitigation strategy. However, this approach necessitates significant socio-political and logistical considerations, as it requires the relocation of millions of people and substantial changes in land-use patterns.

The findings also emphasize the critical role of integrated, system-wide management strategies that include sediment management, climate change mitigation, and adaptive policies to support mangrove resilience. Improved sediment inflows through better upstream river basin management, alongside community engagement and the development of nature-based solutions such as mangrove restoration, are essential to offset the adverse impacts of SLR.

Despite the promising role of managed realignment and sediment management, this study reveals that continued loss of mangrove area is likely, with cascading effects on biodiversity, ecosystem services, and the socio-economic stability of the region. The urgency of addressing these issues is paramount, requiring proactive measures that integrate scientific insights, policy interventions, and stakeholder participation to ensure the sustainability of the Sundarbans mangroves as a globally significant ecosystem. This work contributes valuable insights into the vulnerabilities of coastal ecosystems under climate change and offers a pathway for evidence-based management practices to mitigate these challenges.

The Sundarbans, located in India, stand at a critical juncture. On one hand, the region faces increasing challenges from growing population pressures, unwise land conversions, and unsustainable development patterns, which are significantly amplifying the vulnerability of both the human and natural ecosystems. On the other hand, the escalating impacts of climate-related hazards are threatening the very survival of the mangrove ecosystem, which plays a crucial role in providing vital, yet intangible, ecosystem services for humanity. This delicate balance underscores the urgent need for the formulation and implementation of sustainable policies that foster a blue economy, ensuring inclusive growth and long-term resilience for the region. Now more than ever, it is essential to prioritize both environmental preservation and sustainable socio-economic development, creating a future where the region thrives harmoniously with its natural resources.

References:

1. Abd-El Monsef, H., & Smith, S. E. (2017). A new approach for estimating mangrove canopy cover using Landsat 8 imagery. *Computers and Electronics in Agriculture*, *135*, 183-194. https://doi.org/10.1016/j.compag.2017.02.007
2. Akumu, C. E., Pathirana, S., Baban, S., & Bucher, D. (2011). Examining the potential impacts of sea level rise on coastal wetlands in north-eastern NSW, Australia. *Journal of Coastal Conservation*, *15*, 15-22. https://doi.org/10.1007/s11852-010-0114-3
3. Alcamo, J. (2001). Environment, security and the question of quantification. *International Journal of Sustainable Development*, *4*(2), 139-156. https://doi.org/10.1504/IJSD.2001.001551
4. Alcamo, J., & Henrichs, T. (2008). Chapter two towards guidelines for environmental scenario analysis. *Developments in integrated environmental assessment*, *2*, 13-35. https://doi.org/10.1016/S1574-101X(08)00402-X
5. Ali, S.A., Khatun, R., Ahmad, A. et al. Application of GIS-based analytic hierarchy process and frequency ratio model to flood vulnerable mapping and risk area estimation at Sundarban region, India. Model. Earth Syst. Environ. 5, 1083–1102 (2019). https://doi.org/10.1007/s40808-019-00593-z
6. Allison, M. A. (1998). Geologic framework and environmental status of the Ganges-Brahmaputra Delta. *Journal of Coastal Research*, 827-836.
7. Alongi, D. (2009). *The energetics of mangrove forests*. Springer Science & Business Media.
8. Alongi, D. M. (2008). Mangrove forests: resilience, protection from tsunamis, and responses to global climate change. *Estuarine, coastal and shelf science*, *76*(1), 1-13. https://doi.org/10.1016/j.ecss.2007.08.024
9. Alongi, D. M. (2014). Carbon cycling and storage in mangrove forests. *Annual review of marine science*, *6*(1), 195-219. https://doi.org/10.1146/annurev-marine-010213-135020
10. AppEEARS Team. (2020). *Application for Extracting and Exploring Analysis Ready Samples (AppEEARS); Ver. 2.42.1*. NASA EOSDIS Land Processes Distributed Active Archive Center (LP DAAC), USGS/Earth Resources Observation and Science (EROS) Center: Sioux Falls, SD, USA. Available online: https://lpdaacsvc.cr.usgs.gov/appeears (accessed on 6 June 2020).

11. Arkema, K. K., Guannel, G., Verutes, G., Wood, S. A., Guerry, A., Ruckelshaus, M., ... & Silver, J. M. (2013). Coastal habitats shield people and property from sea-level rise and storms. *Nature climate change*, *3*(10), 913-918. https://doi.org/10.1038/nclimate1944
12. Arsanjani, J. J., Helbich, M., Kainz, W., & Boloorani, A. D. (2013). Integration of logistic regression, Markov chain and cellular automata models to simulate urban expansion. *International Journal of Applied Earth Observation and Geoinformation*, *21*, 265-275. https://doi.org/10.1016/j.jag.2011.12.014
13. Atkinson, P. M., & Tatnall, A. R. (1997). Introduction neural networks in remote sensing. *International Journal of remote sensing*, *18*(4), 699-709. https://doi.org/10.1080/014311697218700
14. Atwood, T. B., Connolly, R. M., Almahasheer, H., Carnell, P. E., Duarte, C. M., Ewers Lewis, C. J., ... & Lovelock, C. E. (2017). Global patterns in mangrove soil carbon stocks and losses. *Nature Climate Change*, *7*(7), 523-528. https://doi.org/10.1038/nclimate3326
15. Awty-Carroll, K., Bunting, P., Hardy, A. and Bell, G., 2019. Using Continuous Change Detection and Classification of Landsat Data to Investigate Long-Term Mangrove Dynamics in the Sundarbans Region. Remote Sensing, 11(23), p.2833. https://doi.org/10.3390/rs11232833
16. B. A. E. & S. (2013). District *statistical handbook, South 24 Parganas and North 24 Parganas*. Department of Statistics and Programme Implementation, The Government of West Bengal. Kolkata, New Secretariat Buildings: Bureau of Applied Economics and Statistics (B.A.E. & S). http://www.wbpspm.gov.in/publications/District%20Statistical%20Handbook. Accessed 22 Nov 2018.
17. Bandyopadhyay, S. (2019). Sundarban: A review of evolution and geomorphology. Retrieved from https://www.academia.edu/download/62538575/Bandyopadhyay_2019_Sundarban_Evolution_and_Geomorphology_World_Bank_Rep20200329-101766-x4920p.pdf
18. Banerjee, K., Senthilkumar, B., Purvaja, R., & Ramesh, R. (2012). Sedimentation and trace metal distribution in selected locations of Sundarbans mangroves and Hooghly estuary, Northeast coast of India. *Environmental geochemistry and health*, *34*, 27-42. https://doi.org/10.1007/s10653-011-9388-0

19. Barbier, E. B., Hacker, S. D., Kennedy, C., Koch, E. W., Stier, A. C., & Silliman, B. R. (2011). The value of estuarine and coastal ecosystem services. *Ecological monographs*, *81*(2), 169-193. https://doi.org/10.1890/10-1510.1
20. Becker, M.; Papa, F.; Karpytchev, M.; Delebecque, C.; Krien, Y.; Khan, J.U.; Ballu, V.; Durand, F.; Cozannet, G.L.; Saiful Islam,A.K.M.; et al. Water level changes, subsidence, and sea-level rise in the Ganges–Brahmaputra–Meghna delta. Proc. Natl. Acad. Sci.USA 2020, 117, 1867–1876. https://doi.org/10.1073/pnas.1912921117
21. Bera, R., & Maiti, R. (2019). Quantitative analysis of erosion and accretion (1975–2017) using DSAS—A study on Indian Sundarbans. *Regional Studies in Marine Science*, *28*, 100583. https://doi.org/10.1016/j.rsma.2019.100583
22. Bhadra, T., Das, S., Hazra, S., & Barman, B. C. (2018). Assessing the demand, availability and accessibility of potable water in Indian Sundarban biosphere reserve area. *Int J Recent Sci Res*, *9*(3), 25437-25.
23. Bhadra, T., Hazra, S., Ray, S. S., & Barman, B. C. (2020). Assessing the groundwater quality of the coastal aquifers of a vulnerable delta: A case study of the Sundarban Biosphere Reserve, India. Groundwater for sustainable development, 11, 100438. https://doi.org/10.1016/j.gsd.2020.100438
24. Bhui, K., Hazra, S., Bhadra, T., & Venugopal, V. (2022). Spatio-temporal variability of tidal velocities in the rivers of the Indian Sundarban Delta: A hydrodynamic modelling approach. *Journal of The Institution of Engineers (India): Series C*, 1-15. https://doi.org/10.1007/s40032-021-00798-1
25. Borón, V., Payán, E., MacMillan, D., & Tzanopoulos, J. (2016). Achieving sustainable development in rural areas in Colombia: Future scenarios for biodiversity conservation under land use change. *Land use policy*, *59*, 27-37. https://doi.org/10.1016/j.landusepol.2016.08.017
26. Brown, S., & Nicholls, R. J. (2015). Subsidence and human influences in mega deltas: the case of the Ganges–Brahmaputra–Meghna. *Science of the Total Environment*, *527*, 362-374. https://doi.org/10.1016/j.scitotenv.2015.04.124
27. Bruun, P. (1962). Sea-level rise as a cause of shore erosion. *Journal of the Waterways and Harbors division*, *88*(1), 117-130. https://doi.org/10.1061/JWHEAU.0000252
28. Bryan, B. A., Nolan, M., McKellar, L., Connor, J. D., Newth, D., Harwood, T., ... & Hatfield-Dodds, S. (2016). Land-use and sustainability under intersecting global change and domestic policy scenarios: Trajectories for Australia to 2050. *Global Environmental Change*, *38*, 130-152. https://doi.org/10.1016/j.gloenvcha.2016.03.002

29. Bryan-Brown, D. N., Connolly, R. M., Richards, D. R., Adame, F., Friess, D. A., & Brown, C. J. (2020). Global trends in mangrove forest fragmentation. *Scientific reports*, *10*(1), 7117. https://doi.org/10.1038/s41598-020-63880-1
30. Cahoon, D. R., & Lynch, J. C. (1997). Vertical accretion and shallow subsidence in a mangrove forest of southwestern Florida, USA. *Mangroves and Salt Marshes*, *1*, 173-186. https://doi.org/10.1023/A:1009904816246
31. Carugati, L., Gatto, B., Rastelli, E., Lo Martire, M., Coral, C., Greco, S., & Danovaro, R. (2018). Impact of mangrove forests degradation on biodiversity and ecosystem functioning. *Scientific reports*, *8*(1), 13298. https://doi.org/10.1038/s41598-018-31683-0
32. Chakrabarti, A. (1992). The Word and the World.
33. Chan, J. C. W., Chan, K. P., & Yeh, A. G. O. (2001). Detecting the nature of change in an urban environment: A comparison of machine learning algorithms. *Photogrammetric Engineering and Remote Sensing*, *67*(2), 213-226.
34. Chand, B. K., Trivedi, R. K., Dubey, S. K., & Beg, M. M. (2012). Aquaculture in changing climate of Sundarban: survey report on climate change vulnerabilities, aquaculture practices & coping measures in Sagar and Basanti blocks of Indian Sundarban. *West Bengal University of Animal & Fishery Sciences, Kolkata, India, 198pp*.
35. Chander, G., Xiong, X. J., Choi, T. J., & Angal, A. (2010). Monitoring on-orbit calibration stability of the Terra MODIS and Landsat 7 ETM+ sensors using pseudo-invariant test sites. *Remote Sensing of Environment*, *114*(4), 925-939. https://doi.org/10.1109/TGRS.2007.907426
36. Chatterjee, M., Shankar, D., Sen, G.K., Sanyal, P., Sundar, D., Michael, G.S., Chatterjee, A., Amol, P., Mukherjee, D., Suprit, K. and Mukherjee, A., 2013. Tidal variations in the Sundarbans estuarine system, India. Journal of Earth System Science, 122, pp.899-933. https://doi.org/10.1007/s12040-013-0314-y
37. Chatterjee, N., Mukhopadhyay, R., & Mitra, D. (2015). Decadal changes in shoreline patterns in Sundarbans, India. http://drs.nio.org/drs/handle/2264/4847
38. Chatterjee, S. (1990). Land reclamations in the Sundarbans – An overview. Retrieved from https://www.jstor.org/stable/44148257
39. Chatterjee, S. (1990). Land reclamations in the Sundarbans-an overview. In *Proceedings of the Indian History Congress* (Vol. 51, pp. 440-446). Indian History Congress.

40. Chatterjee, S. (2016). Strains of settlement: Reclamation and cultivation in the Sundarbans – Myth and history. Retrieved from https://www.academia.edu/download/89133031/Tilling_the_Land_2nd_Proof_with_cover_page_v2.pdf#page=207
41. Chatterjee, S., Maiti, S. K., & Bhattacharyya, S. (2013). Estuarine and coastal geomorphology of the Indian Sundarbans: A remote sensing and GIS approach. Geographical Journal of India, 79(4), 389-405.
42. Chattopadhyay, A. (1994). Some aspects of the village in ancient bengal: size and periphery. In *Proceedings of the Indian History Congress* (Vol. 55, pp. 108-114). Indian History Congress.
43. Chattopadhyaya, I., & Chattopadhyaya, U. C. (1990). The spatial organization of mortuary practices in the Mesolithic Ganga valley: implications for territoriality. *Adaptation and Other Essays*, 103-109.
44. Chaudhuri, A. B. (2007). *Biodiversity of mangroves*. Daya Books.
45. Chaudhuri, A. B., & Choudhury, A. (1994). *Mangroves of the Sundarbans. Volume 1: India* (pp. xii+-247).
46. Chavez, P. S. (1996). Image-based atmospheric corrections-revisited and improved. *Photogrammetric engineering and remote sensing*, *62*(9), 1025-1035.
47. Chellamani, P., Singh, C. P., & Panigrahy, S. (2014). Assessment of the health status of Indian mangrove ecosystems using multi temporal remote sensing data. *Tropical Ecology*, *55*(2), 245-253. ISSN 0564-3295.
48. Chopra, Kanchan & Kapuria, Preeti & Kumar, Pushpam, 2009. "Biodiversity Land Use Change and Human Well being: A Study of Aquaculture in the Indian Sundarbans," OUP Catalogue, Oxford University Press, number 9780198060215, Decembrie.
49. Chowdhury, M. S., & Hafsa, B. (2022). Multi-decadal land cover change analysis over Sundarbans Mangrove Forest of Bangladesh: A GIS and remote sensing-based approach. Retrieved from https://www.sciencedirect.com/science/article/pii/S2351989422001536
50. Civco, D. L. (1993). Artificial neural networks for land-cover classification and mapping. *International journal of geographical information science*, *7*(2), 173-186. https://doi.org/10.1080/02693799308901949
51. Clough, J. S., Park, R. A., & Fuller, R. (2010). SLAMM 6 beta technical documentation, Release 6.0 Beta. *Warren Pinnacle Consulting: Warren, VT*.

52. Clough, J., Polaczyk, A., & Propato, M. (2016). Modeling the potential effects of sea-level rise on the coast of New York: Integrating mechanistic accretion and stochastic uncertainty. *Environmental Modelling & Software*, *84*, 349-362. https://doi.org/10.1016/j.envsoft.2016.06.023
53. Cole Ekberg, M. L., Raposa, K. B., Ferguson, W. S., Ruddock, K., & Watson, E. B. (2017). Development and application of a method to identify salt marsh vulnerability to sea level rise. *Estuaries and Coasts*, *40*, 694-710. https://doi.org/10.1007/s12237-017-0219-0
54. Costanza, R., Sklar, F. H., & White, M. L. (1990). Modeling coastal landscape dynamics. *BioScience*, *40*(2), 91-107. https://doi.org/10.2307/1311342
55. Craft, C., Pennings, S., Clough, J., Park, R., & Ehman, J. (2009). SLR and ecosystem services: a response to Kirwan and Guntenspergen. *Frontiers in Ecology and the Environment*, *7*(3), 127-128.
56. Das, K., & Das, K. (2023). Perils of premature reclamation: Case studies from the Indian Sundarbans. In Springer Climate. https://link.springer.com/chapter/10.1007/978-3-031-42231-7_18
57. Das, S., Ghosh, A., Hazra, S., Ghosh, T., de Campos, R.S. and Samanta, S., 2020. Linking IPCC AR4 & AR5 frameworks for assessing vulnerability and risk to climate change in the Indian Bengal Delta. Progress in Disaster Science, 7, p.100110. https://doi.org/10.1016/j.pdisas.2020.100110
58. DasGupta, R., & Shaw, R. (2019). Resilience building in the Indian Sundarbans through climate-adaptive planning. Sustainability, 11(3), 756. https://doi.org/10.3390/su11030756
59. DasGupta, R., Hashimoto, S., Okuro, T., & Basu, M. (2019). Scenario-based land change modelling in the Indian Sundarban delta: An exploratory analysis of plausible alternative regional futures. *Sustainability Science*, *14*, 221-240. https://doi.org/10.1007/s11625-018-0642-6
60. Datta, D., & Deb, S. (2012). Analysis of coastal land use/land cover changes in the Indian Sunderbans using remotely sensed data. *Geo-spatial Information Science*, *15*(4), 241-250. https://doi.org/10.1080/10095020.2012.714104
61. Didan, K. (2015). *MOD13Q1 MODIS/Terra Vegetation Indices 16-Day L3 Global 250m SIN Grid V006*. NASA EOSDIS Land Processes DAAC. Available online: https://lpdaac.usgs.gov/data/ (accessed on 6 June 2020).

62. Dittmar, T., Hertkorn, N., Kattner, G., & Lara, R. J. (2006). Mangroves, a major source of dissolved organic carbon to the oceans. *Global biogeochemical cycles*, *20*(1). https://doi.org/10.1029/2005GB002570
63. Dodd, R. S., & Ong, J. E. (2008). Future of mangrove ecosystems to 2025.
64. Donato, D. C., Kauffman, J. B., Murdiyarso, D., Kurnianto, S., Stidham, M., & Kanninen, M. (2011). Mangroves among the most carbon-rich forests in the tropics. *Nature geoscience*, *4*(5), 293-297.
65. Doughty, C. L., Langley, J. A., Walker, W. S., Feller, I. C., Schaub, R., & Chapman, S. K. (2016). Mangrove range expansion rapidly increases coastal wetland carbon storage. *Estuaries and Coasts*, *39*, 385-396. https://doi.org/10.1007/s12237-015-9993-8
66. Duarte, C. M., Losada, I. J., Hendriks, I. E., Mazarrasa, I., & Marbà, N. (2013). The role of coastal plant communities for climate change mitigation and adaptation. *Nature climate change*, *3*(11), 961-968. https://doi.org/10.1038/nclimate1970
67. Dubey, S. K., Chand, B. K., Trivedi, R. K., Mandal, B., & Rout, S. K. (2016). Evaluation on the prevailing aquaculture practices in the Indian Sundarban delta: an insight analysis. *Journal of Food, Agriculture & Environment*, *14*(2), 133-141.
68. Duggin, M. J., & Robinove, C. J. (1990). Assumptions implicit in remote sensing data acquisition and analysis. *Remote Sensing*, *11*(10), 1669-1694. https://doi.org/10.1080/01431169008955124
69. Dutta, S. K. (2023). Exploitation, reclamation and struggle: A review of the history of Sundarbans in West Bengal. Retrieved from https://www.researchgate.net/profile/Jayanta-Mete/publication/377768706_EDUCATION_IN_21ST_CENTURY/links/65b7890d1e1ec12eff5ea120/EDUCATION-IN-21ST-CENTURY.pdf#page=142
70. Eastman, J. R. (2009). *IDRISI Taiga guide to GIS and image processing: Manual version 16.02*. Clark Labs.
71. Eastman, J. R., Jiang, H., & Toledano, J. (1998). Multi-criteria and multi-objective decision making for land allocation using GIS. *Multicriteria analysis for land-use management*, 227-251. https://doi.org/10.1007/978-94-015-9058-7_13
72. Eaton, R. M. (1993). *The rise of Islam and the Bengal frontier, 1204-1760* (Vol. 17). Univ of California Press.

73. Farr, T. G., Rosen, P. A., Caro, E., Crippen, R., Duren, R., Hensley, S., ... & Alsdorf, D. (2007). The shuttle radar topography mission. *Reviews of geophysics*, *45*(2). https://doi.org/10.1029/2005RG000183
74. Felsenstein, D., & Lichter, M. (2014). Land use change and management of coastal areas: Retrospect and prospect. *Ocean & coastal management*, *101*, 123-125. https://doi.org/10.1016/j.ocecoaman.2014.09.013
75. Feng, Y., & Liu, Y. (2016). Scenario prediction of emerging coastal city using CA modeling under different environmental conditions: a case study of Lingang New City, China. *Environmental monitoring and assessment*, *188*, 1-15. https://doi.org/10.1007/s10661-016-5558-y
76. FIELD, C., OSBORN, J., HOFFMAN, L., POLSENBERG, J., ACKERLY, D., BERRY, J., ... & MOONEY, H. (1998). Mangrove biodiversity and ecosystem function. *Global Ecology & Biogeography Letters*, *7*(1), 3-14. https://doi.org/10.1111/j.1466-8238.1998.00278.x
77. French, J. (2006). Tidal marsh sedimentation and resilience to environmental change: exploratory modelling of tidal, sea-level and sediment supply forcing in predominantly allochthonous systems. *Marine Geology*, *235*(1-4), 119-136. https://doi.org/10.1016/j.margeo.2006.10.009
78. Ghosh, A., Schmidt, S., Fickert, T. and Nüsser, M., 2015. The Indian Sundarban mangrove forests: history, utilization, conservation strategies, and local perception. Diversity, 7(2), pp.149-169. https://doi.org/10.3390/d7020149
79. Ghosh, M. K., Kumar, L., & Langat, P. K. (2019). Geospatial modelling of the inundation levels in the Sundarbans mangrove forests due to the impact of sea level rise and identification of affected species and regions. *Geomatics, Natural Hazards and Risk*.
80. Ghosh, M. K., Kumar, L., & Roy, C. (2016). Mapping long-term changes in mangrove species composition and distribution in the Sundarbans. *Forests*, *7*(12), 305. https://doi.org/10.3390/f7120305
81. Ghosh, S. (2010). Sustainability potential of suburban gardens: review and new directions. *Australasian Journal of Environmental Management*, *17*(3), 165-175. https://doi.org/10.1080/14486563.2010.9725263
82. Ghosh, S., Hazra, S., Nandy, S., Mondal, P. P., Watham, T., & Kushwaha, S. P. S. (2018). Trends of sea level in the Bay of Bengal using altimetry and other complementary

techniques. *Journal of Spatial Science*, *63*(1), 49-62. https://doi.org/10.1080/14498596.2017.1348309

83. Gilman, E., Van Lavieren, H., Ellison, J., Jungblut, V., Wilson, L., Areki, F., ... & Yuknavage, K. (2006). Pacific Island Mangroves in a Changing Climate and Rising Sea-UNEP Regional Seas Reports and Studies No. 179. *N/A*.
84. Giri, C., Ochieng, E., Tieszen, L. L., Zhu, Z., Singh, A., Loveland, T., ... & Duke, N. (2011). Status and distribution of mangrove forests of the world using earth observation satellite data. *Global ecology and biogeography*, *20*(1), 154-159. https://doi.org/10.1111/j.1466-8238.2010.00584.x
85. Giri, C., Ochieng, E., Tieszen, L. L., Zhu, Z., Singh, A., Loveland, T., ... & Duke, N. (2010). Status and distribution of mangrove forests of the world using earth observation satellite datageb_584.
86. Giri, C., Pengra, B., Zhu, Z., Singh, A. and Tieszen, L.L., 2007. Monitoring mangrove forest dynamics of the Sundarbans in Bangladesh and India using multi-temporal satellite data from 1973 to 2000. Estuarine, coastal and shelf science, 73(1-2), pp.91-100. https://doi.org/10.1016/j.ecss.2006.12.019
87. Giri, P. K., De, S. S., Dehuri, S., & Cho, S. B. (2021). Biogeography based optimization for mining rules to assess credit risk. *Intelligent Systems in Accounting, Finance and Management*, *28*(1), 35-51. https://doi.org/10.1002/isaf.1486
88. Giri, S., Mukhopadhyay, A., Hazra, S., Mukherjee, S., Roy, D., Ghosh, S., ... & Mitra, D. (2014). A study on abundance and distribution of mangrove species in Indian Sundarban using remote sensing technique. *Journal of coastal conservation*, *18*, 359-367. https://doi.org/10.1007/s11852-014-0322-3
89. Giri, S., Samanta, S., Mondal, P.P., Basu, O., Khorat, S., Chanda, A. and Hazra, S., 2022. A geospatial assessment of growth pattern of aquaculture in the Indian Sundarbans Biosphere Reserve. Environment, Development and Sustainability, 24(3), pp.4203-4225. https://doi.org/10.1007/s10668-021-01612-9
90. Goldberg, L., Lagomasino, D., Thomas, N., & Fatoyinbo, T. (2020). Global declines in human-driven mangrove loss. *Global change biology*, *26*(10), 5844-5855. https://doi.org/10.1111/gcb.15275
91. Goodbred Jr, S. L., & Kuehl, S. A. (1999). Holocene and modern sediment budgets for the Ganges-Brahmaputra river system: Evidence for highstand dispersal to flood-plain, shelf, and deep-sea depocenters. *Geology*, *27*(6), 559-562. https://doi.org/10.1130/0091-7613(1999)027%3C0559:HAMSBF%3E2.3.CO;2

92. Goodbred Jr, S. L., & Kuehl, S. A. (2000). The significance of large sediment supply, active tectonism, and eustasy on margin sequence development: Late Quaternary stratigraphy and evolution of the Ganges–Brahmaputra delta. *Sedimentary Geology*, *133*(3-4), 227-248. https://doi.org/10.1016/S0037-0738(00)00041-5

93. Gour, J. (2021). Stages of land reclamation and their impact on the fluvio-geomorphological environment of Indian Sundarbans with special reference to Matla–Bidyadhari Interfluve. Retrieved from https://www.sciencedirect.com/science/article/pii/B9780128238950000221

94. Habib, I. (1999). The agrarian system of Mughal India, 1556-1707. Oxford University Press.

95. Hamilton, S. E., & Casey, D. (2016). Creation of a high spatio-temporal resolution global database of continuous mangrove forest cover for the 21st century (CGMFC-21). *Global Ecology and Biogeography*, *25*(6), 729-738. https://doi.org/10.1111/geb.12449

96. Hashimoto, S., DasGupta, R., Kabaya, K., Matsui, T., Haga, C., Saito, O., & Takeuchi, K. (2019). Scenario analysis of land-use and ecosystem services of social-ecological landscapes: implications of alternative development pathways under declining population in the Noto Peninsula, Japan. *Sustainability Science*, *14*, 53-75. https://doi.org/10.1007/s11625-018-0626-6

97. Hati, J. P., Samanta, S., Chaube, N. R., Misra, A., Giri, S., Pramanick, N., ... & Hazra, S. (2021). Mangrove classification using airborne hyperspectral AVIRIS-NG and comparing with other spaceborne hyperspectral and multispectral data. *The Egyptian Journal of Remote Sensing and Space Science*, *24*(2), 273-281. https://doi.org/10.1016/j.ejrs.2020.10.002

98. Hazra, S. and Samanta, K., 2016. Temporal Change Detection (2001-2008) Study of Sundarban. http://www.iczmpwb.org/main/pdf/ebooks/WWF_FinalReportPDF.pdf

99. Hazra, S., Ghosh, T., Dasgupta, R. and Sen, G., 2002. Sea level and associated changes in the Sundarbans. Science and Culture, 68(9/12), pp.309-321.

100. Hazra, S., Ghosh, T., Dasgupta, R., & Sen, G. (2002). Sea-level and associated changes in the Sundarbans. ScienceDirect, 16(3), 205-213.

101. He, C., Okada, N., Zhang, Q., Shi, P., & Zhang, J. (2006). Modeling urban expansion scenarios by coupling cellular automata model and system dynamic model in Beijing, China. *Applied Geography*, *26*(3-4), 323-345. https://doi.org/10.1016/j.apgeog.2006.09.006

102. Hossain, K. A., Masiero, M., & Pirotti, F. (2024). Land cover change across 45 years in the world's largest mangrove forest (Sundarbans): The contribution of remote sensing in forest monitoring. International Journal of Remote Sensing, 45(1), 75-92. DOI:10.1080/22797254.2022.2097450

103. Huete, A., Didan, K., Miura, T., Rodriguez, E. P., Gao, X., & Ferreira, L. G. (2002). Overview of the radiometric and biophysical performance of the MODIS vegetation indices. *Remote sensing of environment*, *83*(1-2), 195-213. https://doi.org/10.1016/S0034-4257(02)00096-2

104. Huq, S., Ali, S. I., & Rahman, A. A. (1995). Sea-level rise and Bangladesh: A preliminary analysis. *Journal of Coastal Research*, 44-53.

105. India Meteorological Department. (2021). *Grided data download*. Retrieved January 25, 2021, from http://www.imdpune.gov.in/Clim_Pred_LRF_New/Grided_Data_Download.html

106. Irfan, H. (1999). Agrarian System of Mughal India 1556-1707.

107. Ishtiaque, A., Myint, S. W., & Wang, C. (2016). Examining the ecosystem health and sustainability of the world's largest mangrove forest using multi-temporal MODIS products. *Science of the Total Environment*, *569*, 1241-1254. https://doi.org/10.1016/j.scitotenv.2016.06.200

108. Islam, M. J., Alam, M. S., & Elahi, K. M. (1997). Remote sensing for change detection in the Sunderbands, Bangladesh. Geocarto International, 12(3), 91-100. https://doi.org/10.1080/10106049709354601

109. Kates, R. W., Clark, W. C., Corell, R., Hall, J. M., Jaeger, C. C., Lowe, I., ... & Svedin, U. (2001). Sustainability science. *Science*, *292*(5517), 641-642. https://doi.org/10.1126/science.1059386

110. Khan, A. R., Khan, A., Masud, S., & Rahman, R. M. (2021). Analyzing the land cover change and degradation in Sundarbans mangrove forest using machine learning and remote sensing technique.

111. Kirwan, M. L., Guntenspergen, G. R., d'Alpaos, A., Morris, J. T., Mudd, S. M., & Temmerman, S. (2010). Limits on the adaptability of coastal marshes to rising sea level. *Geophysical research letters*, *37*(23). https://doi.org/10.1029/2010GL045489

112. Kok, K. (2009). The potential of Fuzzy Cognitive Maps for semi-quantitative scenario development, with an example from Brazil. *Global environmental change*, *19*(1), 122-133. https://doi.org/10.1016/j.gloenvcha.2008.08.003

113. Kolb, M., & Galicia, L. (2018). Scenarios and story lines: drivers of land use change in southern Mexico. *Environment, Development and Sustainability*, *20*, 681-702. https://doi.org/10.1007/s10668-016-9905-5

114. Kovács, F., & Gulácsi, A. (2019). Spectral index-based monitoring (2000–2017) in lowland forests to evaluate the effects of climate change. *Geosciences*, *9*(10), 411. https://doi.org/10.3390/geosciences9100411

115. Krauss, K. W., McKee, K. L., Lovelock, C. E., Cahoon, D. R., Saintilan, N., Reef, R., & Chen, L. (2014). How mangrove forests adjust to rising sea level. *New Phytologist*, *202*(1), 19-34. https://doi.org/10.1111/nph.12605

116. Kuenzer, C., Bluemel, A., Gebhardt, S., Quoc, T. V., & Dech, S. (2011). Remote sensing of mangrove ecosystems: A review. *Remote Sensing*, *3*(5), 878-928. https://doi.org/10.3390/rs3050878

117. Kulp, S. A., & Strauss, B. H. (2018). CoastalDEM: A global coastal digital elevation model improved from SRTM using a neural network. *Remote sensing of environment*, *206*, 231-239. https://doi.org/10.1016/j.rse.2017.12.026

118. Kumar, T., Mandal, A., Dutta, D., Nagaraja, R., & Dadhwal, V. K. (2019). Discrimination and classification of mangrove forests using EO-1 Hyperion data: a case study of Indian Sundarbans. *Geocarto International*, *34*(4), 415-442. https://doi.org/10.1080/10106049.2017.1408699

119. Kundu, K., Halder, P., & Mandal, J. K. (2019). Forest cover change analysis in Sundarban delta using remote sensing data and GIS. Springer Proceedings in Earth and Environmental Sciences. DOI:10.1007/978-981-13-7334-3_7

120. Kundu, K., Halder, P., & Mandal, J. K. (2021). Change detection and patch analysis of Sundarban forest during 1975–2018 Using Remote Sensing and GIS data. *SN Computer Science*, *2*, 1-14. https://doi.org/10.1007/s42979-021-00749-8

121. LAHIRI, S. (1992). LANDUSE IN THE EASTERN HIMALAYAN REGION. *New Dimensions in Agricultural Geography*, *31*(4), 205.

122. Lee, N. L. Y., Huang, D., Quek, Z. B. R., Lee, J. N., & Wainwright, B. J. (2020). Distinct fungal communities associated with different organs of the mangrove Sonneratia alba in the Malay Peninsula. *IMA fungus*, *11*, 1-9. https://doi.org/10.1186/s43008-020-00042-y

123. Li, L., Chen, Y., Xu, T., Liu, R., Shi, K., & Huang, C. (2015). Super-resolution mapping of wetland inundation from remote sensing imagery based on integration of

back-propagation neural network and genetic algorithm. *Remote Sensing of Environment*, *164*, 142-154. https://doi.org/10.1016/j.rse.2015.04.009

124. Li, S., Meng, X., Ge, Z., & Zhang, L. (2015). Evaluation of the threat from sea-level rise to the mangrove ecosystems in Tieshangang Bay, southern China. *Ocean & Coastal Management*, *109*, 1-8. https://doi.org/10.1016/j.ocecoaman.2015.02.006

125. Lovelock, C. E., Cahoon, D. R., Friess, D. A., Guntenspergen, G. R., Krauss, K. W., Reef, R., ... & Triet, T. (2015). The vulnerability of Indo-Pacific mangrove forests to sea-level rise. *Nature*, *526*(7574), 559-563. https://doi.org/10.1038/nature15538

126. Mahadevia Ghimire, K., & Vikas, M. (2012). Climate change–impact on the Sundarbans, a case study. *International Scientific Journal: Environmental Science*, *2*(1), 7-15.

127. Mandal, A. K., & Nandi, N. C. (1989). Fauna of Sundarban mangrove ecosystem, West Bengal, India.

128. Mandal, M.S.H. and Hosaka, T., 2020. Assessing cyclone disturbances (1988–2016) in the Sundarbans mangrove forests using Landsat and Google Earth Engine. Natural Hazards, 102(1), pp.133-150. https://doi.org/10.1007/s11069-020-03914-z

129. Manna, S., & Raychaudhuri, B. (2020). Mapping distribution of Sundarban mangroves using Sentinel-2 data and new spectral metric for detecting their health condition. *Geocarto International*, *35*(4), 434-452. https://doi.org/10.1080/10106049.2018.1520923

130. Maryantika, N., & Lin, C. (2017). Exploring changes of land use and mangrove distribution in the economic area of Sidoarjo District, East Java using multi-temporal Landsat images. *Information Processing in Agriculture*, *4*(4), 321-332. https://doi.org/10.1016/j.inpa.2017.06.003

131. Mcleod, E., Poulter, B., Hinkel, J., Reyes, E., & Salm, R. (2010). Sea-level rise impact models and environmental conservation: A review of models and their applications. *Ocean & Coastal Management*, *53*(9), 507-517. https://doi.org/10.1016/j.ocecoaman.2010.06.009

132. Menéndez, P., Losada, I. J., Torres-Ortega, S., Narayan, S., & Beck, M. W. (2020). The global flood protection benefits of mangroves. Scientific reports, 10(1), 1-11.

133. Meyer, W. B., & Turner, B. L. (1992). Human population growth and global land-use/cover change. *Annual review of ecology and systematics*, 39-61.

134. Mikhailov, V. N., & Dotsenko, M. A. (2006). Peculiarities of the hydrological regime of the Ganges and Brahmaputra river mouth area. *Water Resources*, *33*, 353-373. https://doi.org/10.1134/S0097807806040014

135. Mishra, V. N., & Rai, P. K. (2016). A remote sensing aided multi-layer perceptron-Markov chain analysis for land use and land cover change prediction in Patna district (Bihar), India. *Arabian Journal of Geosciences*, *9*, 1-18. https://doi.org/10.1007/s12517-015-2138-3

136. Mistri, A., & Das, B. (2020). *Environmental change, livelihood issues and migration*. Springer Singapore.

137. Miththapala, S. (2008). *Mangroves* (Vol. 2). IUCN.

138. Mitra, D., & Karmaker, S. (2010). Mangrove classification in Sundarban using high resolution multi-spectral remote sensing data and GIS. *Asian Journal of Environment and Disaster Management*, *2*(2). 10.3850/S179392402010000268

139. Module, F. L. A. A. S. H. (2009). Atmospheric correction module: Quac and flaash user's guide. *Version*, *4*, 44.

140. Mondal, B., Das, D. N., & Bhatta, B. (2017). Integrating cellular automata and Markov techniques to generate urban development potential surface: a study on Kolkata agglomeration. *Geocarto international*, *32*(4), 401-419. https://doi.org/10.1080/10106049.2016.1155656

141. Montanari, A., Londei, A., & Staniscia, B. (2014). Can we interpret the evolution of coastal land use conflicts? Using Artificial Neural Networks to model the effects of alternative development policies. *Ocean & coastal management*, *101*, 114-122. https://doi.org/10.1016/j.ocecoaman.2014.09.021

142. Morgado, P., Gomes, E., & Costa, N. (2014). Competing visions? Simulating alternative coastal futures using a GIS-ANN web application. *Ocean & coastal management*, *101*, 79-88. https://doi.org/10.1016/j.ocecoaman.2014.09.022

143. Morgan, J. P., & McIntire, W. G. (1959). Quaternary geology of the Bengal basin, East Pakistan and India. *Geological Society of America Bulletin*, *70*(3), 319-342. https://doi.org/10.1130/0016-7606(1959)70[319:QGOTBB]2.0.CO;2

144. Mozumder, C., & Tripathi, N. K. (2014). Geospatial scenario based modelling of urban and agricultural intrusions in Ramsar wetland Deepor Beel in Northeast India using a multi-layer perceptron neural network. *International Journal of Applied Earth Observation and Geoinformation*, *32*, 92-104. https://doi.org/10.1016/j.jag.2014.03.002

145. Mukherjee, S., Banerjee, K., & Ghosh, S. (2021). Cyclone Amphan and its impacts on the coastal ecosystem of the Indian Sundarbans: A remote sensing-based assessment. International Journal of Disaster Risk Reduction, 63, 102463. https://doi.org/10.1016/j.ijdrr.2021.102463

146. Mukhopadhyay, A., Chanda, A., & Ghosh, T. (2018). Land loss and coastal erosion in the Indian Sundarbans: A historical perspective. Regional Studies in Marine Science, 24, 318-329.

147. Mukhopadhyay, A., Wheeler, D., Dasgupta, S., Dey, A., & Sobhan, I. (2018). Aquatic salinization and mangrove species in a changing climate: impact in the Indian Sundarbans. *World Bank Policy Research Working Paper*, (8532).

148. Mukul, S. A., Alamgir, M., Sohel, M. S. I., Pert, P. L., Herbohn, J., Turton, S. M., ... & Laurance, W. F. (2019). Combined effects of climate change and sea-level rise project dramatic habitat loss of the globally endangered Bengal tiger in the Bangladesh Sundarbans. *Science of the total environment*, *663*, 830-840. https://doi.org/10.1016/j.scitotenv.2019.01.383

149. Nagelkerken, I. S. J. M., Blaber, S. J. M., Bouillon, S., Green, P., Haywood, M., Kirton, L. G., ... & Somerfield, P. J. (2008). The habitat function of mangroves for terrestrial and marine fauna: a review. *Aquatic botany*, *89*(2), 155-185. https://doi.org/10.1016/j.aquabot.2007.12.007

150. Nakicenovic, N., Lempert, R. J., & Janetos, A. C. (2014). A framework for the development of new socio-economic scenarios for climate change research: introductory essay: a forthcoming special issue of climatic change. *Climatic change*, *122*, 351-361. https://doi.org/10.1007/s10584-013-0982-2

151. Naskar, K., & Guha Bakshi, D. N. (1987). Mangrove swamps of the Sundarbans: an ecological perspective.

152. Nath, A., Samanta, S., Banerjee, S., Danda, A. A., & Hazra, S. (2021). Threat of arsenic contamination, salinity and water pollution in agricultural practices of Sundarban Delta, India, and mitigation strategies. *SN Applied Sciences*, *3*, 1-15. https://doi.org/10.1007/s42452-021-04544-1

153. National Bureau of Soil Survey and Land Use Planning. (2020, August). *NBSS Publ. No. 176*. https://doi.org/10.13140/RG.2.2.23495.11687

154. Neeti, N., & Eastman, J. R. (2011). A contextual mann-kendall approach for the assessment of trend significance in image time series. *Transactions in GIS*, *15*(5), 599-611. https://doi.org/10.1111/j.1467-9671.2011.01280.x

155. Nicholls, R. J., & Cazenave, A. (2010). Sea-level rise and its impact on coastal zones. *science*, *328*(5985), 1517-1520. https://doi.org/10.1126/science.1185782

156. Nicholls, R. J., Lincke, D., Hinkel, J., Brown, S., Vafeidis, A. T., Meyssignac, B., ... & Fang, J. (2021). A global analysis of subsidence, relative sea-level change and coastal flood exposure. *Nature Climate Change*, *11*(4), 338-342. https://doi.org/10.1038/s41558-021-00993-z

157. Nouri, A., Raman, B., Bozga, M., Legay, A., & Bensalem, S. (2014, September). Faster statistical model checking by means of abstraction and learning. In *International conference on runtime verification* (pp. 340-355). Cham: Springer International Publishing. https://doi.org/10.1007/978-3-319-11164-3_28

158. Office of the Registrar General & Census Commissioner, India. (2011). *Census of India 2011: Provisional population totals*. Government of India. Retrieved from https://censusindia.gov.in/2011-Common/CensusData2011.html

159. Pargiter, F. E. (1934). A revenue history of the Sundarbans, from 1765 to 1870. *(No Title)*.

160. Pargiter, F. E., & Ascoli, F. D. (2002). A revenue history of the Sundarbans. Routledge. https://api.taylorfrancis.com/content/books/mono/download?identifierName=doi&identifierValue=10.4324/9781003005698&type=googlepdf

161. Pastor-Guzman, J., Dash, J., & Atkinson, P. M. (2018). Remote sensing of mangrove forest phenology and its environmental drivers. *Remote sensing of environment*, *205*, 71-84. https://doi.org/10.1016/j.rse.2017.11.009

162. Paul, A. K., Ray, R., Kamila, A., & Jana, S. (2017). Mangrove degradation in the Sundarbans. *Coastal wetlands: alteration and remediation*, 357-392. https://doi.org/10.1007/978-3-319-56179-0_11

163. Payo, A., Mukhopadhyay, A., Hazra, S., Ghosh, T., Ghosh, S., Brown, S., ... & Haque, A. (2016). Projected changes in area of the Sundarban mangrove forest in Bangladesh due to SLR by 2100. *Climatic Change*, *139*, 279-291. https://doi.org/10.1007/s10584-016-1769-z

164. Pethick, J., & Orford, J. D. (2013). Rapid sea-level rise and delta subsidence: Implications for coastal stability. Geology Today, 29(2), 72-77. https://doi.org/10.1111/gto.12036

165. Pocewicz, A., Nielsen-Pincus, M., Goldberg, C. S., Johnson, M. H., Morgan, P., Force, J. E., ... & Vierling, L. (2008). Predicting land use change: comparison of models

based on landowner surveys and historical land cover trends. Landscape Ecology, 23, 195-210. https://doi.org/10.1007/s10980-007-9159-6

166. Prado, P., Alcaraz, C., Benito, X., Caiola, N., & Ibáñez, C. (2019). Pristine vs. human-altered Ebro Delta habitats display contrasting resilience to RSLR. *Science of the Total Environment*, *655*, 1376-1386. https://doi.org/10.1016/j.scitotenv.2018.11.318

167. Quader, M. A., Agrawal, S., & Kervyn, M. (2017). Multi-decadal land cover evolution in the Sundarban, the largest mangrove forest in the world. Journal of Environmental Management, 205, 1-10. DOI:10.1016/j.jenvman.2017.09.034

168. Rahman, A. F., Dragoni, D., & El-Masri, B. (2011). Response of the Sundarbans coastline to sea level rise and decreased sediment flow: A remote sensing assessment. *Remote Sensing of Environment*, *115*(12), 3121-3128. https://doi.org/10.1016/j.rse.2011.06.019

169. Rahman, M. M. (2020). Impact of increased salinity on the plant community of the Sundarbans Mangrove of Bangladesh. *Community Ecology*, *21*(3), 273-284. https://doi.org/10.1007/s42974-020-00028-1

170. Rahman, M. M., Rahman, M. M., & Islam, K. S. (2010). The causes of deterioration of Sundarban mangrove forest ecosystem of Bangladesh: conservation and sustainable management issues. *Aquaculture, Aquarium, Conservation & Legislation*, *3*(2), 77-90.

171. Regmi, R. K., Jung, K., Nakagawa, H., Kang, J., & Lee, G. (2014). Sediment erosion and transport experiments in laboratory using artificial rainfall simulator. *Journal of the Korean Geoenvironmental Society*, *15*(4), 13-27.

172. Reyes, E., White, M. L., Martin, J. F., Kemp, G. P., Day, J. W., & Aravamuthan, V. (2000). Landscape modeling of coastal habitat change in the Mississippi Delta. *Ecology*, *81*(8), 2331-2349. https://doi.org/10.1890/0012-9658(2000)081[2331:LMOCHC]2.0.CO;2

173. Richards, J. F., & Flint, E. P. (1990). Long-term transformations in the Sundarbans wetlands forests of Bengal. Environmental Conservation, 17(1), 35-45. https://link.springer.com/article/10.1007/BF01530433

174. Rikimaru, A., Roy, P. S., & Miyatake, S. (2002). Tropical forest cover density mapping. *Tropical ecology*, *43*(1), 39-47.

175. Rizzoli, P., Martone, M., Gonzalez, C., Wecklich, C., Tridon, D. B., Bräutigam, B., ... & Moreira, A. (2017). Generation and performance assessment of the global

TanDEM-X digital elevation model. *ISPRS Journal of Photogrammetry and Remote Sensing*, *132*, 119-139. https://doi.org/10.1016/j.isprsjprs.2017.08.008

176. Roberts, D. A., Gardner, M., Church, R., Ustin, S., Scheer, G., & Green, R. O. (1998). Mapping chaparral in the Santa Monica Mountains using multiple endmember spectral mixture models. Remote sensing of environment, 65(3), 267-279. https://doi.org/10.1016/S0034-4257(98)00037-6

177. Rogers, K. G., Goodbred, S. L., & Mondal, D. R. (2017). Monsoon sedimentation on the Ganges-Brahmaputra Delta: A comparison of decadal and millennial timescales. Earth Surface Processes and Landforms, 42(4), 585-600. https://doi.org/10.1002/esp.4003

178. Roy, A., & Dhar, S. B. (2021). Forest land degradation and reclamation process in Indian Sundarbans: A case study. ScienceDirect. https://www.sciencedirect.com/science/article/pii/B9780128238950000014

179. Roy, A.B. and Chatterjee, A., 2015. Tectonic framework and evolutionary history of the Bengal Basin in the Indian subcontinent. Current Science, pp.271-279.

180. Roy, S. S., Ghosh, T., & Hewavithana, D. K. (2024). Transformation of coastal wetlands in the Sundarban Delta (1999–2020). Environmental Monitoring and Assessment, 196(2), 12. DOI:10.1007/s10661-024-12901-x

181. Sahana, M. and Sajjad, H., 2019. Assessing influence of erosion and accretion on landscape diversity in Sundarban Biosphere Reserve, Lower Ganga Basin: a geospatial approach. In Quaternary Geomorphology in India (pp. 191-203). Springer, Cham. https://doi.org/10.1007/978-3-319-90427-6_10

182. Sahana, M., Ahmed, R. & Sajjad, H. (2016) Analyzing land surface temperature distribution in response to land use/land cover change using split window algorithm and spectral radiance model in Sundarban Biosphere Reserve, India. *Model. Earth Syst. Environ.* **2**, 81. https://doi.org/10.1007/s40808-016-0135-5

183. Sahana, M., Areendran, G. and Sajjad, H., 2022. Assessment of suitable habitat of mangrove species for prioritizing restoration in coastal ecosystem of Sundarban Biosphere Reserve, India. Scientific Reports, 12(1), p.20997. https://doi.org/10.1038/s41598-022-24953-5

184. Sahana, M., Rehman, S., & Paul, A. K. (2019). Assessing socio-economic vulnerability to climate change-induced disasters: evidence from Sundarban Biosphere Reserve, India. Climate and Development, 12(3), 237-254. https://doi.org/10.1080/24749508.2019.1700670

185. Sahana, M., Rehman, S., Ahmed, R., & Sajjad, H. (2021). Analyzing climate variability and its effects in Sundarban Biosphere Reserve, India: reaffirmation from local communities. Environmental Monitoring and Assessment, 193(7), 456. https://doi.org/10.1007/s10668-020-00682-5

186. Sahana, M., Saini, M., Areendran, G., & Imdad, K. (2022). Assessing wetland ecosystem health in Sundarban Biosphere Reserve using pressure-state-response model and geospatial techniques. Environmental Science & Policy, 135, 152-167. https://doi.org/10.1016/j.envsci.2022.02.003

187. Sahana, M., Sajjad, H., & Ahmed, R. (2015). Assessing spatio-temporal health of forest cover using forest canopy density model and forest fragmentation approach in Sundarban reserve forest, India. *Modeling Earth Systems and Environment*, *1*, 1-10. https://doi.org/10.1007/s40808-015-0043-0

188. Saintilan, N., Khan, N. S., Ashe, E., Kelleway, J. J., Rogers, K., Woodroffe, C. D., & Horton, B. P. (2020). Thresholds of mangrove survival under rapid sea level rise. *Science*, *368*(6495), 1118-1121. https://doi.org/10.1126/science.aba2656

189. Samanta, B. (2018). Coastal erosion in Gabardhanpur and surrounding area, Patharpratima, south 24 parganas, West Bengal, India. *Journal of Geography, Environment and Earth Science International*, *15*(3), 1-10.

190. Samanta, S., Hazra, S., Mondal, P. P., Chanda, A., Giri, S., French, J. R., & Nicholls, R. J. (2021). Assessment and attribution of mangrove Forest changes in the Indian Sundarbans from 2000 to 2020. *Remote Sensing*, *13*(24), 4957. https://doi.org/10.3390/rs13244957

191. Sánchez-Arias, L. E., Rodriguez, J. P., Caballer, M., Asmussen, M. V., & Medina, G. (2011). Diagnostic of health status in Mangrove ecosystems. *Adv. Environ. Res*, *3*, 235-262.

192. Sánchez-Triana, E., Paul, T., & Leonard, O. (2014). Building resilience for sustainable development of the Sundarbans. *The International Bank for Reconstruction and Development, The World Bank, Washington, DC*.

193. Sang, L., Zhang, C., Yang, J., Zhu, D., & Yun, W. (2011). Simulation of land use spatial pattern of towns and villages based on CA–Markov model. *Mathematical and Computer Modelling*, *54*(3-4), 938-943. https://doi.org/10.1016/j.mcm.2010.11.019

194. Sardar, P., & Samadder, S. R. (2021). Understanding the dynamics of landscape of greater Sundarban area using multi-layer perceptron Markov chain and landscape

statistics approach. *Ecological Indicators*, *121*, 106914. https://doi.org/10.1016/j.ecolind.2020.106914

195. Sarkar, A., Sengupta, S. M. J. M., McArthur, J. M., Ravenscroft, P., Bera, M. K., Bhushan, R., ... & Agrawal, S. (2009). Evolution of Ganges–Brahmaputra western delta plain: clues from sedimentology and carbon isotopes. *Quaternary Science Reviews*, *28*(25-26), 2564-2581. https://doi.org/10.1016/j.quascirev.2009.05.016

196. Sarker, S. K., Reeve, R., Thompson, J., Paul, N. K., & Matthiopoulos, J. (2016). Are we failing to protect threatened mangroves in the Sundarbans world heritage ecosystem?. Scientific reports, 6(1), 21234. https://doi.org/10.1038/srep21234

197. Schoemaker, P. J. (2004). Forecasting and scenario planning: The challenges of uncertainty and complexity. *Blackwell handbook of judgment and decision making*, 274-296.

198. Schuerch, M., Spencer, T., Temmerman, S., Kirwan, M. L., Wolff, C., Lincke, D., ... & Brown, S. (2018). Future response of global coastal wetlands to sea-level rise. *Nature*, *561*(7722), 231-234. https://doi.org/10.1038/s41586-018-0476-5

199. Sheeja, R. V., Joseph, S., Jaya, D. S., & Baiju, R. S. (2011). Land use and land cover changes over a century (1914–2007) in the Neyyar River Basin, Kerala: a remote sensing and GIS approach. *International Journal of Digital Earth*, *4*(3), 258-270. https://doi.org/10.1080/17538947.2010.493959

200. Sibanda, S., & Ahmed, F. (2021). Modelling historic and future land use/land cover changes and their impact on wetland area in Shashe sub-catchment, Zimbabwe. *Modeling Earth Systems and Environment*, *7*(1), 57-70. https://doi.org/10.1007/s40808-020-00963-y

201. Simard, M., Fatoyinbo, L., Smetanka, C., Rivera-Monroy, V. H., Castañeda-Moya, E., Thomas, N., & Van der Stocken, T. (2019). Mangrove canopy height globally related to precipitation, temperature and cyclone frequency. *Nature Geoscience*, *12*(1), 40-45. https://doi.org/10.1038/s41561-018-0279-1

202. Sobrino, J. A., Sòria, G., & Prata, A. J. (2004). Surface temperature retrieval from Along Track Scanning Radiometer 2 data: Algorithms and validation. *Journal of geophysical research: atmospheres*, *109*(D11). https://doi.org/10.1029/2003JD004212

203. Song, C., Woodcock, C. E., Seto, K. C., Lenney, M. P., & Macomber, S. A. (2001). Classification and change detection using Landsat TM data: when and how to correct atmospheric effects?. *Remote sensing of Environment*, *75*(2), 230-244. https://doi.org/10.1016/S0034-4257(00)00169-3

204. Spencer, T., Schuerch, M., Nicholls, R. J., Hinkel, J., Lincke, D., Vafeidis, A. T., ... & Brown, S. (2016). Global coastal wetland change under sea-level rise and related stresses: The DIVA Wetland Change Model. *Global and Planetary Change*, *139*, 15-30. https://doi.org/10.1016/j.gloplacha.2015.12.018

205. Stanley, D. J., & Hait, A. K. (2000). Holocene depositional patterns, neotectonics and Sundarban mangroves in the western Ganges-Brahmaputra delta. *Journal of Coastal Research*, 26-39.

206. Swart, R. J., Raskin, P., & Robinson, J. (2004). The problem of the future: sustainability science and scenario analysis. *Global environmental change*, *14*(2), 137-146. https://doi.org/10.1016/j.gloenvcha.2003.10.002

207. Tabak, N. M., Laba, M., & Spector, S. (2016). Simulating the effects of sea level rise on the resilience and migration of tidal wetlands along the Hudson River. *PLoS One*, *11*(4), e0152437. https://doi.org/10.1371/journal.pone.0152437

208. Tang, W., Zheng, M., Zhao, X., Shi, J., Yang, J., & Trettin, C. C. (2018). Big geospatial data analytics for global mangrove biomass and carbon estimation. *Sustainability*, *10*(2), 472. https://doi.org/10.3390/su10020472

209. Thakur, S., Maity, D., Mondal, I. *et al.* Assessment of changes in land use, land cover, and land surface temperature in the mangrove forest of Sundarbans, northeast coast of India. *Environ Dev Sustain* **23**, 1917–1943 (2021). https://doi.org/10.1007/s10668-020-00656-7

210. Thomas, N., Lucas, R., Bunting, P., Hardy, A., Rosenqvist, A., & Simard, M. (2017). Distribution and drivers of global mangrove forest change, 1996–2010. *PloS one*, *12*(6), e0179302. https://doi.org/10.1371/journal.pone.0179302

211. U.S. Geological Survey. (n.d.). EarthExplorer. U.S. Department of the Interior. Retrieved [11 September, 2022], from https://earthexplorer.usgs.gov/

212. Valiela, I., Bowen, J. L., & York, J. K. (2001). Mangrove Forests: One of the World's Threatened Major Tropical Environments: At least 35% of the area of mangrove forests has been lost in the past two decades, losses that exceed those for tropical rain forests and coral reefs, two other well-known threatened environments. *Bioscience*, *51*(10), 807-815. https://doi.org/10.1641/0006-3568(2001)051[0807:MFOOTW]2.0.CO;2

213. Wang, D., Wan, B., Qiu, P., Su, Y., Guo, Q., Wang, R., ... & Wu, X. (2018). Evaluating the performance of Sentinel-2, Landsat 8 and Pléiades-1 in mapping

mangrove extent and species. *Remote Sensing*, *10*(9), 1468. https://doi.org/10.3390/rs10091468

214. Warren Pinnacle. (2016). *SLAMM 6.7 technical documentation*. Warren Pinnacle Consulting, Inc. Available from http://warrenpinnacle.com/prof/SLAMM6/SLAMM_6.7_Technical_Documentation.pdf

215. Weng, Q. (2002). Land use change analysis in the Zhujiang Delta of China using satellite remote sensing, GIS and stochastic modelling. *Journal of environmental management*, *64*(3), 273-284. https://doi.org/10.1006/jema.2001.0509

216. White, E. D., Meselhe, E., Reed, D., Renfro, A., Snider, N. P., & Wang, Y. (2019). Mitigating the effects of sea-level rise on estuaries of the Mississippi Delta Plain using river diversions. *Water*, *11*(10), 2028. https://doi.org/10.3390/w11102028

217. Wolanski, E. (1995). Transport of sediment in mangrove swamps. *Hydrobiologia*, *295*(1), 31-42. https://doi.org/10.1007/BF00029108

218. Woodroffe, C. D., Rogers, K., McKee, K. L., Lovelock, C. E., Mendelssohn, I. A., & Saintilan, N. (2016). Mangrove sedimentation and response to relative sea-level rise. *Annual review of marine science*, *8*(1), 243-266. https://doi.org/10.1146/annurev-marine-122414-034025

219. Wu, G. R., Hong, H. L., & Yan, C. L. (2015). Arsenic accumulation and translocation in mangrove (Aegiceras corniculatum L.) grown in arsenic contaminated soils. *International journal of environmental research and public health*, *12*(7), 7244-7253. https://doi.org/10.3390/ijerph120707244

220. Xu, X., Shrestha, S., Gilani, H., Gumma, M.K., Siddiqui, B.N. and Jain, A.K., 2020. Dynamics and drivers of land use and land cover changes in Bangladesh. Regional Environmental Change, 20, pp.1-11. https://doi.org/10.1007/s10113-020-01650-5

221. Zhang, K., Liu, H., Li, Y., Xu, H., Shen, J., Rhome, J., & Smith III, T. J. (2012). The role of mangroves in attenuating storm surges. *Estuarine, Coastal and Shelf Science*, *102*, 11-23. https://doi.org/10.1016/j.ecss.2012.02.021